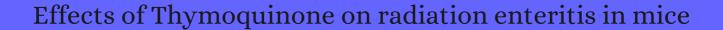
CITATION REPORT List of articles citing



DOI: 10.1038/s41598-018-33214-3 Scientific Reports, 2018, 8, 15122.

Source: https://exaly.com/paper-pdf/70791264/citation-report.pdf

Version: 2024-04-19

This report has been generated based on the citations recorded by exaly.com for the above article. For the latest version of this publication list, visit the link given above.

The third column is the impact factor (IF) of the journal, and the fourth column is the number of citations of the article.

#	Paper	IF	Citations
2338	supp3-2971522.mp3.		
2337	supp1-2971522.mp3.		
2336	supp5-2971522.mp3.		
2335	supp2-2971522.mp3.		
2334	supp6-2971522.mp3.		
2333	supp4-2971522.mp3.		
2332	supp3-2971522.mp3.		
2331	Biogenic Sources of Ice Nucleating Particles at the High Arctic Site Villum Research Station.		
2330	Rattling Transport of Lithium Ion in the Cavities of Model Solid Electrolyte Interphase.		
2329	Critical Size for Carrier Delocalization in Doped Silicon Nanocrystals: A Study by Ultrafast Spectroscopy.		
2328	Quaternary Piperazine-Substituted Rhodamines with Enhanced Brightness for Super-Resolution Imaging.		
2327	Effect of Hydrogen Bonding between lons of Like Charge on the Boundary Layer Friction of Hydroxy-Functionalized Ionic Liquids.		
2326	Water Bridges in Clay Nanopores: Mechanisms of Formation and Impact on Hydrocarbon Transport.		
2325	In Situ Oxygenic Nanopods Targeting Tumor Adaption to Hypoxia Potentiate Image-Guided Photothermal Therapy.		
2324	Highly Stretchable, Directionally Oriented Carbon Nanotube/PDMS Conductive Films with Enhanced Sensitivity as Wearable Strain Sensors.		
2323	Mechanical Reinforcement of Free-Standing Polymeric Nanomembranes via Aluminosilicate Nanotube Scaffolding.		
2322	Polymerization-Based Amplification for Target-Specific Colorimetric Detection of Amplified Mycobacterium tuberculosis DNA on Cellulose.		

2321 Slow Oil, Slow Water: Long-Range Dynamic Coupling across a LiquidLiquid Interface.

Multimodal, in Situ Imaging of Ex Vivo Human Skin Reveals Decrease of Cholesterol Sulfate in the Neoepithelium during Acute Wound Healing.	
2319 Subsurface plant-accessible water in mountain ecosystems with a Mediterranean climate. 2018 , 5, e1277	55
Mass Spectrometry Imaging Shows Cocaine and Methylphenidate Have Opposite Effects on Major Lipids in Drosophila Brain. 2018 , 9, 1462-1468	21
An overview of recent molecular dynamics applications as medicinal chemistry tools for the undruggable site challenge. 2018 , 9, 920-936	21
Reply to the comment on "Synchronizing biological cycles as key to survival under a scenario of global change: The Common quail (Coturnix coturnix) strategy" by Rodriguez-Teijeiro et al. 2018 , 635, 1558-1560	
Piezoelectric materials as stimulatory biomedical materials and scaffolds for bone repair. 2018 , 73, 1-20	130
Clusters of deep-sea egg-brooding octopods associated with warm fluid discharge: An ill-fated fragment of a larger, discrete population?. 2018 , 135, 1-8	7
The partial root-zone saline irrigation system and antioxidant responses in tomato plants. 2018 , 127, 366-379	17
Identification of potential recruitment bottlenecks in larval stages of the giant fan mussel Pinna nobilis using specific quantitative PCR. 2018 , 818, 235-247	2
2311 Fluorescently-tagged polyamines for the staining of siliceous materials. 2018 , 125, 205-211	3
2310 Lateral hardness and the scratch resistance of glasses in the Na2O-CaO-SiO2 system. 2018 , 492, 94-101	18
Distinctive phosphoinositide- and Ca-binding properties of normal and cognitive performance-linked variant forms of KIBRA C2 domain. 2018 , 293, 9335-9344	5
2308 Nano-carriers for targeted delivery and biomedical imaging enhancement. 2018 , 9, 451-468	41
Influence of hydroclimatic variations on solute concentration dynamics in nested subtropical catchments with heterogeneous landscapes. 2018 , 635, 1091-1101	6
Applied microfiber evanescent wave on ZnO nanorods coated glass surface towards temperature sensing. 2018 , 277, 103-111	22
Optical trapping and manipulation of single particles in air: Principles, technical details, and applications. 2018 , 214, 94-119	58
Morphologic and Genomic Analyses of New Isolates Reveal a Second Lineage of Cedratviruses. 2304 2018 , 92,	13

2303	Enhanced magnetic refrigeration capacity in Ni-Mn-Ga micro-particles. 2018, 148, 115-123	22
2302	Structural implications of hERG K channel block by a high-affinity minimally structured blocker. 2018 , 293, 7040-7057	28
2301	Vulnerability in Varying Contexts Affecting Decision Making in Patients With Treatment-Resistant Depression Contemplating Deep Brain Stimulation: Implications for Clinicians. 2018 , 9, 228-230	
2300	Source Study of the 24 August 2016 Mw´6.8 Chauk, Myanmar, Earthquake. 2018 , 89, 1773-1785	4
2299	Everyday information practices: An exploration of intra-individual information behavior across everyday contexts. 2018 , 55, 852-853	
2298	Using Satellite-Borne Remote Sensing Data in Generating Local Warming Maps with Enhanced Resolution. 2018 , 7, 398	1
2297	Properties of Sediment Trap Catchment Areas in Fram Strait: Results From Lagrangian Modeling and Remote Sensing. 2018 , 5,	9
2296	New Insights into Multiclass Damage Classification of Tsunami-Induced Building Damage from SAR Images. 2018 , 10, 2059	18
2295	. 2018 , 6, 74204-74239	11
2294	FSHR Trans-Activation and Oligomerization. 2018 , 9, 760	11
2294	FSHR Trans-Activation and Oligomerization. 2018 , 9, 760 Measurement of phosphate in small samples using capillary electrophoresis with laser-induced luminescence detection. 2018 , 41, 1092-1097	11
<i>,</i>	Measurement of phosphate in small samples using capillary electrophoresis with laser-induced	
2293	Measurement of phosphate in small samples using capillary electrophoresis with laser-induced luminescence detection. 2018 , 41, 1092-1097 A genome-scale metabolic model of potato late blight suggests a photosynthesis suppression	1
2293	Measurement of phosphate in small samples using capillary electrophoresis with laser-induced luminescence detection. 2018, 41, 1092-1097 A genome-scale metabolic model of potato late blight suggests a photosynthesis suppression mechanism. 2018, 19, 863 A Wearable Measurement System for Sole Pressure to Calculate Center of Pressure in Sports Activity. 2018,	1
2293 2292 2291	Measurement of phosphate in small samples using capillary electrophoresis with laser-induced luminescence detection. 2018, 41, 1092-1097 A genome-scale metabolic model of potato late blight suggests a photosynthesis suppression mechanism. 2018, 19, 863 A Wearable Measurement System for Sole Pressure to Calculate Center of Pressure in Sports Activity. 2018, Preparedness for Global Dengue Resurgence: An Urgent Need. 2018, 09,	1
2293 2292 2291 2290	Measurement of phosphate in small samples using capillary electrophoresis with laser-induced luminescence detection. 2018, 41, 1092-1097 A genome-scale metabolic model of potato late blight suggests a photosynthesis suppression mechanism. 2018, 19, 863 A Wearable Measurement System for Sole Pressure to Calculate Center of Pressure in Sports Activity. 2018, Preparedness for Global Dengue Resurgence: An Urgent Need. 2018, 09, Modeling the quantitative nature of neurodevelopmental disorders using Collaborative Cross mice. 2018, 9, 63	1 15 1
2293 2292 2291 2290 2289	Measurement of phosphate in small samples using capillary electrophoresis with laser-induced luminescence detection. 2018, 41, 1092-1097 A genome-scale metabolic model of potato late blight suggests a photosynthesis suppression mechanism. 2018, 19, 863 A Wearable Measurement System for Sole Pressure to Calculate Center of Pressure in Sports Activity. 2018, Preparedness for Global Dengue Resurgence: An Urgent Need. 2018, 09, Modeling the quantitative nature of neurodevelopmental disorders using Collaborative Cross mice. 2018, 9, 63	1 15 1

Quantifying the Spatiotemporal Dynamics of Industrial Land Uses through Mining Free Access Social Datasets in the Mega Hangzhou Bay Region, China. 2018 , 10, 3463	6
Effects of a Meal Replacement on Body Composition and Metabolic Parameters among Subjects with Overweight or Obesity. 2018 , 2018, 2837367	8
Allosteric inhibition induces an open WPD-loop: a new avenue towards glioblastoma therapy 2018 , 8, 40187-40197	15
2282 Bioconversion and Biotransformation Efficiencies of Wild Macrofungi. 2018 , 361-377	4
Three-dimensional numerical simulation and experimental investigation of boundary-driven streaming in surface acoustic wave microfluidics. 2018 , 18, 3645-3654	19
Development of a selective and highly sensitive fluorescence assay for nucleoside triphosphate diphosphohydrolase1 (NTPDase1, CD39). 2018 , 143, 5417-5430	8
In-memory direct processing based on nanoscale perpendicular magnetic tunnel junctions. 2018 , 10, 21225-21230	17
2278 On-chip label-free plasmonic based imaging microscopy for microfluidics. 2018 , 2, 085012	6
2277 Impact of Cubic Symmetry on Optical Activity of Dielectric 8-srs Networks. 2018 , 8, 2104	3
2276 Cut-and-Project Schemes for Pisot Family Substitution Tilings. 2018 , 10, 511	2
2275 Microbial Interconversion of Alkanes to Electricity. 2018 , 6,	2
2275 Microbial Interconversion of Alkanes to Electricity. 2018 , 6, Support Tool for Identifying In Situ Remediation Technology for Sites Contaminated by Hexavalent Chromium. 2018 , 10, 1344	4
Support Tool for Identifying In Situ Remediation Technology for Sites Contaminated by Hexavalent	
Support Tool for Identifying In Situ Remediation Technology for Sites Contaminated by Hexavalent Chromium. 2018, 10, 1344 From Picture to Movie: Twenty Years of Ground Deformation Recording Over Tuscany Region	4
Support Tool for Identifying In Situ Remediation Technology for Sites Contaminated by Hexavalent Chromium. 2018, 10, 1344 From Picture to Movie: Twenty Years of Ground Deformation Recording Over Tuscany Region (Italy) With Satellite InSAR. 2018, 6,	29
Support Tool for Identifying In Situ Remediation Technology for Sites Contaminated by Hexavalent Chromium. 2018, 10, 1344 From Picture to Movie: Twenty Years of Ground Deformation Recording Over Tuscany Region (Italy) With Satellite InSAR. 2018, 6, Capturing motivation and emotion regulation during a learning process. 2018, 85-104	4 29 17
Support Tool for Identifying In Situ Remediation Technology for Sites Contaminated by Hexavalent Chromium. 2018, 10, 1344 From Picture to Movie: Twenty Years of Ground Deformation Recording Over Tuscany Region (Italy) With Satellite InSAR. 2018, 6, Capturing motivation and emotion regulation during a learning process. 2018, 85-104 Genetic Variants in Preeclampsia: Lessons From Studies in Latin-American Populations. 2018, 9, 1771	4 29 17 18

2267	A Novel Optosensor for Rapid Detection of Difenoconazole Using Molecularly Imprinted Polymers. 2018 , 18, 9466-9470		5
2266	Triggering Endogenous Cardiac Repair and Regeneration via Extracellular Vesicle-Mediated Communication. 2018 , 9, 1497		21
2265	Optimal positioning of storage systems in microgrids based on complex networks centrality measures. <i>Scientific Reports</i> , 2018 , 8, 16658	4.9	7
2264	Head and neck cancer organoids established by modification of the CTOS method can be used to predict in vivo drug sensitivity. 2018 , 87, 49-57		59
2263	Unsupervised calibration for noninvasive glucose-monitoring devices using mid-infrared spectroscopy. 2018 , 11, 1850038		6
2262	Biosurfactant production by fungi as a sustainable alternative. 2018 , 85,		15
2261	VIOLA-A Multi-Purpose and Web-Based Visualization Tool for Neuronal-Network Simulation Output. 2018 , 12, 75		7
2260	Titania-Based Hybrid Materials with ZnO, ZrOland MoSlA Review. 2018, 11,		38
2259	A baroclinic coastal trapped wave event in the Gulf of Naples (Tyrrhenian Sea). 2018 , 68, 1683-1694		12
2258	Interpersonal Variations in Gut Microbiota Profiles Supersedes the Effects of Differing Fecal Storage Conditions. <i>Scientific Reports</i> , 2018 , 8, 17367	4.9	28
2257	Study on Compaction Characteristics and Construction Control of Mixtures of Red Clay and Gravel. 2018 , 2018, 1-8		О
2256	Micro-Nano Scale Surface Coating for Nucleate Boiling Heat Transfer: A Critical Review. 2018 , 11, 3189		38
2255	3D printing for chemical, pharmaceutical and biological applications. 2018 , 2, 422-436		128
2254	Eye tracking technology in sports-related concussion: a systematic review and meta-analysis. 2018 , 39, 12TR01		30
2253	Determining minimal output sets that ensure structural identifiability. 2018, 13, e0207334		5
2252	Characterization of Bacillus thuringiensis isolates by their insecticidal activity and their production of Cry and Vip3 proteins. 2018 , 13, e0206813		11
2251	The Effects of a Combination of Ion Channel Inhibitors in Female Rats Following Repeated Mild Traumatic Brain Injury. 2018 , 19,		11
2250	Insight into micro-cracking in 3D-printed Fe-based BMGs by selective laser melting. 2018 , 103, 101-106		15

Versatility of cell-penetrating peptides for intracellular delivery of siRNA. 2018 , 25, 1996-2006	33
2248 [Hypertension-related cognitive impairment: Not as easy as it looks like]. 2018 , 35, 149-151	
Robustness of the reproductive number estimates in vector-borne disease systems. 2018 , 12, e0006999	2
Nanostructures of diamond, graphene oxide and graphite inhibit CYP1A2, CYP2D6 and CYP3A4 enzymes and downregulate their genes in liver cells. 2018 , 13, 8561-8575	8
GSFLOWIGRASS v1.0.0: GIS-enabled hydrologic modeling of coupled groundwater urface-water systems. 2018 , 11, 4755-4777	13
Upconversion of low-energy photons in semiconductor nanostructures for solar energy harvesting. 2244 2018 , 5, 1	9
Theoretical study of some structures of titanium(IV) complexes derived from 2-, 3- and 4-hydroxyl-benzoic acids. 2018 , 32, 571	1
A Perspective Study of Mechanical Characterisation of Graphene for Potential Applications in Thermal Management of Microsystems. 2018 ,	
Reducing the Effect of Spurious Phase Variations in Neural Oscillatory Signals. 2018 , 12, 82	3
Quantifying site-specific chromatin mechanics and DNA damage response. <i>Scientific Reports</i> , 2018 , 8, 18084	1 .9 9
	1
3-D Super-Resolution Ultrasound Imaging Using a 2-D Sparse Array with High Volumetric Imaging	
3-D Super-Resolution Ultrasound Imaging Using a 2-D Sparse Array with High Volumetric Imaging Rate. 2018 ,	
3-D Super-Resolution Ultrasound Imaging Using a 2-D Sparse Array with High Volumetric Imaging Rate. 2018, 2238 A computational intelligence-based filter for lung sound separation. 2018, Pharmacological Effect of Quercetin in Hypertension and Its Potential Application in	1
3-D Super-Resolution Ultrasound Imaging Using a 2-D Sparse Array with High Volumetric Imaging Rate. 2018, 2238 A computational intelligence-based filter for lung sound separation. 2018, Pharmacological Effect of Quercetin in Hypertension and Its Potential Application in Pregnancy-Induced Hypertension: Review of , , and Clinical Studies. 2018, 2018, 7421489	23
3-D Super-Resolution Ultrasound Imaging Using a 2-D Sparse Array with High Volumetric Imaging Rate. 2018, 2238 A computational intelligence-based filter for lung sound separation. 2018, Pharmacological Effect of Quercetin in Hypertension and Its Potential Application in Pregnancy-Induced Hypertension: Review of , , and Clinical Studies. 2018, 2018, 7421489 2236 Applications of Raman spectroscopy in cancer diagnosis. 2018, 37, 691-717	1 23 93
3-D Super-Resolution Ultrasound Imaging Using a 2-D Sparse Array with High Volumetric Imaging Rate. 2018, 2238 A computational intelligence-based filter for lung sound separation. 2018, Pharmacological Effect of Quercetin in Hypertension and Its Potential Application in Pregnancy-Induced Hypertension: Review of , , and Clinical Studies. 2018, 2018, 7421489 2236 Applications of Raman spectroscopy in cancer diagnosis. 2018, 37, 691-717 2237 The many faces of mathematical modelling in oncology. 2019, 92, 20180856 Scaffolds for Chondrogenic Cells Cultivation Prepared from Bacterial Cellulose with Relaxed Fibers	1 23 93 3

2231	Epidermal epidemic: unravelling the pathogenesis of chytridiomycosis. 2019 , 222,	5
2230	Functional Assessment of Patient-Derived Retinal Pigment Epithelial Cells Edited by CRISPR/Cas9. 2018 , 19,	12
2229	Macrocheles species (Acari: Macrochelidae) associated with human corpses in Europe. 2018 , 76, 453-471	12
2228	Mimicking Epithelial Tissues in Three-Dimensional Cell Culture Models. 2018 , 6, 197	41
2227	Sea Spray Aerosol: Where Marine Biology Meets Atmospheric Chemistry. 2018 , 4, 1617-1623	21
2226	Can Daytime Napping Assist the Process of Skills Acquisition After Stroke?. 2018 , 9, 1002	4
2225	Effects of CT FOV displacement and acquisition parameters variation on texture analysis features. 2018 , 63, 235021	4
2224	A discontinuous Galerkin model for fluorescence loss in photobleaching of intracellular polyglutamine protein aggregates. 2018 , 11, 7	O
2223	Engineering of the cellular translational machinery and non-coding RNAs to enhance CHO cell growth, recombinant product yields and quality. 2018 , 22, 199-208	3
2222	Zika Virus Epidemic in Brazil. II. Post-Mortem Analyses of Neonates with Microcephaly, Stillbirths, and Miscarriage. 2018 , 7,	15
2221	Efficient immunoaffinity chromatography of lymphocytes directly from whole blood. <i>Scientific Reports</i> , 2018 , 8, 16731	9
2220	How pupil responses track value-based decision-making during and after reinforcement learning. 2018 , 14, e1006632	24
2219	Methyl benzoate exhibits insecticidal and repellent activities against Bemisia tabaci (Gennadius) (Hemiptera: Aleyrodidae). 2018 , 13, e0208552	12
2218	Microfluidic Devices for Drug Assays. 2018 , 7,	30
2217	Remote Sensing Is Changing Our View of the Coast: Insights from 40 Years of Monitoring at Narrabeen-Collaroy, Australia. 2018 , 10, 1744	53
2216	Drag Effect of Water Consumption on Urbanization A Case Study of the Yangtze River Economic Belt from 2000 to 2015. 2018 , 10, 1115	12
2215	Predicting the Binding of Fatty Acid Amide Hydrolase Inhibitors by Free Energy Perturbation. 2018 , 14, 5815-5822	8
2214	Chronic Intracortical Recording and Electrochemical Stability of Thiol-ene/Acrylate Shape Memory Polymer Electrode Arrays. 2018 , 9,	31

	Nonpolar Matrix. 2018 , 90, 12592-12600	12
2212	Primates in peril: the significance of Brazil, Madagascar, Indonesia and the Democratic Republic of the Congo for global primate conservation. 2018 , 6, e4869	67
2211	Micromanaging Immunity in the Murine Host vs. the Mosquito Vector: Microbiota-Dependent Immune Responses to Intestinal Parasites. 2018 , 8, 308	7
2210	Coral reef degradation affects the potential for reef recovery after disturbance. 2018 , 142, 48-58	23
2209	Bright Prospects for Arctic Sea Ice Prediction on Subseasonal Time Scales. 2018 , 45, 9731-9738	38
2208	Improved production of polysaccharides in Ganoderma lingzhi mycelia by plasma mutagenesis and rapid screening of mutated strains through infrared spectroscopy. 2018 , 13, e0204266	12
2207	Synthesis of copper-loaded activated carbon for enhancing the photocatalytic removal of methylene blue. 2018 , 272, 353-360	4
2206	Theta Bursts Precede, and Spindles Follow, Cortical and Thalamic Downstates in Human NREM Sleep. 2018 , 38, 9989-10001	19
2205	Graphene aerogel based room temperature chemiresistive detection of hydrogen peroxide: A key explosive ingredient. 2018 , 282, 97-113	6
2204	Rapid eye movement density during REM sleep in dogs (Canis familiaris). 2018 , 46, 554-560	5
2204	Rapid eye movement density during REM sleep in dogs (Canis familiaris). 2018 , 46, 554-560 Raman spectroscopy as a novel tool for fast characterization of the chemical composition of perivascular adipose tissue. 2018 , 143, 5999-6005	9
	Raman spectroscopy as a novel tool for fast characterization of the chemical composition of	
2203	Raman spectroscopy as a novel tool for fast characterization of the chemical composition of perivascular adipose tissue. 2018 , 143, 5999-6005 Controlling the Wetting Properties of Superhydrophobic Titanium Surface Fabricated by UV	9
2203	Raman spectroscopy as a novel tool for fast characterization of the chemical composition of perivascular adipose tissue. 2018 , 143, 5999-6005 Controlling the Wetting Properties of Superhydrophobic Titanium Surface Fabricated by UV Nanosecond-Pulsed Laser and Heat Treatment. 2018 , 8, A comparative review of recent bioinformatics tools for inferring gene regulatory networks using	9
2203	Raman spectroscopy as a novel tool for fast characterization of the chemical composition of perivascular adipose tissue. 2018, 143, 5999-6005 Controlling the Wetting Properties of Superhydrophobic Titanium Surface Fabricated by UV Nanosecond-Pulsed Laser and Heat Treatment. 2018, 8, A comparative review of recent bioinformatics tools for inferring gene regulatory networks using time-series expression data. 2018, 20, 320 Enhanced contrast in X-ray microtomographic images of the membranous labyrinth using different	9 21 3
2203 2202 2201 2200	Raman spectroscopy as a novel tool for fast characterization of the chemical composition of perivascular adipose tissue. 2018, 143, 5999-6005 Controlling the Wetting Properties of Superhydrophobic Titanium Surface Fabricated by UV Nanosecond-Pulsed Laser and Heat Treatment. 2018, 8, A comparative review of recent bioinformatics tools for inferring gene regulatory networks using time-series expression data. 2018, 20, 320 Enhanced contrast in X-ray microtomographic images of the membranous labyrinth using different X-ray sources and scanning modes. 2018, 233, 770-782 Thigh-Derived Inertial Sensor Metrics to Assess the Sit-to-Stand and Stand-to-Sit Transitions in the	9 21 3
2202 2201 2200 2199	Raman spectroscopy as a novel tool for fast characterization of the chemical composition of perivascular adipose tissue. 2018, 143, 5999-6005 Controlling the Wetting Properties of Superhydrophobic Titanium Surface Fabricated by UV Nanosecond-Pulsed Laser and Heat Treatment. 2018, 8, A comparative review of recent bioinformatics tools for inferring gene regulatory networks using time-series expression data. 2018, 20, 320 Enhanced contrast in X-ray microtomographic images of the membranous labyrinth using different X-ray sources and scanning modes. 2018, 233, 770-782 Thigh-Derived Inertial Sensor Metrics to Assess the Sit-to-Stand and Stand-to-Sit Transitions in the Timed Up and Go (TUG) Task for Quantifying Mobility Impairment in Multiple Sclerosis. 2018, 9, 684 Nano-targeted relaxin impairs fibrosis and tumor growth in pancreatic cancer and improves the	9 21 3 3

2195	Endocannabinoid Virodhamine Is an Endogenous Inhibitor of Human Cardiovascular CYP2J2 Epoxygenase. 2018 , 57, 6489-6499	11
2194	C5a anaphylatoxin and its role in critical illness-induced organ dysfunction. 2018 , 48, e13028	18
2193	MolPharm/CABS 2018. 2018 , 13, 11-54	
2192	Land Suitability and Insurance Premiums: A GIS-based Multicriteria Analysis Approach for Sustainable Rice Production. 2018 , 10, 1759	17
2191	Feedback of action outcome retrospectively influences sense of agency in a continuous action task. 2018 , 13, e0202690	4
2190	Effect of Electrode Shape and Flow Conditions on the Electrochemical Detection with Band Microelectrodes. 2018 , 18,	5
2189	Exchange stiffness influence on Terfenol-D magnetic states. 2018 , 1, 014001	2
2188	The Current Status and Development of Insect-Resistant Genetically Engineered Poplar in China. 2018 , 9, 1408	17
2187	Regional Landslide Identification Based on Susceptibility Analysis and Change Detection. 2018, 7, 394	9
2186	Chemical-mediated counter defense: attraction of two parasitoid species to the defensive secretion of host larvae. 2018 , 28, 153-162	1
2185	Injectable long-acting human immunodeficiency virus antiretroviral prodrugs with improved pharmacokinetic profiles. 2018 , 552, 371-377	5
2184	Molecular recognition of the beta-glucans laminarin and pustulan by a SusD-like glycan-binding protein of a marine Bacteroidetes. 2018 , 285, 4465-4481	7
2183	Sustained Release from Ionic-Gradient Liposomes Significantly Decreases ETIDOCAINE Cytotoxicity. 2018 , 35, 229	6
2182	Thermo-diffusion and non-uniform heat source/sink effects on hydromagnetic flow of Cu and TiO2 water - based nanofluid partially filled with a porous medium. 2018 , 13, 51-61	11
2181	Climate-Related Limitations on Photosynthesis and Drought-Resistance Strategies of Ziziphus spina-christi. 2018 , 1,	8
2180	Feasibility of a Three-Dimensional Porous Uncalcined and Unsintered Hydroxyapatite/poly-d/l-lactide Composite as a Regenerative Biomaterial in Maxillofacial Surgery. 2018 , 11,	8
2179	Monocytes in rheumatoid arthritis: Circulating precursors of macrophages and osteoclasts and, their heterogeneity and plasticity role in RA pathogenesis. 2018 , 65, 348-359	85
2178	Network Neuroscience Reveals Distinct Neuromarkers of Flow During Media Use. 2018 , 68, 872-895	15

2177	Estrogen alpha receptor antagonists for the treatment of breast cancer: a review. 2018, 12, 107		37
2176	Neural measures of the causal role of observers' facial mimicry on visual working memory for facial expressions. 2018 , 13, 1281-1291		13
2175	Body-relative horizontal-vertical anisotropy in human representations of traveled distances. 2018 , 236, 2811-2827		7
2174	Single-Cell Transcriptomics. 2018 , 1-22		
2173	Effects of Water Column Mixing and Stratification on Planktonic Primary Production and Dinitrogen Fixation on a Northern Red Sea Coral Reef. 2018 , 9, 2351		7
2172	A polymorphism in the fatty acid desaturase-2 gene is associated with the arachidonic acid metabolism in pigs. <i>Scientific Reports</i> , 2018 , 8, 14336	4.9	24
2171	A Personalized Point-of-Care Platform for Real-Time ECG Monitoring. 2018 , 64, 452-460		11
2170	Modulation of gene expression in rat muscle cells following treatment with nanoceria in different gravity regimes. 2018 , 13, 2821-2833		9
2169	ZnO-pHEMA Nanocomposites: An Ecofriendly and Reusable Material for Water Remediation. 2018 , 10, 40100-40110		30
2168	Adaptive Matching Transmitter With Dual-Band Antenna for Intraoral Tongue Drive System. 2018 , 12, 1279-1288		12
2167	Impaired myogenic development, differentiation and function in hESC-derived SMA myoblasts and myotubes. 2018 , 13, e0205589		12
2166	Soil bulb mites as trace evidence for the location of buried money. 2018 , 292, e25-e30		3
2165	Effects of polymethylmethacrylate nanoplastics on Dicentrarchus labrax. 2018, 110, 435-441		80
2164	A Deep Eastern Equatorial Pacific Thermocline During the Last Glacial Maximum. 2018 , 45, 11,806		9
2163	Nanomedicines for Malaria Chemotherapy: Encapsulation vs. Polymer Therapeutics. 2018 , 35, 237		12
2162	Evaluation of Breed and Parity Order Effects on the Lipid Composition of Porcine Colostrum. 2018 , 66, 12911-12920		8
2161	Showcasing the role of seawater in bacteria recruitment and microbiome stability in sponges. <i>Scientific Reports</i> , 2018 , 8, 15201	4.9	25
2160	Improving Electron Extraction Ability and Device Stability of Perovskite Solar Cells Using a Compatible PCBM/AZO Electron Transporting Bilayer. 2018 , 8,		23

2159	Structural analysis of magnetic nanocomposites based on chitosan. 2018 , 72, 202-213		17
2158	Concepts for Developing Physical Gels of Chitosan and of Chitosan Derivatives. 2018 , 4,		50
2157	Strong LightMatter Interaction in Lithography-Free Planar Metamaterial Perfect Absorbers. 2018 , 5, 4203-4221		65
2156	Transcriptome analysis of extended-spectrum <code>#actamase-producing Escherichia coli</code> and methicillin-resistant Staphylococcus aureus exposed to cefotaxime. <i>Scientific Reports</i> , 2018 , 8, 16076	4.9	4
2155	Training Population Optimization for Prediction of Cassava Brown Streak Disease Resistance in West African Clones. 2018 , 8, 3903-3913		17
2154	Candida albicans interdigital foot infection: A case report highlighting the importance of antifungal susceptibility testing. 2018 , 12, 889-896		O
2153	Chemical Removal of Phosphorus from Swine Effluent: the Impact of Previous Effluent Treatment Technologies on Process Efficiency. 2018 , 229, 1		10
2152	Image segmentation for whole tomato plant recognition at night. 2018 , 154, 434-442		14
2151	Triatomine Fauna and Recent Epidemiological Dynamics of Chagas Disease in an Endemic Area of Northeast Brazil. 2018 , 2018, 7020541		4
2150	Targeting the Bacterial Protective Armour; Challenges and Novel Strategies in the Treatment of Microbial Biofilm. 2018 , 11,		20
2149	Zika Virus Vaccines: Challenges and Perspectives. 2018 , 6,		14
2148	Systematic Analysis of Gene Expression Profiles Controlled by hnRNP Q and hnRNP R, Two Closely Related Human RNA Binding Proteins Implicated in mRNA Processing Mechanisms. 2018 , 5, 79		7
2147	Lack of improvement in multiplication is associated with reverting from verbal retrieval to numerical operations. 2018 , 183, 859-871		6
2146	Selective serotonin reuptake inhibitors affect structure, function and metabolism of skeletal muscle: A systematic review. 2018 , 136, 194-204		5
2145	Testing the transferability of track-based habitat models for sound marine spatial planning. 2018 , 24, 1772-1787		10
2144	Effect of different water application rates and nitrogen fertilisation on growth and essential oil of clove basil (Ocimum gratissimum L.). 2018 , 125, 186-197		14
2143	Double-split labyrinth resonator with defective ground system for wide-band band-stop filter application. 2018 , 8, 085127		1
2142	Heterogeneous Organocatalysts Based on a Triazine-Triazole Silane Ligand. 2018 , 2018, 4206-4214		8

2141	Study on healing technique for weak interlayer and related mechanical properties based on microbially-induced calcium carbonate precipitation. 2018 , 13, e0203834	4	
2140	Animal Models of the Impact of Social Stress on Cocaine Use Disorders. 2018 , 140, 131-169	11	
2139	Towards the minimum-cost control of target nodes in directed networks with linear dynamics. 2018 , 355, 8141-8157	3	
2138	Whitefly-transmitted viruses threatening cassava production in Africa. 2018 , 33, 167-176	21	
2137	Microbial enterotypes in personalized nutrition and obesity management. 2018, 108, 645-651	78	
2136	Bryozoan framework composition in the oddly shaped reefs from Abrolhos Bank, Brazil, southwestern Atlantic: taxonomy and ecology. 2018 , 4483, 155-186	7	
2135	Magneto-Optical Kerr Effect Driven by Spin Accumulation on Cu, Au, and Pt. 2018 , 8, 1378	1	
2134	Targeting Breast Cancer Stem Cells to Overcome Treatment Resistance. 2018, 23,	67	
2133	Liquid gated ZnO nanorod FET sensor for ultrasensitive detection of Hepatitis B surface antigen with vertical electrode configuration. 2018 , 122, 58-67	15	
2132	Genome Editing in Rice: Recent Advances, Challenges, and Future Implications. 2018 , 9, 1361	90	
2131	In ovo exposure to triclosan alters the hepatic proteome in chicken embryos. 2018 , 165, 495-504	8	
2130	Research on photonic generation of quadrupling triangular-shaped waveform using external modulation. 2018 , 45, 352-358	5	
2129	Ferroelectric Materials: A Novel Pathway for Efficient Solar Water Splitting. 2018 , 8, 1526	14	
2128	Reinventing an Organelle: The Reduced Mitochondrion in Parasitic Protists. 2018 , 34, 1038-1055	33	
2127	Temperature dependence of piezo- and ferroelectricity in ultrathin P(VDF-TrFE) films 2018 , 8, 29164-29171	6	
2126	The utility and application of electrophysiological methods in the study of visual hallucinations. 2018 , 129, 2361-2371	6	
2125	Antimicrobial Photodynamic Inactivation Mediated by Rose Bengal and Erythrosine Is Effective in the Control of Food-Related Bacteria in Planktonic and Biofilm States. 2018 , 23,	26	
2124	Biokinetics of microbial consortia using biogenic sulfur as a novel electron donor for sustainable denitrification. 2018 , 270, 359-367	42	

2123	Home-based training of rhythmic skills with a serious game in Parkinson's disease: Usability and acceptability. 2018 , 61, 380-385	19
2122	Chitosan, gelatin and methylcellulose films incorporated with tannic acid for food packaging. 2018 , 120, 1119-1126	56
2121	Effect of activated carbon on microbial-induced calcium carbonate precipitation of sand. 2018 , 77, 1	7
2120	Influenza [A new pathogen every year. 2018 , 12, 12-21	3
2119	Classification of Paris species according to botanical and geographical origins based on spectroscopic, chromatographic, conventional chemometric analysis and data fusion strategy. 2018 , 143, 367-378	16
2118	Relationship Between Amyloid-Positivity and Progression to Mild Cognitive Impairment or Dementia over 8 Years in Cognitively Normal Older Adults. 2018 , 65, 1313-1325	14
2117	On the Mobile Communication Requirements for the Demand-Side Management of Electric Vehicles. 2018 , 11, 1220	35
2116	Nutrient recovery technologies integrated with energy recovery by waste biomass anaerobic digestion. 2018 , 269, 520-531	102
2115	Chemotaxonomic potential of exocrine alkyl esters in julid millipedes (Diplopoda: Julidae: Cylindroiulini). 2018 , 81, 1-11	1
2114	Thermal tuning of graphene-embedded waveguide filters based on the polymer-silica hybrid structure 2018 , 8, 30755-30760	2
2113	Automated approach for indirect immunofluorescence images classification based on unsupervised clustering method. 2018 , 12, 989-995	8
2112	The Genus Corynebacterium in the Genomic Era. 2018 ,	Ο
2111	Role of Solid-Gas Interface of Nanobubbles for Therapeutic Applications. 2018 , 35, 469-494	15
2110	Complex microbial systems across different levels of description. 2018 , 15, 051002	2
2109	Heterogeneous photocatalysis and its potential applications in water and wastewater treatment: a review. 2018 , 29, 342001	244
2108	Cost Effective, Green Synthesis of Copper Oxide Nanoparticles Using Fruit Extract of Syzygium alternifolium (Wt.) Walp., Characterization and Evaluation of Antiviral Activity. 2018 , 29, 743-755	41
2107	Onward and upward: Optimizing motor performance. 2018 , 60, 107-114	24
2106	Tribonucleation: A New Mechanism for Generating the Soda Geyser. 2018 , 95, 1345-1349	3

2105	Nash Equilibrium-Based Asymptotic Stability Analysis of Multi-Group Asymmetric Evolutionary Games in Typical Scenario of Electricity Market. 2018 , 6, 32064-32086	33
2104	Boat noise in an estuarine soundscape - A potential risk on the acoustic communication and reproduction of soniferous fish in the May River, South Carolina. 2018 , 133, 246-260	17
2103	A multi-band switchable antenna for Wi-Fi, 3G Advanced, WiMAX, and WLAN wireless applications. 2018 , 10, 991-997	15
2102	Antibacterial effectiveness meets improved mechanical properties: Manuka honey/gellan gum composite hydrogels for cartilage repair. 2018 , 198, 462-472	40
2101	Synthesis of non-toxic, biocompatible, and colloidal stable silver nanoparticle using egg-white protein as capping and reducing agents for sustainable antibacterial application 2018 , 8, 23213-23229	34
2100	Meeting report - INDEPTH kick-off meeting. 2018 , 131,	4
2099	The Untapped Pharmacopeic Potential of Helminths. 2018, 34, 828-842	26
2098	Actinoplanes deserti sp. nov., isolated from a desert soil sample. 2018 , 111, 2303-2310	5
2097	Effects of nanoplastics on Mytilus galloprovincialis after individual and combined exposure with carbamazepine. 2018 , 643, 775-784	173
2096	Metabolic mechanisms underpinning vegetative bud dormancy release and shoot development in sweet cherry. 2018 , 155, 1-11	22
2095	Graphene-Incorporated Biopolymeric Mixed-Matrix Membrane for Enhanced CO Separation by Regulating the Support Pore Filling. 2018 , 10, 27810-27820	26
2094	Effect of triclosan-coated sutures on surgical site infections in pilonidal disease: prospective randomized study. 2018 , 33, 1445-1452	7
2093	HSP70 as a Biomarker: an Excellent Tool in Environmental Contamination Analysis Review. 2018 , 229, 1	10
2092	Silicon transcriptionally regulates sulfur and ABA metabolism and delays leaf senescence in barley under combined sulfur deficiency and osmotic stress. 2018 , 155, 394-410	32
2091	Up-regulated RxLR effector genes of Plasmopara viticola in synchronized host-free stages and infected leaves of hosts with different susceptibility. 2018 , 122, 1125-1133	6
2090	Nonlinear dynamics of solitary and optically injected two-element laser arrays with four different waveguide structures: a numerical study. <i>Optics Express</i> , 2018 , 26, 4751-4765	9
2089	Mapping bifurcation structure and parameter dependence in quantum dot spin-VCSELs. <i>Optics Express</i> , 2018 , 26, 14636-14649	12
2088	Multimodal 3D DenseNet for IDH Genotype Prediction in Gliomas. 2018 , 9,	64

2087	Shale Kerogen: Hydraulic Fracturing Fluid Interactions and Contaminant Release. 2018, 32, 8966-8977	26
2086	Wing twisting by elastic instability: A purely passive approach. 2018 , 206, 750-761	2
2085	One pot reflux synthesis of reduced graphene oxide decorated with silver/cobalt oxide: A novel nano composite material for high capacitance applications. 2018 , 44, 20524-20530	16
2084	Application of nuclear techniques to environmental plastics research. 2018 , 192, 368-375	21
2083	Trinity of Three-Dimensional (3D) Scaffold, Vibration, and 3D Printing on Cell Culture Application: A Systematic Review and Indicating Future Direction. 2018 , 5,	25
2082	Synergism of nitrogen and reduced graphene in the electrocatalytic behavior of resorcinol - Formaldehyde based carbon aerogels. 2018 , 139, 872-879	20
2081	Liquid Biopsy in Oral Cancer. 2018 , 19,	44
2080	Structural and functional characterization of a novel lipolytic enzyme from a Brazilian Cerrado soil metagenomic library. 2018 , 40, 1395-1406	6
2079	Functional changes in reef systems in warmer seas: Asymmetrical effects of altered grazing by a widespread crustacean mesograzer. 2018 , 644, 976-981	2
2078	MM-PBSA and per-residue decomposition energy studies on 7-Phenyl-imidazoquinolin-4(5H)-one derivatives: Identification of crucial site points at microsomal prostaglandin E synthase-1 (mPGES-1) active site. 2018 , 119, 352-359	17
2077	An environmental DNA sampling method for aye-ayes from their feeding traces. 2018 , 8, 9229-9240	13
2076	Comparative analysis of humoral immune responses and pathologies of BALB/c and C57BL/6 wildtype mice experimentally infected with a highly virulent Rodentibacter pneumotropicus (Pasteurella pneumotropica) strain. 2018 , 18, 45	22
2075	High CO2 Under Nutrient Fertilization Increases Primary Production and Biomass in Subtropical Phytoplankton Communities: A Mesocosm Approach. 2018 , 5,	12
2074	The Role of Dissolved Oxygen Levels on Human Mesenchymal Stem Cell Culture Success, Regulatory Compliance, and Therapeutic Potential. 2018 , 27, 1303-1321	14
2073	Cognitive Bias in Zoo Animals: An Optimistic Outlook for Welfare Assessment. 2018, 8,	15
2072	Review of Parameter Determination for Thermal Modeling of Lithium Ion Batteries. 2018 , 4, 20	19
2071	Centuries-Old DNA from an Extinct Population of Aesculapian Snake (Zamenis longissimus) Offers New Phylogeographic Insight. 2018 , 10, 14	4
2070	An Abstraction-Refinement Methodologyfor Reasoning about Network Games 2018, 9, 39	1

2069	The Present and Future of Whole Genome Sequencing (WGS) and Whole Metagenome Sequencing (WMS) for Surveillance of Antimicrobial Resistant Microorganisms and Antimicrobial Resistance Genes across the Food Chain. 2018 , 9,	59
2068	Characterization of sickness behavior in zebrafish. 2018 , 73, 596-602	23
2067	Modelling Hydrodynamic Impacts of Sea-Level Rise on Wave-Dominated Australian Estuaries with Differing Geomorphology. 2018 , 6, 66	11
2066	Spared CA1 pyramidal neuron function and hippocampal performance following antisense knockdown of microRNA-134. 2018 , 59, 1518-1526	12
2065	Impact of an InxGa1⊠As Capping Layer in Impeding Indium Desorption from Vertically Coupled InAs/GaAs Quantum Dot Interfaces. 2018 , 1, 4317-4331	8
2064	Microwave Assisted Hydrothermal Carbonization and Solid State Postmodification of Carbonized Polypropylene. 2018 , 6, 11105-11114	23
2063	A Hearty Dose of Noncoding RNAs: The Imprinted Locus in Cardiac Development and Disease. 2018 , 5,	15
2062	High performance hybrid supercapacitors with LiNi1/3Mn1/3Co1/3O2/activated carbon cathode and activated carbon anode. 2018 , 43, 15365-15369	8
2061	Na1.4 DI-S4 periodic paralysis mutation R222W enhances inactivation and promotes leak current to attenuate action potentials and depolarize muscle fibers. <i>Scientific Reports</i> , 2018 , 8, 10372	9
2060	The oligosaccharides 6'-sialyllactose, 2'-fucosyllactose or galactooligosaccharides do not directly modulate human dendritic cell differentiation or maturation. 2018 , 13, e0200356	10
2059	Exploring the physiological information of Sun-induced chlorophyll fluorescence through radiative transfer model inversion. 2018 , 215, 97-108	26
2058	Optically-Monitored Nanopore Fabrication Using a Focused Laser Beam. <i>Scientific Reports</i> , 2018 , 8, 9765 _{4.9}	37
2057	Effect of the combination of Cu and CdTe plasmas on the structural and optical properties of CdTe:Cu thin films deposited by laser ablation. 2018 , 87, 7-12	5
2056	Successful treatment of hepatic gas gangrene by open drainage: A case report and review of the Japanese literature. 2018 , 49, 121-125	2
2055	Controlling the properties of radiation-synthesized thermoresponsive oligoether methacrylate hydrogels by varying the monomer side-chain length; self-composite network containing crystalline phase. 2018 , 150, 275-288	10
2054	Representation of Multidecadal Sahel Rainfall Variability in 20th Century Reanalyses. <i>Scientific Reports</i> , 2018 , 8, 10937	11
2053	Thermal spikes from the urban heat island increase mortality and alter physiology of lizard embryos. 2018 , 221,	34
2052	Performance Enhancement of Al2O3/H-Diamond MOSFETs Utilizing Vacuum Annealing and V2O5 as a Surface Electron Acceptor. 2018 , 39, 1354-1357	14

2051	Understanding and Designing the Strategies for the Microbe-Mediated Remediation of Environmental Contaminants Using Omics Approaches. 2018 , 9, 1132		144
2050	Juvenile survival, competing risks, and spatial variation in mortality risk of a marine apex predator. 2018 , 55, 2888-2897		19
2049	Engineering thermoresponsive phase separated vesicles formed emulsion phase transfer as a content-release platform. 2018 , 9, 4851-4858		24
2048	Highly Efficient Optical Beam Steering Using an In-Fiber Diffraction Grating for Full Duplex Indoor Optical Wireless Communication. 2018 , 36, 4618-4625		30
2047	A quick test of cognitive speed in older adults with Alzheimer's disease and mild cognitive impairment: A preliminary behavioral and brain imaging study. 2018 , 280, 30-38		4
2046	The functional role of sodium taurocholate cotransporting polypeptide NTCP in the life cycle of hepatitis B, C and D viruses. 2018 , 75, 3895-3905		11
2045	Hybrid cell reactor system from Escherichia coli protoplast cells and arrayed lipid bilayer chamber device. <i>Scientific Reports</i> , 2018 , 8, 11757	4.9	5
2044	Multi-residue analysis of chiral and achiral trace organic contaminants in soil by accelerated solvent extraction and enantioselective liquid chromatography tandem-mass spectrometry. 2018 , 1572, 62-71		19
2043	Development and Validation of the Computerised Adaptive Beat Alignment Test (CA-BAT). <i>Scientific Reports</i> , 2018 , 8, 12395	4.9	15
2042	Weak proactive cognitive/motor brain control accounts for poor children's behavioral performance in speeded discrimination tasks. 2018 , 138, 211-222		6
2041	Hydrodynamics in a shallow seasonally low-inflow estuary following eelgrass collapse. 2018 , 213, 160-17	75	5
2040	Lack of Galectin-3 Disrupts Thymus Homeostasis in Association to Increase of Local and Systemic Glucocorticoid Levels and Steroidogenic Machinery. 2018 , 9, 365		7
2039	Dynamic process connectivity explains ecohydrologic responses to rainfall pulses and drought. 2018 , 115, E8604-E8613		21
2038	Genetic Analysis of a Commercial Egg Laying Line Challenged With Newcastle Disease Virus. 2018 , 9, 326		14
2037	Facile synthesis of carbon-coated layered double hydroxide and its comparative characterisation with Zn-Al LDH: application on crystal violet and malachite green dye adsorption-isotherm, kinetics and Box-Behnken design. <i>Environmental Science and Pollution Research</i> , 2018 , 25, 30236-30254	5.1	42
2036	Assessing modern river sediment discharge to the ocean using satellite gravimetry. 2018 , 9, 3384		26
2035	Breaking the frontiers of cosmetology with antimicrobial peptides. 2018 , 36, 2019-2031		15
2034	Increasing beta-amyloid deposition in cognitively healthy aging predicts nonlinear change in BOLD modulation to difficulty. 2018 , 183, 142-149		6

2033	Genotype-specific response of winter wheat (Triticum aestivum L.) to irrigation and inoculation with ACC deaminase bacteria. 2018 , 8, 1-7	7
2032	Applications of tumor chip technology. 2018 , 18, 2893-2912	58
2031	Development of robust, fast and efficient QRS complex detector: a methodological review. 2018 , 41, 581-600	21
2030	Duty-cycle characterisation of large-format automotive lithium ion pouch cells for high performance vehicle applications. 2018 , 19, 170-184	6
2029	A synthesis of ecological and evolutionary determinants of bat diversity across spatial scales. 2018 , 18, 18	21
2028	New40Ar/39Ar dating of the Antrim Plateau Volcanics, Australia: clarifying an age for the eruptive phase of the Kalkarindji continental flood basalt province. 2018 , 175, 974-985	4
2027	Transcriptome Sequencing Approaches to Elucidate Host-Microbe Interactions in Opportunistic Human Fungal Pathogens. 2019 , 422, 193-235	5
2026	A new analysis approach based on Haralick texture features for the characterization of microstructure on the example of low-alloy steels. 2018 , 144, 584-596	23
2025	Photoacoustic tomography of intact human prostates and vascular texture analysis identify prostate cancer biopsy targets. 2018 , 11, 46-55	11
2024	Past climate changes and strong oceanographic barriers structured low-latitude genetic relics for the golden kelp Laminaria ochroleuca. 2018 , 45, 2326-2336	26
2023	Simultaneous determination of the size and concentration of AgNPs in water samples by UV-vis spectrophotometry and chemometrics tools. 2018 , 188, 393-403	16
2022	MicroRNAs and the neural crest: From induction to differentiation. 2018 , 154, 98-106	14
2021	Distinguishing skin cancer cells and normal cells using electrical impedance spectroscopy. 2018 , 823, 531-536	24
2020	Layer-by-layer self-assembly of ternary MoS2-rGO@PPyNTs nanocomposites for high performance supercapacitor electrode. 2018 , 243, 75-89	24
2019	Spatial Wavelet-Based Coherence and Coupling in EEG Signals With Eye Open and Closed During Resting State. 2018 , 6, 37003-37022	11
2018	Nano boron nitride modified reactive powder concrete. 2018 , 179, 186-197	21
2017	Human health risk assessment data of trace elements concentration in tap water-Abeokuta South, Nigeria. 2018 , 18, 1416-1426	5
2016	Optimal Control of an Endoreversible Solar Power Plant. 2018 , 43, 255-271	19

Epithelial-to-mesenchymal transition of A549 lung cancer cells exposed to electronic cigarettes. 2015 2018 , 122, 224-233		25
Green synthesis of platinum nanoparticles using Saudi Dates extract and their usage on the cancer cell treatment. <i>Arabian Journal of Chemistry</i> , 2019 , 12, 330-349	5.9	89
Hepcidin Mediates Transcriptional Changes in Ferroportin mRNA in Differentiated Neuronal-Like PC12 Cells Subjected to Iron Challenge. 2019 , 56, 2362-2374		3
Real-Time Crawling Wave Sonoelastography for Human Muscle Characterization: Initial Results. 2019 , 66, 563-571		7
2011 Perylene-embedded electrospun PS fibers for white light generation. 2019 , 160, 501-508		18
2010 Radiation effects on Drosophila suzukii (Diptera: Drosophilidae) reproductive behaviour. 2019 , 143, 88-	-94	14
Variability of winter haze over the Beijing-Tianjin-Hebei region tied to wind speed in the lower troposphere and particulate sources. 2019 , 215, 1-11		31
Interstitial fluid flow under the microscope: is it a future drug target for high grade brain tumours such as glioblastoma?. 2019 ,		2
2007 Reconciling Color Vision Models With Midget Ganglion Cell Receptive Fields. 2019 , 13, 865		13
2006 Pilonidal sinus disease¶86 years since Mayo. 2019 , 41, 94-95		
Graphene nanoplatelets: A promising corrosion inhibitor and toughening inclusion in plasma sprayed cerium oxide coating. 2019 , 809, 151819		9
Systems biology studies in Pseudomonas aeruginosa PA01 to understand their role in biofilm formation and multidrug efflux pumps. 2019 , 136, 103668		21
Brain functional connectivity in individuals with callosotomy and agenesis of the corpus callosum: A systematic review. 2019 , 105, 231-248		18
2002 The Evolving Neural Tissue Engineering Landscape of India 2019 , 2, 5446-5459		2
The association between frailty and MRI features of cerebral small vessel disease. <i>Scientific Reports</i> , 2001 , 9, 11343	4.9	19
	<u> </u>	12
2000 GR Dimerization and the Impact of GR Dimerization on GR Protein Stability and Half-Life. 2019 , 10, 169	3	
Strategy Shift Toward Lower Spatial Frequencies in the Recognition of Dynamic Facial Expressions of Basic Emotions: When It Moves It Is Different. 2019 , 10, 1563	٥	3

1997	Microplastics in the environment: A critical review of current understanding and identification of future research needs. 2019 , 254, 113011	190
1996	Depression biomarkers using non-invasive EEG: A review. 2019 , 105, 83-93	55
1995	The effect of maxillary-mandibular advancement surgery on two-dimensional cephalometric analysis, polysomnographic and patient-reported outcomes in 32 patients with sleep disordered breathing: A retrospective cohort study. 2019 , 5, 100112	1
1994	A water-resilient carbon nanotube based strain sensor for monitoring structural integrity. 2019 , 7, 19996-2000	0 5 2
1993	Synthesis temperature and NaOH concentration dependences of microstructure and magnetic properties of MnNi-Fe2O4 nanoparticles. 2019 , 546, 042041	
1992	Persulphide-responsive transcriptional regulation and metabolism in bacteria. 2020 , 167, 125-132	3
1991	The CaMKII inhibitor KN93-calmodulin interaction and implications for calmodulin tuning of Na1.5 and RyR2 function. 2019 , 82, 102063	17
1990	Understanding soil biodiversity using two orthogonal 1000km transects across New South Wales, Australia. 2019 , 354, 113860	5
1989	Revisiting the overlap between autistic and schizotypal traits in the non-clinical population using meta-analysis and network analysis. 2019 , 212, 6-14	15
1988	Influence of the Aliphatic Side Chain on the Near Atmospheric Pressure Plasma Polymerization of 2-Alkyl-2-oxazolines for Biomedical Applications. 2019 , 11, 31356-31366	12
1987	Local Overheating Explains the Rate Enhancement of Xylose Dehydration under Microwave Heating. 2019 , 7, 14273-14279	11
1986	Microalgal Enzymes with Biotechnological Applications. 2019 , 17,	30
1985	Modelling the spatio-temporal bycatch dynamics in an estuarine small-scale shrimp trawl fishery. 2019 , 219, 105336	3
1984	Fabrication of Eco-Friendly Solid-State Symmetric Ultracapacitor Device Based on Co-Doped PANI/GO Composite. 2019 , 11,	21
1983	Green Corrosion Inhibitors. 2019,	3
1982	In vivo surveillance and elimination of teratoma-forming human embryonic stem cells with monoclonal antibody 2448 targeting annexin A2. 2019 , 116, 2996-3005	10
1981	Role of Beta-blockers in Cardiovascular Disease in 2019. 2019 , 72, 844-852	8
1980	Factors Affecting Microalgae Production for Biofuels and the Potentials of Chemometric Methods in Assessing and Optimizing Productivity. 2019 , 8,	24

1979	More data on in vitro assessment of comparative and combined toxicity of metal oxide nanoparticles. 2019 , 133, 110753	11
1978	Lutein: A potential antibiofilm and antiquorum sensing molecule from green microalga Chlorella pyrenoidosa. 2019 , 135, 103658	14
1977	Ionic Liquid-Derived Co3O4-N/S-Doped Carbon Catalysts for the Enhanced Water Oxidation. 2019 , 7, 14889-14898	13
1976	Quantifying multiple crystallite orientations and crystal heterogeneities in complex thin film materials. 2019 , 21, 5707-5720	10
1975	Copper nanoparticles incorporated porous carbon nanofibers as a freestanding binder-free electrode for symmetric supercapacitor with enhanced electrochemical performance. 2019 , 6, 105005	11
1974	Multi-connection load compensation and load information calculation for an upper-limb exoskeleton based on a six-axis force/torque sensor. 2019 , 16, 172988141986318	2
1973	Examining the predictive accuracy of metabolomics for small-for-gestational-age babies: a systematic review. 2019 , 9, e031238	11
1972	Dysregulated Irritability as a Window on Young Children's Psychiatric Risk: Transdiagnostic Effects via the Family Check-Up. 2019 , 31, 1887-1899	11
1971	Superior Memory Reduces 8-year Risk of Mild Cognitive Impairment and Dementia But Not Amyloid Associated Cognitive Decline in Older Adults. 2019 , 34, 585-598	11
1970	Nonpoint source pollution. 2019 , 91, 1114-1128	8
1970 1969	Nonpoint source pollution. 2019 , 91, 1114-1128 Optical Cavities for Optical Atomic Clocks, Atom Interferometry and Gravitational-Wave Detection. 2019 ,	1
1969	Optical Cavities for Optical Atomic Clocks, Atom Interferometry and Gravitational-Wave Detection.	
1969	Optical Cavities for Optical Atomic Clocks, Atom Interferometry and Gravitational-Wave Detection. 2019,	1
1969 1968	Optical Cavities for Optical Atomic Clocks, Atom Interferometry and Gravitational-Wave Detection. 2019, Introduction to Optical Cavities, Atomic Clocks, Cold Atoms and Gravitational Waves. 2019, 1-25	1
1969 1968 1967	Optical Cavities for Optical Atomic Clocks, Atom Interferometry and Gravitational-Wave Detection. 2019, Introduction to Optical Cavities, Atomic Clocks, Cold Atoms and Gravitational Waves. 2019, 1-25 Interstitial-Free Bake Hardening Realized by Epsilon Martensite Reverse Transformation. 2019, 50, 3985-3991 Amyloid cross-seeding raises new dimensions to understanding of amyloidogenesis mechanism.	9
1969 1968 1967 1966	Optical Cavities for Optical Atomic Clocks, Atom Interferometry and Gravitational-Wave Detection. 2019, Introduction to Optical Cavities, Atomic Clocks, Cold Atoms and Gravitational Waves. 2019, 1-25 Interstitial-Free Bake Hardening Realized by Epsilon Martensite Reverse Transformation. 2019, 50, 3985-3991 Amyloid cross-seeding raises new dimensions to understanding of amyloidogenesis mechanism. 2019, 56, 100937 A machine learning approach to modelling solar irradiation of urban and terrain 3D models. 2019,	9
1969 1968 1967 1966	Optical Cavities for Optical Atomic Clocks, Atom Interferometry and Gravitational-Wave Detection. 2019, Introduction to Optical Cavities, Atomic Clocks, Cold Atoms and Gravitational Waves. 2019, 1-25 Interstitial-Free Bake Hardening Realized by Epsilon Martensite Reverse Transformation. 2019, 50, 3985-3991 Amyloid cross-seeding raises new dimensions to understanding of amyloidogenesis mechanism. 2019, 56, 100937 A machine learning approach to modelling solar irradiation of urban and terrain 3D models. 2019, 78, 101387 Influence of Hydrolyzed Polyacrylamide Hydrogel Stiffness on Podocyte Morphology, Phenotype,	9 20 5

1961	Preparation of electrospun polycaprolactone nanofiber mats loaded with microalgal extracts. 2019 , 19, 691-699	3
1960	On the oxidation mechanism of refractory high entropy alloys. 2019 , 159, 108161	55
1959	Galvanic corrosion in a eutectic high entropy alloy. 2019 , 848, 113331	13
1958	Catalytic Production of Levulinic Acid (LA) from Actual Biomass. 2019 , 24,	47
1957	Seedling Characteristics of Three Oily Species before and after Root Pruning and Transplant. 2019 , 8,	2
1956	Moral rigidity as a proximate facilitator of group cohesion and combativeness. 2019 , 42, e130	O
1955	Geometric principles of second messenger dynamics in dendritic spines. <i>Scientific Reports</i> , 2019 , 9, 1167 6 .9	22
1954	Dual-band reconfigurable coding metasurfaces hybridized with vanadium dioxide for wavefront manipulation at terahertz frequencies. 2019 , 61, 2847-2853	4
1953	Acoustophoretic rapid media exchange and continuous-flow electrotransfection of primary human T cells for applications in automated cellular therapy manufacturing. 2019 , 19, 2978-2992	12
1952	Commensal Bacteria Regulate Gene Expression and Differentiation in Vertebrate Olfactory Systems Through Transcription Factor REST. 2019 , 44, 615-630	6
1951	Intrinsic tryptophan fluorescence spectroscopy reliably determines galectin-ligand interactions. Scientific Reports, 2019 , 9, 11851 4.9	31
1950	Effect of Heat Treatment on Microstructure and Mechanical Properties of Extruded Mg-4Zn-1.5Al-2Sn Alloy. 2019 , 28, 4565-4573	
1949	Enhancing Hepatitis C virus pseudoparticles infectivity through p7NS2 cellular expression. 2019 , 274, 113714	5
1948	Sexual trauma history is associated with reduced orbitofrontal network strength in substance-dependent women. 2019 , 24, 101973	4
1947	Interconnection between circadian clocks and thyroid function. 2019 , 15, 590-600	51
1946	Patrolling the vascular borders: platelets in immunity to infection and cancer. 2019 , 19, 747-760	54
1945	Designing a brain computer interface for control of an assistive robotic manipulator using steady state visually evoked potentials. 2019 , 2019, 1067-1072	4
1944	Evolutionary drivers of seasonal plumage colours: colour change by moult correlates with sexual selection, predation risk and seasonality across passerines. 2019 , 22, 1838-1849	16

1943	Attenuation of Zika Virus by Passage in Human HeLa Cells. 2019 , 7,	7
1942	Grape seed flour intake decreases adiposity gain in high-fat-diet induced obese mice by activating thermogenesis. 2019 , 62, 103509	9
1941	Effect of peroxomonosulfate, peroxodisulfate and hydrogen peroxide on graphene oxide photocatalytic performances in methyl orange dye degradation. 2019 , 237, 124479	32
1940	Mapping the consequences of artificial light at night for intertidal ecosystems. 2019 , 691, 760-768	21
1939	Anthropogenic Marine Debris assessment with Unmanned Aerial Vehicle imagery and deep learning: A case study along the beaches of the Republic of Maldives. 2019 , 693, 133581	64
1938	Selective Metallization of 3D Printable Thermoplastic Polyurethanes. 2019 , 7, 104947-104955	4
1937	Investigating the construct of motor competence in middle childhood using the BOT-2 Short Form: An item response theory perspective. 2019 , 29, 1980-1987	13
1936	Prevalence of Syphilis among Pregnant Women Attending Antenatal Care Clinic, Sede Muja District, South Gondar, Northwest Ethiopia. 2019 , 2019, 1584527	6
1935	Categorising use patterns of non-marine environments by elasmobranchs and a review of their extinction risk. 2019 , 29, 689-710	11
1934	Construction of surfactant/polymer/copolymer-templated mesoporous reduced graphene oxide nanoparticles for adsorption applications. 2019 , 4, 53-59	2
1933	Reversible Adsorption of Nanoparticles at Surfactant-Laden Liquid-Liquid Interfaces. 2019 , 35, 11089-11098	12
1932	Selective Laser Melting of Duplex Stainless Steel 2205: Effect of Post-Processing Heat Treatment on Microstructure, Mechanical Properties, and Corrosion Resistance. 2019 , 12,	34
1931	The Influence of Viscoelastic Crustal Rheologies on Volcanic Ground Deformation: Insights From Models of Pressure and Volume Change. 2019 , 124, 8127-8146	17
1930	Modelling the Effects of Snail Control and Health Education in Clonorchiasis Infection in Foshan, China. 2019 , 2019, 1-14	1
1929	MOF-Derived ZnSe/N-Doped Carbon Composites for Lithium-Ion Batteries with Enhanced Capacity and Cycling Life. 2019 , 14, 237	11
1928	Applications of Deep Learning to Neuro-Imaging Techniques. 2019 , 10, 869	55
1927	A Decoy-Receptor Approach Using Nicotinic Acetylcholine Receptor Mimics Reveals Their Potential as Novel Therapeutics Against Neurotoxic Snakebite. 2019 , 10, 848	16
1926	Influence of denoising on classification results in the context of hyperspectral data: High Definition FT-IR imaging. 2019 , 1085, 39-47	11

1925	Sense of agency in continuous action is influenced by outcome feedback in one-back trials. 2019 , 199, 102897	2
1924	Fe-Mn (oxyhydr)oxides as an indicator of REY enrichment in deep-sea sediments from the central North Pacific. 2019 , 112, 103044	13
1923	Goat milk oligosaccharides: Composition, analytical methods and bioactive and nutritional properties. 2019 , 92, 152-161	16
1922	Building a synthetic mechanosensitive signaling pathway in compartmentalized artificial cells. 2019 , 116, 16711-16716	58
1921	Ultrasensitive THz Refractive Index Sensor Based on a Controllable Perfect MTM Absorber. 2019 , 19, 10490-10497	40
1920	Creating impactful characters. 2019 , 38, 1-12	1
1919	AM Fungi and Trichoderma Interaction for Biological Control of Soilborne Plant Pathogen Fusarium oxysporum. 2019 , 95-128	3
1918	Floral traits determine pollinator visitation in Rhododendron species across an elevation gradient in the Sikkim Himalaya. 2019 , 129, 81-94	6
1917	Characterization of the cone-rod dystrophy retinal phenotype caused by novel homozygous DRAM2 mutations. 2019 , 187, 107752	3
1916	Complete mitochondrial genomes of the Spondias tuberosa Arr. Cam and Spondias mombin L. reveal highly repetitive DNA sequences. 2019 , 720, 144026	3
1915	Room-Temperature Ferromagnetism Induced by High-Pressure Hydrogenation of ZnO. 2019 , 123, 19851-198	61 8
1914	Capsaicin and Piperine as Functional Excipients for Improved Drug Delivery across Nasal Epithelial Models. 2019 , 85, 1114-1123	5
1913	Health economic evaluation of current vaccination strategies and new vaccines against tuberculosis: a systematic review. 2019 , 18, 897-911	4
1912	Reliability of ultrasound strain elastography in the assessment of the quadriceps and patellar tendon in healthy adults. 2019 , 27, 252-261	10
1911	Conversion of Chitin to Defined Chitosan Oligomers: Current Status and Future Prospects. 2019 , 17,	58
1910	CRISPR/Cas9-mediated gfp gene inactivation in Arabidopsis suspension cells. 2019 , 46, 5735-5743	5
1909	Evaluating causal associations between chronotype and fatty acids and between fatty acids and type 2 diabetes: A Mendelian randomization study. 2019 , 29, 1176-1184	4
1908	Drift frequency of kilometric radio burst type III with solar wind speed and density. 2019 , 1152, 012032	

1907	Is TRMM product good proxy for gauge precipitation over peat land area of the South Sumatera?. 2019 , 1282, 012021	4
1906	D-Amphetamine Exposure Differentially Disrupts Signaling Across Ontogeny in the Zebrafish. 2019 , 1, 85-104	O
1905	Comparison of dictionary learning methods for reverberation suppression in photoacoustic microscopy: Invited presentation. 2019 ,	
1904	Bioenergy from biofuel residues and waste. 2019 , 91, 1199-1204	7
1903	Polymeric chains and petrolic imaginaries: world literature, plastic, and negative value. 2019 , 23, 179-193	Ο
1902	Recent advances in plasmid-based tools for establishing novel microbial chassis. 2019, 37, 107433	13
1901	Cross state-dependent memory retrieval between morphine and norharmane in the mouse dorsal hippocampus. 2019 , 153, 24-29	2
1900	Precise DNA Concentration Measurements with Nanopores by Controlled Counting. 2019 , 91, 12228-12237	21
1899	Insight by Cryo-TEM into the growth and crystallization processes of calcium phosphate nanoparticles in aqueous medium. 2019 , 237, 121862	4
1898	Insights into Computational Drug Repurposing for Neurodegenerative Disease. 2019 , 40, 565-576	32
1897	Realization of Bidirectional, Bandwidth-Enhanced Metamaterial Absorber for Microwave Applications. <i>Scientific Reports</i> , 2019 , 9, 10058	9
1896	S-shaped microfiber based diaphragm supported optical microphone. 2019 , 1, 025005	7
1895	Comparative genomics reveals complex natural product biosynthesis capacities and carbon metabolism across host-associated and free-living Aquimarina (Bacteroidetes, Flavobacteriaceae) species. 2019 , 21, 4002-4019	10
1894	RAFTSG: an efficient and versatile clustering software to analyses in large protein datasets. 2019 , 20, 392	1
1893	Dissemination of Multidrug-Resistant Commensal in Feedlot Lambs in Southeastern Brazil. 2019 , 10, 1394	5
1892	Liquid Biopsy for the Detection of Resistance Mechanisms in NSCLC: Comparison of Different Blood Biomarkers. 2019 , 8,	18
1891	Soil Metagenomics: Unculturable Microbial Diversity and Its Function. 2019 , 355-362	13
1890	Differences in bifunctionality of ZnO and ZrO2 in Cu/ZnO/ZrO2/Al2O3 catalysts in hydrogenation of carbon oxides for methanol synthesis. 2019 , 258, 117971	25

1889	Neural responses to electrical stimulation in 2D and 3D in vitro environments. 2019 , 152, 265-284	15
1888	NO/cGMP/PKG activation protects Drosophila cells subjected to hypoxic stress. 2019 , 223, 106-114	5
1887	Elevated aerosol layer over South Asia worsens the Indian droughts. <i>Scientific Reports</i> , 2019 , 9, 10268 4.9	15
1886	Direct observation of confinement-induced diffusophoresis. 2019 , 30, 41LT01	Ο
1885	Folic acid and cyanocobalamin effects on the expression of genes involved in DNA methylation of the oyster Crassostrea gigas. 2019 , 50, 1903-1911	1
1884	Inter-specific differences in invader and native fish functional responses illustrate neutral effects on prey but superior invader competitive ability. 2019 , 64, 1655-1663	13
1883	Inactive Sulfide Ecosystems in the Deep Sea: A Review. 2019 , 6,	19
1882	Between Science and Art: Thin Sound Absorbers Inspired by Slavic Ornaments. 2019 , 6,	2
1881	Preparation, characterization and cost analysis of activated biochar and hydrochar derived from agricultural waste: a comparative study. 2019 , 1, 1	15
1880	Influences of watershed characteristics on long-term annual and intra-annual water balances over India. 2019 , 577, 123970	17
1879	Quantification of location-dependence in a large-scale additively manufactured build through experiments and micromechanical modeling. 2019 , 7, 100397	8
1878	Complex Transmission Patterns and Age-Related Dynamics of a Selfish mtDNA Deletion. 2019 , 59, 983-993	3
1877	Plant Proteins and Processes Targeted by Parasitic Nematode Effectors. 2019 , 10, 970	31
1876	Selective laser melting processing of 316L stainless steel: effect of microstructural differences along building direction on corrosion behavior. 2019 , 104, 2669-2679	13
1875	Rapid evaporative ionization mass spectrometry coupled with an electrosurgical knife for the rapid identification of Mediterranean Sea species. 2019 , 411, 6603-6614	8
1874	Endoplasmic reticulum stress: A master regulator of metabolic syndrome. 2019 , 860, 172553	39
1873	Exploring the synergistic interactions of TiO2, rGO, and g-C3N4 catalyst admixtures in a polystyrene nanocomposite photocatalytic film for wastewater treatment: Unary, binary and ternary systems. 2019 , 7, 103246	6
1872	Sustainable hydrogen production for the greener environment by quantum dots-based efficient photocatalysts: A review. 2019 , 248, 109246	80

1871	Density functional theory model for carbon dot surfaces and their interaction with silver nanoparticles. 2019 , 114, 113640	8
1870	Papel de los bloqueadores beta en la enfermedad cardiovascular en 2019. 2019 , 72, 844-852	9
1869	Well-Ordered Monolayer Growth of Crown-Ether Ring Molecules on Cu(111) in Ultra-High Vacuum: An STM, UPS, and DFT Study. 2019 , 123, 18939-18950	5
1868	Colorimetric and Near-Absolute Polarization-Insensitive Refractive-Index Sensing in All-Dielectric Guided-Mode Resonance Based Metasurface. 2019 , 123, 19125-19134	19
1867	Ge nanoparticles in SiO for near infrared photodetectors with high performance. <i>Scientific Reports</i> , 2019 , 9, 10286	14
1866	Investigation into the Potential of Lachancea fermentati Strain KBI 12.1 for Low Alcohol Beer Brewing. 2019 , 77, 157-169	13
1865	Frontiers in positron emission tomography imaging of the vulnerable atherosclerotic plaque. 2019 , 115, 1952-1962	12
1864	Early life microbial exposure shapes subsequent animal health. 2019 , 99, 661-677	3
1863	Root diversity in sesame (Sesamum indicum L.): insights into the morphological, anatomical and gene expression profiles. 2019 , 250, 1461-1474	10
1862	Stability of Selected Hydrogen Bonded Semiconductors in Organic Electronic Devices. 2019 , 31, 6315-6346	33
1861	Recent advances in the use of TiO2 nanotube powder in biological, environmental, and energy applications. 2019 , 1, 2801-2816	49
1860	A Novel HIF Inhibitor Halofuginone Prevents Neurodegeneration in a Murine Model of Retinal Ischemia-Reperfusion. 2019 , 20,	17
1859	Artificial Intelligence-Based Classification of Multiple Gastrointestinal Diseases Using Endoscopy Videos for Clinical Diagnosis. 2019 , 8,	26
1858	Stable Deuterium Labeling of Histidine-Rich Lysine-Based Dendrimers. 2019 , 24,	13
1857	Synthesis of a polydopamaine nanoparticle/bacterial cellulose composite for use as a biocompatible matrix for laccase immobilization. 2019 , 26, 8337-8349	7
1856	Horses prefer to solicit a person who previously observed a food-hiding process to access this food: A possible indication of attentional state attribution. 2019 , 166, 103906	7
1855	Perylene Bisimide Dyes with up to Five Independently Introduced Substituents: Controlling the Functionalization Pattern and Photophysical Properties Using Regiospecific Bay Substitution. 2019 , 84, 9532-9547	16
1854	Single Silicon Vacancy Centers in 10 nm Diamonds for Quantum Information Applications. 2019 , 2, 4765-4772	12

1853	Auditory findings associated with Zika virus infection: an integrative review. 2019 , 85, 642-663		11
1852	Spin transport in antiferromagnetic insulators: progress and challenges. 2019 , 11,		25
1851	Adapt or die-Response of large herbivores to environmental changes in Europe during the Holocene. 2019 , 25, 2915-2930		17
1850	Recent Trends to Study the Functional Analysis of Mycorrhizosphere. 2019 , 181-190		6
1849	Electrospun Mesoporous Mnl/[email´protected] Nanofibers for High-Performance Asymmetric Supercapacitor Devices with High Stability. 2019 , 7, 13471-13480		46
1848	Intra-articularly injected mesenchymal stem cells promote cartilage regeneration, but do not permanently engraft in distant organs. <i>Scientific Reports</i> , 2019 , 9, 10153	4.9	35
1847	Polymer/glass hybrid DC-MZI thermal optical switch for 3D-integrated chips 2019 , 9, 10651-10656		2
1846	Close Kin Proximity in Yellowfin Tuna (Thunnus albacares) as a Driver of Population Genetic Structure in the Tropical Western and Central Pacific Ocean. 2019 , 6,		6
1845	Landslide-Induced Damage Probability Estimation Coupling InSAR and Field Survey Data by Fragility Curves. 2019 , 11, 1486		22
1844	Are traded forest tree seeds a potential source of nonnative pests?. 2019 , 29, e01971		18
1843	Timing the Brain to Time the Mind: Critical Contributions of Time-Resolved Neuroimaging for Temporal Cognition. 2019 , 1-50		О
1842	Deep learning derived tumor infiltration maps for personalized target definition in Glioblastoma radiotherapy. 2019 , 138, 166-172		17
1841	Prospective environmental risk assessment of nanocellulose for Europe. 2019 , 6, 2520-2531		11
1840	Proteases in Pemphigoid Diseases. 2019 , 10, 1454		9
1839	Frontline Science: Abnormalities in the gut mucosa of non-obese diabetic mice precede the onset of type 1 diabetes. 2019 , 106, 513-529		25
1838	A DNA based visual and colorimetric aggregation assay for the early growth factor receptor (EGFR) mutation by using unmodified gold nanoparticles. 2019 , 186, 546		13
1837	Department of Earth Sciences, University of Florence. 2019 , 16, 1809-1813		1
1836	Surface and bulk phase analysis of the tribolayer of nanocrystalline diamond films sliding against steel balls. 2019 , 97, 107472		10

1835	Blue lemon@quaternary graphene oxide open frameworks: As a novel nanostructure for performance enhancement of thin film nanocomposite forward osmosis membrane. 2019 , 148, 451-459	15
1834	A revised experimental protocol for implementing the actinometry method with the Reineckell salt. 2019 , 382, 111934	5
1833	Structure and dynamics of Becretase with presenilin 2 compared to presenilin 1 2019 , 9, 20901-20916	12
1832	Big data in pharmacogenomics: current applications, perspectives and pitfalls. 2019 , 20, 609-620	4
1831	Relationships between Cytokine Levels and Disease Parameters during the Development of a Collagen-induced Arthritis Model in Cynomolgus Macaques (). 2019 , 69, 228-239	2
1830	Changing landscape of optical imaging in skeletal metastases. 2019 , 17, 100249	5
1829	Towards understanding partial adaptation to the subterranean habitat in the European cave spider, Meta menardi: An ecocytological approach. <i>Scientific Reports</i> , 2019 , 9, 9121	6
1828	Assessing radiomic feature robustness to interpolation in F-FDG PET imaging. <i>Scientific Reports</i> , 2019 , 9, 9649	26
1827	Auditory Stream Segregation Can Be Modeled by Neural Competition in Cochlear Implant Listeners. 2019 , 13, 42	2
1826	Economical production of androstenedione and 9thydroxyandrostenedione using untreated cane molasses by recombinant mycobacteria. 2019 , 290, 121750	10
1825	Biodegradable nanocomposite Fe-Ag load-bearing scaffolds for bone healing. 2019 , 98, 246-254	6
1824	Physical and physiological changes in phenotypes of nance [Byrsonima crassifolia (L.) H.B.K.] with different harvest maturity. 2019 , 256, 108620	4
1823	Recovery of scandium from Canadian bauxite residue utilizing acid baking followed by water leaching. 2019 , 95, 549-559	37
1822	Simply Extending the Mass Range in Electron Transfer Higher Energy Collisional Dissociation Increases Confidence in N-Glycopeptide Identification. 2019 , 91, 10401-10406	25
1821	Separated Schmidt modes in the angular spectrum of biphotons. 2019 , 16, 085207	0
1820	Epigenetic Regulation at the Interplay Between Gut Microbiota and Host Metabolism. 2019 , 10, 638	71
1819	Cytoplasmic conductivity as a marker for bioprocess monitoring: Study of Chinese hamster ovary cells under nutrient deprivation and reintroduction. 2019 , 116, 2896-2905	5
1818	Current advances in bone tissue engineering concerning ceramic and bioglass scaffolds: A review. 2019 , 45, 21051-21061	61

1817	Bioinspired, Multidisciplinary, Iterative Catalyst Design Creates the Highest Performance Peroxidase Mimics and the Field of Sustainable Ultradilute Oxidation Catalysis (SUDOC). 2019 , 9, 7023-7037	20
1816	Synthetic Flavonoids as Novel Modulators of Platelet Function and Thrombosis. 2019 , 20,	8
1815	Extremeness of recent drought events in Switzerland: dependence on variable and return period choice. 2019 ,	
1814	Biodegradation of lignin of Bambusa nutans by the isolate Inonotus pachyphloeus JP-1. 2019 , 2, 125-133	1
1813	Analysis of drugprotein interaction in bio-inspired microwells. 2019 , 1, 1	4
1812	Green synthesis of silver nanoparticles using Combretum erythrophyllum leaves and its antibacterial activities. 2019 , 31, 100191	59
1811	Brine ions impacts on water-oil dynamic interfacial properties considering asphaltene and maltene constituents. 2019 , 579, 123665	14
1810	Exercise physiology: exercise hyperpnea. 2019 , 10, 166-172	3
1809	Transforming agricultural land use through marginal gains in the food system. 2019 , 57, 101932	14
1808	Synthesis, characterization and catalytic activity of supported vanadium Schiff base complex as a magnetically recoverable nanocatalyst in epoxidation of alkenes and oxidation of sulfides. 2019 , 897, 200-206	23
1807	Comparative analyses of chloroplast genomes among three Firmiana species: Identification of mutational hotspots and phylogenetic relationship with other species of Malvaceae. 2019 , 19, 100199	36
1806	Biomonitoring of mycotoxin exposure using urinary biomarker approaches: a review. 2019 , 1-21	11
1805	Evaluation of rice grain yield and yield components of Nona Bokra chromosome segment substitution lines with the genetic background of Koshihikari, in a saline paddy field. 2019 , 11, plz040	2
1804	Meta-analysis of GWA studies provides new insights on the genetic architecture of skin pigmentation in recently admixed populations. 2019 , 20, 59	17
1803	Genetic Analyses of Tanzanian Local Chicken Ecotypes Challenged with Newcastle Disease Virus. 2019 , 10,	8
1802	Is brain connectome research the future frontier for subjective cognitive decline? A systematic review. 2019 , 130, 1762-1780	13
1801	Gut microbiome and serum metabolome analyses identify molecular biomarkers and altered glutamate metabolism in fibromyalgia. 2019 , 46, 499-511	49
1800	Prolonged nearwork affects the ciliary muscle morphology. 2019 , 186, 107741	3

1799	Biomass enhancement and bioconversion of brown marine microalgal lipid using heterogeneous catalysts mediated transesterification from biowaste derived biochar and bionanoparticle. 2019 , 255, 115789	21
1798	Early-life social environment alters juvenile behavior and neuroendocrine function in a highly social cichlid fish. 2019 , 115, 104552	10
1797	Engineered nanomaterials in the context of global element cycles. 2019 , 6, 2697-2711	38
1796	I'm Sensing in the Rain. 2019 ,	16
1795	Quantifying sediment mass redistribution from joint time-lapse gravimetry and photogrammetry surveys. 2019 ,	
1794	CRISPR/Cas9-Mediated Genetic Engineering of Hybridomas for Creation of Antibodies that Allow for Site-Specific Conjugation. 2019 , 2033, 81-93	1
1793	The Functional Role of Critical Dynamics in Neural Systems. 2019 ,	5
1792	A Broad Family of Carbon Nanomaterials: Classification, Properties, Synthesis, and Emerging Applications. 2019 , 451-490	1
1791	Weak Acid-Base Interactions of Histidine and Cysteine Affect the Charge States, Tertiary Structure, and Zn(II)-Binding of Heptapeptides. 2019 , 30, 2068-2081	7
1790	Terminologia Histologica 10 years on: some disputable terms in need of discussion and recent developments. 2019 , 226, 16-22	3
1789	DNA repair and neurological disease: From molecular understanding to the development of diagnostics and model organisms. 2019 , 81, 102669	16
1788	Investigating the accumulation and translocation of titanium dioxide nanoparticles with different surface modifications in static and dynamic human placental transfer models. 2019 , 142, 488-497	23
1787	Unraveling the mechanism of peptidoglycan amidation by the bifunctional enzyme complex GatD/MurT: A comparative structural approach. 2019 , 309, 151334	1
1786	Widespread activation of awake mouse cortex by electrical stimulation. 2019 , 2019, 1113-1117	O
1785	Changes in the Ileal, but Not Fecal, Microbiome in Response to Increased Dietary Protein Level and Enterotoxigenic Exposure in Pigs. 2019 , 85,	15
1784	A comparative analysis of the optoelectronic performance of conventional and inverted design organic photodetectors. 2019 , 95, 109273	9
1783	Searching for the optimal tDCS target for motor rehabilitation. 2019 , 16, 90	17
1782	Scene semantics involuntarily guide attention during visual search. 2019 , 26, 1683-1689	22

1781	Bone marrow macrophage M2 polarization and adipose-derived stem cells osteogenic differentiation synergistically promote rehabilitation of bone damage. 2019 , 120, 19891-19901	12
1780	Hippocampal CA1 and cortical interictal oscillations in the pilocarpine model of epilepsy. 2019 , 1722, 146351	4
1779	The Association between Prefrontal Cortex Activity and Turning Behavior in People with and without Freezing of Gait. 2019 , 416, 168-176	15
1778	Electrically Compact SRR-Loaded Metamaterial Inspired Quad Band Antenna for Bluetooth/WiFi/WLAN/WiMAX System. 2019 , 8, 790	18
1777	Diabetic Retinopathy, lncRNAs, and Inflammation: A Dynamic, Interconnected Network. 2019 , 8,	25
1776	Defects in Trabecular Development Contribute to Left Ventricular Noncompaction. 2019 , 40, 1331-1338	10
1775	Advancing our understanding of the connectivity, evolution and management of marine lobsters through genetics. 2019 , 29, 669-687	4
1774	Electrochemistry and morphology of graphite negative electrodes containing silicon as capacity-enhancing electrode additive. 2019 , 320, 134602	9
1773	Profile and content of sialylated oligosaccharides in donkey milk at early lactation. 2019 , 115, 108437	11
1772	Nonmonotonic Plasticity: How Memory Retrieval Drives Learning. 2019 , 23, 726-742	51
1771	Biobased Ketal D iester Additives Derived from Levulinic Acid: Synthesis and Effect on the Thermal Stability and Thermo-Mechanical Properties of Poly(vinyl chloride). 2019 , 7, 13920-13931	16
1770	Effects of oxytocin-family peptides and substance P on locomotor activity and filial preferences in visually naMe chicks. 2019 , 50, 3674-3687	8
1769	Horizontal and vertical self-paced saccades as a diagnostic marker of traumatic brain injury. 2019 , 4, CNC60	15
1768	Nitrogen-utilization efficiency during early deficiency after a luxury consumption is improved by sustaining nitrate reductase activity and photosynthesis in cotton plants. 2019 , 443, 185-198	2
1767	Neurodevelopmental and Metabolomic Responses from Prenatal Coexposure to Perfluorooctanesulfonate (PFOS) and Methylmercury (MeHg) in Sprague-Dawley Rats. 2019 , 32, 1656-1669	9
1766	Strategies for Membrane Protein Analysis by Mass Spectrometry. 2019 , 1140, 289-298	2
1765	Multi-endpoint toxicological assessment of polystyrene nano- and microparticles in different biological models in vitro. 2019 , 61, 104610	76
1764	MerMAIDs: a family of metagenomically discovered marine anion-conducting and intensely desensitizing channelrhodopsins. 2019 , 10, 3315	33

1763	A system for site-specific integration of transgenes in mammalian cells. 2019 , 14, e0219842		11
1762	Impact of ROS Generated by Chemical, Physical, and Plasma Techniques on Cancer Attenuation. 2019 , 11,		67
1761	Characterization of Phase I and Glucuronide Phase II Metabolites of 17 Mycotoxins Using Liquid Chromatography-High-Resolution Mass Spectrometry. 2019 , 11,		9
1760	Improved methodologies for Earth system modelling of atmospheric soluble iron and observation comparisons using the Mechanism of Intermediate complexity for Modelling Iron (MIMI v.1.0). 2019		
1759	Beetle and maize yield response to plant residue application and manual weeding under two tillage systems in northern Zimbabwe. <i>Applied Soil Ecology</i> , 2019 , 144, 139-146	5	2
1758	Oligosaccharide-marker approach for qualitative and quantitative analysis of specific polysaccharide in herb formula by ultra-high-performance liquid chromatography-quadrupole-time-of-flight mass spectrometry: Dendrobium officinale, a case		11
1757	Voltammetric determination of iron(III) using sputtered platinum thin film. 2019 , 320, 134607		6
1756	Inter- and intra-lineage genetic diversity of wild-type Zika viruses reveals both common and distinctive nucleotide variants and clusters of genomic diversity. 2019 , 8, 1126-1138		10
1755	Reflections on glass. 2019 , 19, 26		7
1754	Distinct temporal mechanisms modulate numerosity perception. 2019 , 19, 19		4
1754 1753	Distinct temporal mechanisms modulate numerosity perception. 2019 , 19, 19 Visual plasticity and exercise revisited: No evidence for a "cycling lane". 2019 , 19, 21		7
1753	Visual plasticity and exercise revisited: No evidence for a "cycling lane". 2019 , 19, 21 The bulb retouchers in the Levant: New insights into Middle Palaeolithic retouching techniques and		7
1753 1752	Visual plasticity and exercise revisited: No evidence for a "cycling lane". 2019 , 19, 21 The bulb retouchers in the Levant: New insights into Middle Palaeolithic retouching techniques and mobile tool-kit composition. 2019 , 14, e0218859		7
1753 1752 1751	Visual plasticity and exercise revisited: No evidence for a "cycling lane". 2019 , 19, 21 The bulb retouchers in the Levant: New insights into Middle Palaeolithic retouching techniques and mobile tool-kit composition. 2019 , 14, e0218859 The influence of referent type and familiarity on word-referent mapping. 2019 , 14, e0219552 Habitual sugar intake and cognitive impairment among multi-ethnic Malaysian older adults. 2019 ,		7 7 0
1753 1752 1751 1750	Visual plasticity and exercise revisited: No evidence for a "cycling lane". 2019, 19, 21 The bulb retouchers in the Levant: New insights into Middle Palaeolithic retouching techniques and mobile tool-kit composition. 2019, 14, e0218859 The influence of referent type and familiarity on word-referent mapping. 2019, 14, e0219552 Habitual sugar intake and cognitive impairment among multi-ethnic Malaysian older adults. 2019, 14, 1331-1342 Epidemic IncX3 plasmids spreading carbapenemase genes in the United Arab Emirates and		7 7 0
1753 1752 1751 1750 1749	Visual plasticity and exercise revisited: No evidence for a "cycling lane". 2019, 19, 21 The bulb retouchers in the Levant: New insights into Middle Palaeolithic retouching techniques and mobile tool-kit composition. 2019, 14, e0218859 The influence of referent type and familiarity on word-referent mapping. 2019, 14, e0219552 Habitual sugar intake and cognitive impairment among multi-ethnic Malaysian older adults. 2019, 14, 1331-1342 Epidemic IncX3 plasmids spreading carbapenemase genes in the United Arab Emirates and worldwide. 2019, 12, 1729-1742 Charcoal Fine Residues Effects on Soil Organic Matter Humic Substances, Composition, and		7 7 0 16 28

1745	Effects of Chestnut Tannin Extract, Vescalagin and Gallic Acid on the Dimethyl Acetals Profile and Microbial Community Composition in Rumen Liquor: An In Vitro Study. 2019 , 7,	11
1744	Comparison of Cloud Properties from Himawari-8 and FengYun-4A Geostationary Satellite Radiometers with MODIS Cloud Retrievals. 2019 , 11, 1703	26
1743	Genome Analysis of A Novel South African Cydia pomonella granulovirus (CpGV-SA) with Resistance-Breaking Potential. 2019 , 11,	3
1742	Classification of iron oxide aerosols by a single particle soot photometer using supervised machine learning. 2019 , 12, 3885-3906	6
1741	Oxytocin and pair compatibility in adult male rhesus macaques (Macaca mulatta). 2019 , 81, e23031	1
1740	Proteoglycan degradation mimics static compression by altering the natural gradients in fibrillar organisation in cartilage. 2019 , 97, 437-450	14
1739	Influence of background oxygen pressure and post - deposition annealing on the structural, morphological, optical and luminescence properties of laser ablated SrWO4 thin films. 2019 , 103, 104615	4
1738	Nano-bio interactions: a neutrophil-centric view. 2019 , 10, 569	41
1737	CoreBhell assembly of Co3O4@NiO-ZnO nanoarrays as battery-type electrodes for high-performance supercapatteries. 2019 , 6, 2481-2487	21
1736	Evaluation of non-invasive toxicological analysis of nano-polystyrene in relative in vivo conditions to D. magna. 2019 , 6, 2832-2849	4
1735	Visual Imprinting in Birds: Behavior, Models, and Neural Mechanisms. 2019 , 10, 658	20
1734	Proteolytic Rafts for Improving Intraparenchymal Migration of Minimally Invasively Administered Hydrogel-Embedded Stem Cells. 2019 , 20,	2
1733	Preliminary Review of Sources, Fate, Analytical Challenges and Regulatory Status of Emerging Organic Contaminants in Aquatic Environments in Selected African Countries. 2019 , 2, 573-585	9
1732	Performance and competitive displacement of Bemisia tabaci MEAM1 and MED cryptic species on different host plants. 2019 , 124, 104860	14
1731	Monocytes contribute to DNA sensing through the TBK1 signaling pathway in type 1 diabetes patients. 2019 , 105, 102294	12
1730	Isolation of intact bacteria from blood by selective cell lysis in a microfluidic porous silica monolith. 2019 , 5, 30	9
1729	Drones and convolutional neural networks facilitate automated and accurate cetacean species identification and photogrammetry. 2019 , 10, 1490-1500	35
1728	Dietary supplementation of garlic (Allium sativum) modulates gut microbiota and health status of tilapia (Oreochromis niloticus) against Streptococcus iniae infection. 2019 , 50, 2107-2116	20

1727	Vector competence of Aedes aegypti for different strains of Zika virus in Argentina. 2019 , 13, e0007433	9
1726	Role of Endometrial Autophagy in Physiological and Pathophysiological Processes. 2019 , 10, 3459-3471	13
1725	Coastal habitats and their importance for the diversity of benthic communities: A species- and trait-based approach. 2019 , 226, 106272	21
1724	The Interaction of Person-Affect-Cognition-Execution (I-PACE) model for addictive behaviors: Update, generalization to addictive behaviors beyond internet-use disorders, and specification of the process character of addictive behaviors. 2019 , 104, 1-10	347
1723	Lysine-based dendrimer with double arginine residues 2019 , 9, 18018-18026	16
1722	Impact of pre-treatment on the stability of color, flavor, and microbial profile of coriander paste. 2019 , 43, e14091	2
1721	Reference genes for real-time RT-PCR expression studies in an Antarctic Pseudomonas exposed to different temperature conditions. 2019 , 23, 625-633	7
1720	Anthocyanins and flavonols from the flowers of Amherstia nobilis endemic to Myanmar. 2019 , 86, 103906	5
1719	Characteristics and evolution of the late Permian Bource-to-sink system of the Beisantai area in the eastern Junggar Basin, NW China. 2019 , 181, 103907	2
1718	Chromosomal Locations and Interactions of Four Loci Associated With Seed Coat Color in Watermelon. 2019 , 10, 788	8
1717	Phase-dependent optical and photocatalytic performance of synthesized titanium dioxide (TiO2) nanoparticles. 2019 , 193, 163011	28
1716	Morphologically bioinspired hierarchical nylon 6,6 electrospun assembly recreating the structure and performance of tendons and ligaments. 2019 , 71, 79-90	15
1715	Through the eyes of a pathogen: light perception and signal transduction in Acinetobacter baumannii. 2019 , 18, 2363-2373	4
1714	Meta-analysis of Factors Influencing Population Differentiation in Yellowfin Tuna (Thunnus albacares). 2019 , 27, 517-532	2
1713	Enhanced Photoresponsivity of All-Inorganic (CsPbBr3) Perovskite Nanosheets Photodetector with Carbon Nanodots (CDs). 2019 , 8, 678	15
1712	Amphidinol 22, a New Cytotoxic and Antifungal Amphidinol from the Dinoflagellate. 2019 , 17,	40
1711	Application of Biodegradable and Biocompatible Nanocomposites in Electronics: Current Status and Future Directions. 2019 , 9,	52
1710	Changes in Forest Net Primary Productivity in the Yangtze River Basin and Its Relationship with Climate Change and Human Activities. 2019 , 11, 1451	11

Young adult binge drinkers have immunophenotypical disarrangements in peripheral natural killer 1709 cells. 2019, 81, 70-78 Crystal Structures and Nuclear Magnetic Resonance Studies of the Apo Form of the c-MYC:MAX 1708 14 bHLHZip Complex Reveal a Helical Basic Region in the Absence of DNA. 2019, 58, 3144-3154 Solution-based synthesis of lithium thiophosphate superionic conductors for solid-state batteries: a 1707 52 chemistry perspective. **2019**, 7, 17735-17753 Patterns, dynamics and consequences of microplastic ingestion by the temperate coral, Astrangia 1706 53 poculata. **2019**, 286, 20190726 Switch rates for orthogonally oriented kinetic-depth displays are correlated across observers. 2019, 1705 4 19.1 Bisubstrate Inhibitors of Nicotinamide -Methyltransferase (NNMT) with Enhanced Activity. 2019, 32 62, 6597-6614 Single-cell RNA-seq variant analysis for exploration of genetic heterogeneity in cancer. Scientific 1703 4.9 15 Reports, 2019, 9, 9524 Unraveling the effects of the gut microbiota composition and function on horse endurance 1702 4.9 14 physiology. Scientific Reports, 2019, 9, 9620 Tau pathology reduction with SM07883, a novel, potent, and selective oral DYRK1A inhibitor: A 1701 19 potential therapeutic for Alzheimer's disease. 2019, 18, e13000 Plant-Based Natural Product Chemistry for Integrated Pest Management of Drosophila suzukii. 13 2019, 45, 626-637 1699 Surface manipulation techniques of Roman denarii. 2019, 493, 818-828 5 High photoresponse performance of self-powered n-Cu2O/p-CuI heterojunction based UV-Visible 1698 9 photodetector. **2019**, 296, 61-69 1697 Meiotic DNA Repair in the Nucleolus Employs a Nonhomologous End-Joining Mechanism. 2019, 31, 2259-2275 23 Prevalence of depression among the elderly (60 years and above) population in India, 1997-2016: a 1696 56 systematic review and meta-analysis. 2019, 19, 832 Adaptation and sustainability of water management for rice agriculture in temperate regions: The 1695 17 Italian case-study. 2019, 30, 2033-2047 Honeycomb-like porous activated carbon for efficient copper (II) adsorption synthesized from 1694 33 natural source: Kinetic study and equilibrium isotherm analysis. 2019, 7, 103236 Forward osmosis research trends in desalination and wastewater treatment: A review of research 1693 77 trends over the past decade. 2019, 31, 100886 Evaluation of DC-MS and HiPIMS TiB2 and TaN coatings as diffusion barriers against molten 1692 aluminum: An insight into the wetting mechanism. 2019, 375, 171-181

1691	Antenatal exposure to solar radiation and learning disabilities: Population cohort study of 422,512 children. <i>Scientific Reports</i> , 2019 , 9, 9356	4.9	2	
1690	TouristsDesthetic assessment of environmental changes, linking conservation planning to sustainable tourism development. 2019 , 27, 1477-1494		15	
1689	A dynamic yet vulnerable pipeline: Integration and coordination of hydraulic traits across whole plants. 2019 , 42, 2789-2807		31	
1688	Combining Phase Advancement and Period Correction Explains Rushing during Joint Rhythmic Activities. <i>Scientific Reports</i> , 2019 , 9, 9350	4.9	7	
1687	DNA processing by the MOBH family relaxase Tral encoded within the gonococcal genetic island. 2019 , 47, 8136-8153		0	
1686	Reduced Graphene Oxide/Silicon Nanowire Heterojunction for High Sensitivity and Broadband Photodetector. 2019 , 3, 1-4		3	
1685	Chameleonfishes in Bangladesh: hipshot taxonomy, sibling species, elusive species, and limits of species delimitation (Teleostei: Badidae). 2019 , 4586, zootaxa.4586.2.7		2	
1684	A dose-dependent response to MEK inhibition determines hypoblast fate in bovine embryos. 2019 , 19, 13		11	
1683	Smoking is associated with greater pain intensity and pain-related occupational disability in Japanese workers. 2019 , 33, 523-530		1	
1682	Continental-Scale Landscape Evolution: A History of North American Topography. 2019 , 124, 2689-272	:2	13	
1681	Observed Northward Migration of Agro-Climate Zones in Europe Will Further Accelerate Under Climate Change. 2019 , 7, 1088-1101		31	
1680	CRISPR-mediated gene silencing reveals involvement of the archaeal S-layer in cell division and virus infection. 2019 , 10, 4797		22	
1679	Geochemical Evidence for the Control of Fire by Middle Palaeolithic Hominins. <i>Scientific Reports</i> , 2019 , 9, 15368	4.9	18	
1678	Effect of Nb and W on Fe2(Nb,W) laves phase in Fe-9Cr-6.5Al-Nb-W alloys. 2019 , 6, 116504		1	
1677	Multifunctional Silica-Silicone Nanocomposite with Regenerative Superhydrophobic Capabilities. 2019 , 11, 42827-42837		19	
1676	The impact of decellularization methods on extracellular matrix derived hydrogels. <i>Scientific Reports</i> , 2019 , 9, 14933	4.9	69	
1675	Coupling Multi-Angle Light Scattering to Reverse-Phase Ultra-High-Pressure Chromatography (RP-UPLC-MALS) for the characterization monoclonal antibodies. <i>Scientific Reports</i> , 2019 , 9, 14965	4.9	7	
1674	Polystyrene nanoplastics disrupt glucose metabolism and cortisol levels with a possible link to behavioural changes in larval zebrafish. 2019 , 2, 382		66	

1673	Peer pressure: evolutionary responses to biotic pressures in wine yeasts. 2019 , 19,	13
1672	Multiple-trait selection of soybean for biodiesel production in Brazil. 2019 , 140, 111721	18
1671	NAFLD and Atherosclerosis: Two Sides of the Same Dysmetabolic Coin?. 2019 , 30, 891-902	42
1670	Adsorption of Surface Active Ionic Liquids on Different Rock Types under High Salinity Conditions. Scientific Reports, 2019 , 9, 14760 4.9	29
1669	Does the addition of a supportive chatbot promote user engagement with a smoking cessation app? An experimental study. 2019 , 5, 2055207619880676	20
1668	Interleaved deep brain stimulation for dyskinesia management in Parkinson's disease. 2019 , 34, 1722-1727	11
1667	Simulated real-time dose reconstruction for moving tumors in stereotactic liver radiotherapy. 2019 , 46, 4738-4748	7
1666	Invasion success of a widespread invasive predator may be explained by a high predatory efficacy but may be influenced by pathogen infection. 2019 , 21, 3545-3560	4
1665	Memory deficits in males and females long after subchronic immune challenge. 2019 , 158, 60-72	8
1664	Pharmacological and toxicological in vitro and in vivo effect of higher doses of oxime reactivators. 2019 , 383, 114776	2
1663	Balanced cholinergic modulation of spinal locomotor circuits via M2 and M3 muscarinic receptors. Scientific Reports, 2019 , 9, 14051	8
1662	Nanoscale engineered surfaces for cooling in electronic devices. 2019 ,	1
1661	A Study of Fine-Tuning CNN Models Based on Thermal Imaging for Breast Cancer Classification. 2019 ,	16
1660	Bacterial and Fungal Diversity Inside the Medieval Building Constructed with Sandstone Plates and Lime Mortar as an Example of the Microbial Colonization of a Nutrient-Limited Extreme Environment (Wawel Royal Castle, Krakow, Poland). 2019 , 7,	5
1659	Sabotage at the Powerhouse? Unraveling the Molecular Target of 2-Isopropylbenzaldehyde Thiosemicarbazone, a Specific Inhibitor of Aflatoxin Biosynthesis and Sclerotia Development in , Using Yeast as a Model System. 2019 , 24,	4
1658	High-Temperature Stress and Photosynthesis Under Pathological Impact. 2019 , 39-64	
1657	Instruments and methods: hot-water borehole drilling at a high-elevation debris-covered glacier. 2019 , 65, 822-832	3
1656	Clinical presentation of FMD virus SAT1 infections in experimentally challenged indigenous South African goats. 2019 , 180, 15-20	4

1655	Identifying and mapping very small (<0.5 km2) mountain glaciers on coarse to high-resolution imagery. 2019 , 65, 873-888		21
1654	Predicting the affective tone of everyday dreams: A prospective study of state and trait variables. <i>Scientific Reports</i> , 2019 , 9, 14780	4.9	5
1653	A Novel Approach for the Integral Management of Water Extremes in Plain Areas. 2019 , 6, 70		2
1652	Fabricating Laser-Induced Periodic Surface Structures on Medical Grade CobaltthromeMolybdenum: Tribological, Wetting and Leaching Properties. 2019 , 7, 70		8
1651	Microphysiological systems in the evaluation of hematotoxicities during drug development. 2019 , 17, 18-22		4
1650	A novel approach to monitoring wetland dynamics using CYGNSS: Everglades case study. 2019 , 233, 11	1417	39
1649	Duplicated Vagus Nerve in Adolescence: Case Report and Review of Literature. 2019 , 131, 180-185		1
1648	Electrospun 5-chloro-8-hydroxyquinoline-Loaded Cellulose Acetate/Polyethylene Glycol Antifungal Membranes Against Esca. 2019 , 11,		8
1647	Direct detection of brown adipose tissue thermogenesis in UCP1-/- mice by hyperpolarized Xe MR thermometry. <i>Scientific Reports</i> , 2019 , 9, 14865	4.9	21
1646	Differential Susceptibility of Catheter Biomaterials to Biofilm-Associated Infections and Their Remedy by Drug-Encapsulated Eudragit RL100 Nanoparticles. 2019 , 20,		12
1645	Microencapsulation of Enteric Bacteriophages in a pH-Responsive Solid Oral Dosage Formulation Using a Scalable Membrane Emulsification Process. 2019 , 11,		28
1644	Data on draft genome sequence of sp. strain MHSD28, a bacterial endophyte isolated from. 2019 , 26, 104524		4
1643	Elastic geobarometry for anisotropic inclusions in cubic hosts. 2019 , 350-351, 105218		17
1642	Radiomics and MGMT promoter methylation for prognostication of newly diagnosed glioblastoma. <i>Scientific Reports</i> , 2019 , 9, 14435	4.9	26
1641	Methods Used for the Eradication of Staphylococcal Biofilms. 2019 , 8,		8
1640	Design of Dense Brush Conformation Bearing Gold Nanoparticles as Theranostic Agent for Cancer. 2019 , 189, 709-728		3
1639	Novel green synthesis of silver nanoparticles using clammy cherry (Cordia obliqua Willd) fruit extract and investigation on its catalytic and antimicrobial properties. 2019 , 1, 1		9
1638	Predictive coding in a multisensory path integration task: An fMRI study. 2019 , 19, 13		1

1637	Characterization and probiotic properties of from human breast milk. 2019 , 9, 398	17
1636	Superhydrophobic cotton fabrics based on ZnO nanoparticles functionalization. 2019 , 1, 1	8
1635	Amino-functionalized MIL-88B(Fe)-based porous carbon for enhanced adsorption toward ciprofloxacin pharmaceutical from aquatic solutions. 2019 , 22, 804-812	29
1634	Exploring T & B-cell epitopes and designing multi-epitope subunit vaccine targeting integration step of HIV-1 lifecycle using immunoinformatics approach. 2019 , 137, 103791	16
1633	One-carbon metabolism supplementation improves outcome after stroke in aged male MTHFR-deficient mice. 2019 , 132, 104613	5
1632	Ultrasmall Mode Volume Hyperbolic Nanocavities for Enhanced Light-Matter Interaction at the Nanoscale. 2019 , 13, 11770-11780	18
1631	Design and radiation mechanism analysis of a multi-usage ultra-high frequency radio frequency identification tag antenna. 2019 , 13, 1989-1996	2
1630	Advanced DSP for Coherent Optical Fiber Communication. 2019 , 9, 4192	15
1629	Folic Acid Antagonists: Antimicrobial and Immunomodulating Mechanisms and Applications. 2019 , 20,	43
1628	Effect of organic carbon and nutrient supplementation on the digestate-grown microalga, Parachlorella kessleri. 2019 , 294, 122232	4
1627	Laser-induced breakdown spectroscopy for food authentication. 2019 , 28, 96-103	11
1626	Structural analysis of premolar roots in Middle Pleistocene hominins from China. 2019 , 136, 102669	5
1625	Optimisation of bioimpedance measurements of neuronal activity with an ex vivo preparation of Cancer pagurus peripheral nerves. 2019 , 327, 108322	1
1624	Microstructure and chemical composition of a Sardinian bronze axe of the Iron Age from Motya (Sicily, Italy). 2019 , 158, 109957	8
1623	Amplified CO2 reduction of greenhouse gas emissions with C2CNT carbon nanotube composites. 2019 , 6, 100023	12
1622	The relationship between male social status, ejaculate and circulating testosterone concentration and female yolk androgen transfer in red junglefowl (Gallus gallus). 2019 , 116, 104580	2
1621	Antineoplastic properties of zafirlukast against hepatocellular carcinoma via activation of mitochondrial mediated apoptosis. 2019 , 109, 104489	8
1620	Facing death: How does the subterranean termite Coptotermes gestroi (Isoptera: Rhinotermitidae) deal with corpses?. 2019 , 137, 125712	2

1619	Gel electrophoresis separation and origins of light emission in fluorophores prepared from citric acid and ethylenediamine. <i>Scientific Reports</i> , 2019 , 9, 14665	9	9
1618	Nestling carcasses from colonially breeding wading birds: patterns of access and energetic relevance for a vertebrate scavenger community. <i>Scientific Reports</i> , 2019 , 9, 14512	9	2
1617	CortiWatch: watch-based cortisol tracker. 2019 , 5, FSO416		20
1616	Bacterial Metabolites Mirror Altered Gut Microbiota Composition in Patients with Parkinson's Disease. 2019 , 9, S359-S370		17
1615	How Can We Assess Positive Welfare in Ruminants?. 2019 , 9,		37
1614	Correlating nano-scale surface replication accuracy and cavity temperature in micro-injection moulding using in-line process control and high-speed thermal imaging. 2019 , 47, 367-381		20
1613	Non-reciprocal biasing for performance enhancement of the resonant fiber gyroscope with B eflector lising In-line Faraday rotators: Design, analysis and characterization. 2019 , 53, 102038		3
1612	Mechanical properties and morphology of electrospun mats made of poly (Epentadecalactone). 2019 , 1310, 012013		1
1611	An Innovation of Interaction Method Based on Force Feedback in HMD System. 2019 , 1335, 012004		
1610	One-pot synthesis of ZnS-rGO nanocomposites using single-source molecular precursor for photodegradation of methylene blue and reduction towards toxic Cr(VI) under solar light. 2019 , 6, 105536	5	10
1609	An interaction between host and microbe genotypes determines colonization success of a key bumble bee gut microbiota member. 2019 , 73, 2333-2342		5
1608	Floral organs act as environmental filters and interact with pollinators to structure the yellow monkeyflower (Mimulus guttatus) floral microbiome. 2019 , 28, 5155-5171		18
1607	Biocompatible Aloe vera and Tetracycline Hydrochloride Loaded Hybrid Nanofibrous Scaffolds for Skin Tissue Engineering. 2019 , 20,		28
1606	Influence of the First Chromophore-Forming Residue on Photobleaching and Oxidative Photoconversion of EGFP and EYFP. 2019 , 20,		5
1605	An Update on Core Jasmonate Signalling Networks, Physiological Scenarios, and Health Applications. 2019 , 387-452		6
1604	Basics of Expansion Microscopy. 2019 , 91, e67		2
1603	Predicting resilience of ecosystem functioning from co-varying species' responses to environmental change. 2019 , 9, 11775-11790		1
1602	Differentially methylated gene patterns between age-matched sarcopenic and non-sarcopenic women. 2019 , 10, 1295-1306		11

1601 Effects of pollution on marine organisms. 2019 , 91, 1229-1252		8
Visible-enhanced silver-doped PbI2 nanostructure/Si heterojunction photodetector: effect of doping concentration on photodetector parameters. 2019 , 51, 1		7
1599 Genetic and epigenetic determinants of muscle mass. 2019 , 251-272		
1598 The Gut Microbiome. 2019 , 61-98		1
1597 Cannabis prices on the dark web. 2019 , 120, 103306		6
An economic and environmental assessment of a glyphosate ban for the example of maize production. 2019 ,		5
DempsterBhafer Fusion Based on a Deep Boltzmann Machine for Blood Pressure Estimation. 20 9, 96)19,	4
Structure Based Multitargeted Molecular Docking Analysis of Selected Furanocoumarins agains Breast Cancer. <i>Scientific Reports</i> , 2019 , 9, 15743	st 4·9	40
Asian and African lineage Zika viruses show differential replication and innate immune response human dendritic cells and macrophages. <i>Scientific Reports</i> , 2019 , 9, 15710	es in 4.9	10
Association Between Renal Function and Troponin T Over Time in Stable Chronic Kidney Diseas Patients. 2019 , 8, e013091	se	17
Fungal feature tracker (FFT): A tool for quantitatively characterizing the morphology and growt filamentous fungi. 2019 , 15, e1007428	th of	10
Strong anthropogenic control of secondary organic aerosol formation from isoprene in Beijing. 2019 ,		
Hypoxia-induced HIF-1\(\text{\text{\text{H}}}\) are critical for the malignant transformation of ameloblastom via TGF-\(\text{\texi}\texi{\text{\text{\texiclex{\text{\text{\text{\text{\text{\text{\t	a	26
$_{15}88$ Collective turns in jackdaw flocks: kinematics and information transfer. 2019 , 16, 20190450		14
1587 Least-squares solutions to polynomial systems of equations with quantum annealing. 2019 , 18,	1	5
Numerical Study on Zika Epidemic Early Warning Algorithms Driven by Dynamical Network Biomarker. 2019 , 2019, 1-5		1
First Evidence of Realized Selection Response on Fillet Yield in Rainbow Trout , Using Sib Select or Based on Correlated Ultrasound Measurements. 2019 , 10, 1225	ion:	11
1584 Short-Term Free-Floating Slice Cultures from the Adult Human Brain. 2019 ,		4

1583	Impact of chronically alternating light-dark cycles on circadian clock mediated expression of cancer (glioma)-related genes in the brain. 2019 , 15, 1816-1834	7
1582	Simultaneous production of DHA and squalene from sp. grown on forest biomass hydrolysates. 2019 , 12, 255	32
1581	Assessment of gamma-rays and fast neutron beam attenuation features of Er2O3-doped B2O3InOBi2O3 glasses using XCOM and simulation codes (MCNP5 and Geant4). 2019 , 125, 1	12
1580	Enhancement of the therapeutic efficacy of praziquantel in murine Schistosomiasis mansoni using silica nanocarrier. 2019 , 118, 3519-3533	10
1579	Smart cancer nanomedicine. 2019 , 14, 1007-1017	447
1578	Stiff Composite Cylinders for Extremely Expandable Structures. <i>Scientific Reports</i> , 2019 , 9, 15955 4.9	4
1577	Reconstruction and analysis of a Kluyveromyces marxianus genome-scale metabolic model. 2019 , 20, 551	21
1576	Assessing reliability of intra-tumor heterogeneity estimates from single sample whole exome sequencing data. 2019 , 14, e0224143	9
1575	Digital Assessment of Stained Breast Tissue Images for Comprehensive Tumor and Microenvironment Analysis. 2019 , 7, 246	11
1574	Alder Distribution and Expansion Across a Tundra Hillslope: Implications for Local N Cycling. 2019 , 10, 1099	17
1573	Frequency Dependency of the Delta-E Effect and the Sensitivity of Delta-E Effect Magnetic Field Sensors. 2019 , 19,	14
1572	Prey and Venom Efficacy of Male and Female Wandering Spider, (Araneae: Ctenidae). 2019, 11,	6
1571	Native-Osteoarthritic Joint Resident Stem and Progenitor Cells for Cartilage Cell-Based Therapies: A Quantitative Comparison With Respect to Concentration and Biological Performance. 2019 , 47, 3521-3530	8
1570	Co-existence of Leclercia adecarboxylata (LSE-1) and Bradyrhizobium sp. (LSBR-3) in nodule niche for multifaceted effects and profitability in soybean production. 2019 , 35, 172	11
1569	Trends in and factors associated with the adoption of digital aids for smoking cessation and alcohol reduction: A population survey in England. 2019 , 205, 107653	6
1568	Pollutant gas and particulate material emissions in ethanol production in Brazil: social and environmental impacts. <i>Environmental Science and Pollution Research</i> , 2019 , 26, 35082-35093	2
1567	Collaborative Approaches to Archaeology Programming and the Increase of Digital Literacy Among Archaeology Students. 2019 , 5, 137-154	4
1566	Transcranial Direct Current Stimulation to Improve the Dysfunction of Descending Pain Modulatory System Related to Opioids in Chronic Non-cancer Pain: An Integrative Review of Neurobiology and Meta-Analysis. 2019 , 13, 1218	17

1565	Picosecond Laser Interference Patterning of Periodical Micro-Architectures on Metallic Molds for Hot Embossing. 2019 , 12,		13
1564	. 2019,		2
1563	Phenolic compounds increase their concentration in Carica papaya leaves under drought stress. 2019 , 41, 1		7
1562	PRODIGY: personalized prioritization of driver genes. 2020 , 36, 1831-1839		8
1561	Microhabitat use and body size drive the evolution of colour patterns in snapping shrimps (Decapoda: Alpheidae: Alpheus). 2019 ,		1
1560	Integration of Hybrid Plasmonic Au-BaTiO Metamaterial on Silicon Substrates. 2019 , 11, 45199-45206		19
1559	Neural oscillations during cognitive processes in an App knock-in mouse model of Alzheimer's disease pathology. <i>Scientific Reports</i> , 2019 , 9, 16363	4.9	8
1558	mTOR and autophagy pathways are dysregulated in murine and human models of Schaaf-Yang syndrome. <i>Scientific Reports</i> , 2019 , 9, 15935	4.9	11
1557	The microbiome of the upper respiratory tract in health and disease. 2019 , 17, 87		118
1556	Pathological pain processing in mouse models of multiple sclerosis and spinal cord injury: contribution of plasma membrane calcium ATPase 2 (PMCA2). 2019 , 16, 207		8
1555	Smoking index, lifestyle factors, and genomic instability assessed by single-cell gel electrophoresis: a cross-sectional study in subjects from Yucatan, Mexico. 2019 , 11, 150		1
1554	The autophagic inducer and inhibitor display different activities on the meiotic and developmental competencies of porcine oocytes derived from small and medium follicles. 2019 , 65, 527-532		5
1553	PRMT Inhibitors. 2019 , 159-196		1
1552	Perspective on the Future Role of Aptamers in Analytical Chemistry. 2019 , 91, 15335-15344		47
1551	Influence of Hydrogen Bonding between Ions of Like Charge on the Ionic Liquid Interfacial Structure at a Mica Surface. 2019 , 10, 7368-7373		15
1550	Freshwater mussels house a diverse mussel-associated leech assemblage. <i>Scientific Reports</i> , 2019 , 9, 16449	4.9	12
1549	Phloroglucinol Treatment Induces Transgenerational Epigenetic Inherited Resistance Against Infections and Thermal Stress in a Brine Shrimp () Model. 2019 , 10, 2745		21
1548	The characteristics of krill swarms in relation to aggregating Antarctic blue whales. <i>Scientific Reports</i> , 2019 , 9, 16487	4.9	10

1547	Latitudinal gradient of cyanobacterial diversity in tidal flats. 2019 , 14, e0224444		1
1546	A Novel LSTM Approach for Asynchronous Multivariate Time Series Prediction. 2019,		5
1545	Carbon sequestration via afforestation as a sustainable action to mitigate climate change in Western Iran. 2019 , 43, 194-202		О
1544	Complete chloroplast genomes of all six Hosta species occurring in Korea: molecular structures, comparative, and phylogenetic analyses. 2019 , 20, 833		20
1543	A Multi-Scale Temporal Feature Aggregation Convolutional Neural Network for Portfolio Management. 2019 ,		2
1542	Evolution of Structural Diversity of Triterpenoids. 2019 , 10, 1523		25
1541	Biofilm Formation by Clinical Isolates is Differentially Affected by Glucose and Sodium Chloride Supplemented Culture Media. 2019 , 8,		22
1540	Nanocomposites of ZnO for Water Remediation. 2019 , 179-233		3
1539	Anti-inflammatory activity of polyamide dendrimers bearing bile acid termini synthesized via SPAAC. 2019 , 21, 1		7
1538	High-Frequency soft magnetic properties of Fe-Si-B-P-Mo-Cu amorphous and nanocrystalline alloys. 2019 , 526, 119702		13
1537	Baby-SPIME: A dynamic in vitro piglet model mimicking gut microbiota during the weaning process. 2019 , 167, 105735		3
1536	Proneness of European Catchments to Multiyear Streamflow Droughts. 2019 , 55, 8881-8894		15
1535	In vivo fluorescence imaging of conjunctival goblet cells. Scientific Reports, 2019, 9, 15457	4.9	4
1534	Nanohydroxyapatite Reinforced Chitosan Composite Hydrogel with Tunable Mechanical and Biological Properties for Cartilage Regeneration. <i>Scientific Reports</i> , 2019 , 9, 15957	4.9	28
1533	Chicken toll-like receptors and their significance in immune response and disease resistance. 2019 , 38, 284-306		16
1532	L modulates the immune system in a multiple sclerosis mouse model. 2021 , 24, 843-849		2
1531	The rise of flexible electronics in neuroscience, from materials selection to in vitro and in vivo applications. 2019 , 4, 1664319		6
1530	Supplemental effects of dietary nucleotides on intestinal health and growth performance of newly weaned pigs. 2019 , 97, 4875-4882		21

1529	Profiling Bacterial Diversity and Potential Pathogens in Wastewater Treatment Plants Using High-Throughput Sequencing Analysis. 2019 , 7,	2	23
1528	Ultrasonic-assisted melt blending for polyvinyl alcohol/carbon dots luminescent flexible films. 2019	C)
1527	Effector mining from the Erysiphe pisi haustorial transcriptome identifies novel candidates involved in pea powdery mildew pathogenesis. 2019 , 20, 1506-1522	1	11
1526	Genome-wide analysis, transcription factor network approach and gene expression profile of GH3 genes over early somatic embryogenesis in Coffea spp. 2019 , 20, 812	8	3
1525	An Assessment of Computer-Generated Stimuli for Use in Studies of Body Size Estimation and Bias. 2019 , 10, 2390	ϵ	6
1524	SiO2@Al2O3 core-shell nanoparticles based molten salts nanofluids for thermal energy storage applications. 2019 , 26, 101033	2	20
1523	Decoupling Catalyst Dewetting, Gas Decomposition, and Surface Reactions in Carbon Nanotube Forest Growth Reveals Dependence of Density on Nucleation Temperature. 2019 , 123, 28726-28738	1	12
1522	Deep Origin of the Dome-Shaped Hyblean Plateau, Southeastern Sicily: A New Tectono-Magmatic Model. 2019 , 38, 4488-4515	5	5
1521	Genetic Markers for Species Conservation and Timber Tracking: Development of Microsatellite Primers for the Tropical African Tree Species Prioria balsamifera and Prioria oxyphylla. 2019 , 10, 1037	2	2
1520	Free-Space-Optical Quantum Key Distribution Systems: Challenges and Trends. 2019,	1	[
1519	Evidence for incentive salience sensitization as a pathway to alcohol use disorder. 2019 , 107, 897-926	2	26
1518	Behavioural plasticity and the transition to order in jackdaw flocks. 2019 , 10, 5174	2	28
1517	Solution blown polymer/biowaste derived carbon particles nanofibers: An optimization study and energy storage applications. 2019 , 26, 100962	5	5
1516	Non-Gaussian models of diffusion weighted imaging for detection and characterization of prostate cancer: a systematic review and meta-analysis. <i>Scientific Reports</i> , 2019 , 9, 16837) 7	7
1515	An unusual bird (Theropoda, Avialae) from the Early Cretaceous of Japan suggests complex evolutionary history of basal birds. 2019 , 2, 399	5	5
1514	A conserved miRNA-183 cluster regulates the innate antiviral response. 2019 , 294, 19785-19794	1	1
1513	ANISEED 2019: 4D exploration of genetic data for an extended range of tunicates. 2020 , 48, D668-D675	1	16
1512	Thymically-derived Foxp3+ regulatory T cells are the primary regulators of type 1 diabetes in the non-obese diabetic mouse model. 2019 , 14, e0217728	7	7

1511 Voltage-Gated Calciu	m Channels and ⊞ynuclein: Implications in Parkinson's Disease. 2019 , 12, 237	15
1510 A New Adaptive Imag	ge Interpolation Method to Define the Shoreline at Sub-Pixel Level. 2019 , 11, 1880	9
A Multilayer Microflu 2019 ,	idic Platform for the Conduction of Prolonged Cell-Free Gene Expression.	4
1508 Artificial Photosynthe	esis. 2019 , 271-309	2
A range-wide model of desert tortoise. 2019	of contemporary, omnidirectional connectivity for the threatened Mojave , 10, e02847	6
1506 A review of smartpho	one point-of-care adapter design. 2019 , 1, e12039	17
Plasma-activated met Pd and zeolite catalys	thane partial oxidation reaction to oxygenate platform chemicals over Fe, Mo, sts. 2019 , 43, 8085	6
	tes microglia phagocytosis and increases transient receptor potential vanilloid ssion on the plasma membrane. 2019 , 67, 2294-2311	14
Drosophila ClC-a is re neural circuits. 2019 ,	quired in glia of the stem cell niche for proper neurogenesis and wiring of 67, 2374-2398	8
	al phantom analyses for preprocessing evaluation and detection of a robust adiomics of the brain. 2019 , 46, 5116-5123	22
1501 Anaerobic digestion.	2019 , 91, 1253-1271	27
1500 Selected nucleos(t)id	e-based prescribed drugs and their multi-target activity. 2019 , 865, 172747	18
	ght-dependent proton pumps increase boundary layer pH in tropical sed mechanism to sustain calcification under ocean acidification. 2019 , 521, 151208	13
1498 Nucleic acid amplifica	ation-based HER2I655V molecular detection for breast cancer. 2019 , 5, 31-41	
1497 Biodegradability of h	ydrothermally altered deep-sea dissolved organic matter. 2019 , 217, 103706	5
Structural and function gut microbe. 2019 , 29	onal aspects of mannuronic acid-specific PL6 alginate lyase from the human 94, 17915-17930	21
1495 What Does a Horgous	s Look Like? Nonsense Words Elicit Meaningful Drawings. 2019 , 43, e12791	4
	atinine level in patient blood samples by Fourier NIR spectroscopy and in comparison with biochemical assay. 2019 , 12, 1950015	3

1493	Prediction in goal-directed action. 2019 , 19, 10		21
1492	The influence of feedstock characteristics on enzyme production in : a review on productivity, gene regulation and secretion profiles. 2019 , 12, 238		37
1491	Crosstalk Between Signaling Pathways Involved in the Regulation of Airway Smooth Muscle Cell Hyperplasia. 2019 , 10, 1148		10
1490	Half-Century Changes in LULC and Fire in Two Iberian Inner Mountain Areas. 2019 , 2, 45		2
1489	From Science to Practice: A Review of Laterality Research on Ungulate Livestock. 2019 , 11, 1157		8
1488	Nanoscopic Imaging of Human Tissue Sections via Physical and Isotropic Expansion. 2019 ,		1
1487	Improved methodologies for Earth system modelling of atmospheric soluble iron and observation comparisons using the Mechanism of Intermediate complexity for Modelling Iron (MIMI v1.0). 2019 , 12, 3835-3862		18
1486	Tracing post-depositional processes and preservation of architectural materials and deposits in the semi-arid environment of southern Cyprus: A micromorphological approach. 2019 , 27, 101986		2
1485	Hydrophobically associating polymers for enhanced oil recovery [Part B: A review of modelling approach to flow in porous media. 2019 , 293, 111495		14
1484	Photonic crystal for graphene plasmons. 2019 , 10, 4780		30
1483	Bioprocessing of common pulses changed seed microstructures, and improved dipeptidyl peptidase-IV and Eglucosidase inhibitory activities. <i>Scientific Reports</i> , 2019 , 9, 15308	4.9	20
1482	Preventative effects of the partial RANKL peptide MHP1-AcN in a mouse model of imiquimod-induced psoriasis. <i>Scientific Reports</i> , 2019 , 9, 15434	4.9	3
1481	Smooth muscle contractility causes the gut to grow anisotropically. 2019 , 16, 20190484		8
1480	Off-State Operation of a Three Terminal Ionic FET for Logic-in-Memory. 2019 , 7, 1232-1238		О
1479	Topical and spatial repellent bioassays against the Australian paralysis tick, Ixodes holocyclus (Acari: Ixodidae). 2019 , 58, 866-874		3
1478	Will Entrepreneurship Promote Productivity Growth in China?. 2019 , 28, 73		
1477	Characterising extinction debt following habitat fragmentation using neutral theory. 2019 , 22, 2087-209)6	13
1476	Association between depressive symptoms and sleep neurophysiology in early adolescence. 2019 , 60, 1334-1342		11

1475	The effects of diadromy and its loss on genomic divergence: The case of amphidromous Galaxias maculatus populations. 2019 , 28, 5217-5231	21
1474	Distinct functional roles for hopanoid composition in the chemical tolerance of Zymomonas mobilis. 2019 , 112, 1564-1575	14
1473	Composition and volatility of SOA formed from oxidation of real tree emissions compared to single VOC-systems. 2019 ,	
1472	Enantioselective Fluorocyclizations Mediated by Amino-Acid-Derived Phthalazine. 2019 , 361, 5334-5339	10
1471	Female-biased gape and body-size dimorphism in the New World watersnakes (tribe: Thamnophiini) oppose predictions from Rensch's rule. 2019 , 9, 9624-9633	5
1470	Multipath mitigation in GPS receiver using Taylor integrated bidirectional least mean square algorithm. 2019 , 30, e3760	3
1469	Lipase production from mutagenic strain of KU377454 and its immobilization using Au@Ag core shells nanoparticles for application in waste cooking oil degradation. 2019 , 9, 411	6
1468	Temporal Features of Muscle Synergies in Sit-to-Stand Motion Reflect the Motor Impairment of Post-Stroke Patients. 2019 , 27, 2118-2127	21
1467	The spatial and temporal properties of attentional selectivity for saccades and reaches. 2019 , 19, 12	5
1466	Comparison of post-traumatic changes in circulating and bone marrow leukocytes between BALB/c and CD-1 mouse strains. 2019 , 14, e0222594	3
1465	Retrieval of sea ice thickness using global navigation satellite system reflected signals. 2019 , 52, 1131-1136	2
1464	An Assembly and Interfacial Templating Route to Carbon Supercapacitors with Simultaneously Tailored Meso- and Microstructures. 2019 , 11, 43509-43519	3
1463	Large Summer Contribution of Organic Biogenic Aerosols to Arctic Cloud Condensation Nuclei. 2019 , 46, 11500-11509	9
1462	Migrations and Clusters of Shallow Very Low Frequency Earthquakes in the Regions Surrounding Shear Stress Accumulation Peaks Along the Nankai Trough. 2019 , 46, 11830-11840	11
1461	Pathways of carrier recombination in Si/SiO2 nanocrystal superlattices. 2019 , 126, 163101	Ο
1460	Birefringence of nonlinearity in all-normal dispersion photonic crystal fibers. 2019 , 21, 125502	O
1459	Krill spatial distribution in the Spanish Mediterranean Sea in summer time. 2019 , 41, 491-505	3
1458	Nanostructured Core Active Fiber Based on Ytterbium Doped Phosphate Glass. 2019 , 37, 5885-5891	2

1457	Breadth of the thermal response captures individual and geographic variation in temperature-dependent sex determination. 2019 , 33, 1928-1939	14
1456	Maternal versus artificial rearing shapes the rumen microbiome having minor long-term physiological implications. 2019 , 21, 4360-4377	13
1455	Effect of walking on depression prevalence for diabetes using information communication technology: Prospective study. 2019 , 19, 1147-1152	2
1454	Role of light-intensity-dependent changes in thiol and amino acid metabolism in the adaptation of wheat to drought. 2019 , 205, 562-570	3
1453	Co-evolution of cerebral and cerebellar expansion in cetaceans. 2019 , 32, 1418-1431	5
1452	Integrating data to redescribe Euschistus taurulus Berg (Hemiptera: Pentatomidae). 2019 , 4688, zootaxa.4688	8.4.7
1451	Including Wave Diffraction in XBeach: Model Extension and Validation. 2019 , 36, 116	2
1450	One-Volt, Solution-Processed Organic Transistors with Self-Assembled Monolayer-TaO Gate Dielectrics. 2019 , 12,	12
1449	Symbiosis in Sustainable Agriculture: Can Olive Fruit Fly Bacterial Microbiome Be Useful in Pest Management?. 2019 , 7,	7
1448	Physiologic Patient Derived 3D Spheroids for Anti-neoplastic Drug Screening to Target Cancer Stem Cells. 2019 ,	4
1447	Microstructure and Texture Evolution During Thermomechanical Processing of Al0.25CoCrFeNi High-Entropy Alloy. 2019 , 50, 5433-5444	4
1446	Characterization of CsI(Tl) and LYSO(Ce) scintillator detectors by measurements and Monte Carlo simulations. 2019 , 154, 108878	6
1445	Anti-inflammatory Surface Coatings Based on Polyelectrolyte Multilayers of Heparin and Polycationic Nanoparticles of Naproxen-Bearing Polymeric Drugs. 2019 , 20, 4015-4025	18
1444	Cardiomyogenesis Modeling Using Pluripotent Stem Cells: The Role of Microenvironmental Signaling. 2019 , 7, 164	17
1443	From Green Remediation to Polymer Hybrid Fabrication with Improved Optical Band Gaps. 2019 , 20,	44
1442	Polarization Control of the Interface Ferromagnetic to Antiferromagnetic Phase Transition in Co/Pb(Zr,Ti)O. 2019 , 11, 34399-34407	4
1441	The antitoxic effects of quercetin and quercetin-conjugated iron oxide nanoparticles (QNPs) against HO-induced toxicity in PC12 cells. 2019 , 14, 6813-6830	10
1440	Composite Membranes of Poly(Etaprolactone) with Bisphosphonate-Loaded Bioactive Glasses for Potential Bone Tissue Engineering Applications. 2019 , 24,	10

1439	Pore Scale Visualization of Drainage in 3D Porous Media by Confocal Microscopy. <i>Scientific Reports</i> , 2019 , 9, 12333	.9	9
1438	Biodistribution of nanodiamonds in the body of mice using EPR spectrometry. 2019 , 13, 984-988		1
1437	2 Stages-region-based P300 Speller in BrainComputer Interface. 2019 , 65, 740-748		7
1436	Iontophoresis in lateral epicondylitis: a randomized, double-blind clinical trial. 2019 , 28, 1743-1749		6
1435	Effects of photochemical and microbiological changes in terrestrial dissolved organic matter on its chemical characteristics and phytotoxicity towards cyanobacteria. 2019 , 695, 133901		5
1434	Yields and resilience outcomes of organic, cover crop, and conventional practices in a Mediterranean climate. <i>Scientific Reports</i> , 2019 , 9, 12283	.9	14
1433	28-GHz Wireless Carrier Heterodyned From Orthogonally Polarized Tri-Color Laser Diode for Fading-Free Long-Reach MMWoF. 2019 , 37, 3388-3400		9
1432	Modelling and Simulation of a portable, size- discriminating Capacitive Particulate Matter sensor. 2019 ,		1
1431	Factors associated with black bear density and implications for management. 2019 , 83, 1527-1539		7
1430	Reflections on the crooked timber of red blood cell physiology. 2019 , 79, 102354		3
1429	Production and use of triploid zebrafish for surrogate reproduction. 2019 , 140, 33-43		11
1428	Humid Subtropical Forests Constitute a Net Methane Source: A Catchment-Scale Study. 2019 , 124, 2927-2	942	2
1427	Parameter-free image resolution estimation based on decorrelation analysis. 2019 , 16, 918-924		81
1426	Corrosion behavior of metastable AISI 321 austenitic stainless steel: Investigating the effect of grain size and prior plastic deformation on its degradation pattern in saline media. <i>Scientific Reports</i> 4, 2019 , 9, 12116	.9	21
1425	Resting-state fMRI: comparing default mode network connectivity between normal and low auditory working memory groups. 2019 , 1248, 012005		3
1424	. 2019 , 7, 96223-96231		
1423	Sulfidation Behaviour of Blast Furnace Dust at High Temperatures. 2019 , 60, 363-371		1
1422	InN Nanowires Based Near-Infrared Broadband Optical Detector. 2019 , 31, 1526-1529		6

1421	Gazing into the anthosphere: considering how microbes influence floral evolution. 2019 , 224, 1012-1020	24
1420	Understanding the Signaling Pathways Related to the Mechanism and Treatment of Diabetic Peripheral Neuropathy. 2019 , 160, 2119-2127	16
1419	Thermal illumination limits in 3D Raman microscopy: A comparison of different sample illumination strategies to obtain maximum imaging speed. 2019 , 14, e0220824	2
1418	The Use of Murine Models for Studying Mechanistic Insights of Genomic Instability in Multiple Myeloma. 2019 , 10, 740	3
1417	Prokaryotic Diversity and Community Patterns in Antarctic Continental Shelf Sponges. 2019 , 6,	26
1416	Fungal Physiology and Immunopathogenesis. 2019,	1
1415	Lassa fever: With 50 years of study, hundreds of thousands of patients and an extremely high disease burden, what have we learned?. 2019 , 37, 123-131	9
1414	Tribological and mechanical properties of diamond films synthesized with high methane concentration. 2019 , 85, 105057	6
1413	Neurobiological and behavioural responses of cleaning mutualisms to ocean warming and acidification. <i>Scientific Reports</i> , 2019 , 9, 12728	15
1412	How to optimise photosynthetic biogas upgrading: a perspective on system design and microalgae selection. 2019 , 37, 107444	34
1411	Raney Nickel 2.0: Development of a high-performance bifunctional electrocatalyst. 2019 , 322, 134687	10
1410	Integrative study of microbial community dynamics and water quality along The Apatlaco River. 2019 , 255, 113158	15
1409	Development and characterization of novel composite glycerol-plasticized films based on sodium caseinate and lipid fraction of tomato pomace by-product. 2019 , 139, 128-138	16
1408	Insights into Membrane Protein-Lipid Interactions from Free Energy Calculations. 2019 , 15, 5727-5736	33
1407	Molecular Characterization of Human Lymph Node Stromal Cells During the Earliest Phases of Rheumatoid Arthritis. 2019 , 10, 1863	11
1406	Can Herbivore Management Increase the Persistence of Indo-Pacific Coral Reefs?. 2019 , 6,	15
1405	Effect of Chronic Corticosterone Treatment on Depression-Like Behavior and Sociability in Female and Male C57BL/6N Mice. 2019 , 8,	10
1404	Genetics, Toxicity, and Distribution of Enterohemorrhagic Hemolysin. 2019 , 11,	13

1403	Intermittent-Excessive and Chronic-Moderate Ethanol Intake during Adolescence Impair Spatial Learning, Memory and Cognitive Flexibility in the Adulthood. 2019 , 418, 205-217	17
1402	Multi-Color Laser Diode Heterodyned 28-GHz Millimeter-Wave Carrier Encoded With DMT for 5G Wireless Mobile Networks. 2019 , 7, 122697-122706	11
1401	Wavelength Switchable Mode-Locked Fiber Laser With Tapered Two-Mode Fiber. 2019 , 11, 1-8	4
1400	A Dual-Output Reconfigurable Shared-Inductor Boost-Converter/Current-Mode Inductive Power Management ASIC With 750% Extended Output-Power Range, Adaptive Switching Control, and Voltage-Power Regulation. 2019 , 13, 1075-1086	8
1399	An update on advances in new developing DNA conjugation diagnostics and ultra-resolution imaging technologies: Possible applications in medical and biotechnological utilities. 2019 , 144, 111633	7
1398	Evidence for provenance change in deep sea sediments of the Bengal Fan: A 7 million year record from IODP U1444A. 2019 , 186, 104008	2
1397	LSTM-based Short-term Load Forecasting for Building Electricity Consumption. 2019,	6
1396	. 2019,	2
1395	Scalable integration of nano-, and microfluidics with hybrid two-photon lithography. 2019 , 5, 40	28
1394	A thin-film extensional flow model for biofilm expansion by sliding motility. 2019 , 475, 20190175	4
1393	Smart Biosensor for Rapid and Simultaneous Detection of Waterborne Pathogens in Tap Water. 2019 ,	1
1392	Electroseismocardiography System for Non-Invasive Human Diseases Diagnosis. 2019,	
1391	Recent advances in non-ionic surfactant vesicles (niosomes): Fabrication, characterization, pharmaceutical and cosmetic applications. 2019 , 144, 18-39	109
1390	Essential oil from Negramina (Siparuna guianensis) plants controls aphids without impairing survival and predatory abilities of non-target ladybeetles. 2019 , 255, 113153	12
1389	Epitranscriptomic systems regulate the translation of reactive oxygen species detoxifying and disease linked selenoproteins. 2019 , 143, 573-593	10
1388	Exploring the extracellular matrix in health and disease using proteomics. 2019, 63, 417-432	53
1387	The Shocking History of Procter & Gamble Rely Tampons. 2019 , 6, 222-224	
1386	3-D fluid channel location from noise tremors using matched field processing. 2019 , 219, 1550-1561	2

1385	Characterization of pepper accessions using molecular markers linked to pungency and SSR. 2019 , 37, 152-160	O
1384	Influence of Cell Type and Culture Medium on Determining Cancer Selectivity of Cold Atmospheric Plasma Treatment. 2019 , 11,	52
1383	MMP14 in Sarcoma: A Regulator of Tumor Microenvironment Communication in Connective Tissues. 2019 , 8,	30
1382	Prediction of Peptide Vascularization Inhibitory Activity in Tumor Tissue as a Possible Target for Cancer Treatment. 2019 , 21, 15	
1381	The impact of increases in South Asian anthropogenic emissions of SO₂ on sulfate loading in the upper troposphere and lower stratosphere during the monsoon season and the associated radiative impact. 2019 ,	
1380	Meeting climate targets by direct CO₂ injections: What price would the ocean have to pay?. 2019 ,	
1379	Cancer invasion regulates vascular complexity in a three-dimensional biomimetic model. 2019 , 119, 179-193	18
1378	COX-2/iNOS regulation during experimental hepatic injury and its mitigation by cloudy apple juice. 2019 , 140, 1006-1017	2
1377	More than Microtubules: The Structure and Function of the Subpellicular Array in Trypanosomatids. 2019 , 35, 760-777	13
1376	Engineering of a fungal laccase to develop a robust, versatile and highly-expressed biocatalyst for sustainable chemistry. 2019 , 21, 5374-5385	25
1375	Biocompatible chitosan-collagen-hydroxyapatite nanofibers coated with platelet-rich plasma for regenerative engineering of the rotator cuff of the shoulder 2019 , 9, 27013-27020	4
1374	Synthesis and thermal stability of ZrO@SiO core-shell submicron particles 2019 , 9, 26902-26914	6
1373	Thermal integrity modelling using finite-element, finite-volume, and algebraic topological methods. 2019 ,	1
1372	Understanding membrane remodelling initiated by photosensitized lipid oxidation. 2019 , 254, 106263	23
1371	The cardiovascular effects of electronic cigarettes: A systematic review of experimental studies. 2019 , 127, 105770	27
1370	Graphene Oxide Nanocarriers for Fluorescent Sensing of Calcium Ion Accumulation and Direct Assessment of Ion-Induced Enzymatic Activities in Cells. 2019 , 2, 5594-5603	3
1369	Bifurcation analysis of the dynamics of interacting subnetworks of a spiking network. <i>Scientific Reports</i> , 2019 , 9, 11397	4
1368	Effect of Arc Pressure on the Digging Process in Variable Polarity Plasma Arc Welding of A5052P Aluminum Alloy. 2019 , 12,	7

1367	Biomaterials in Orthopaedics and Bone Regeneration. 2019,		4
1366	OSM-induced CD44 contributes to breast cancer metastatic potential through cell detachment but not epithelial-mesenchymal transition. 2019 , 11, 7721-7737		4
1365	Functions of subventricular zone neural precursor cells in stroke recovery. 2019 , 376, 112209		4
1364	Defect-induced enhanced dissociative adsorption, optoelectronic properties and interfacial contact in Ce doped TiO2: Solar photocatalytic degradation of Rhodamine B. 2019 , 45, 22253-22263		16
1363	Lactate and pyruvate promote oxidative stress resistance through hormetic ROS signaling. 2019 , 10, 653		66
1362	The large repertoire of conifer NLR resistance genes includes drought responsive and highly diversified RNLs. <i>Scientific Reports</i> , 2019 , 9, 11614	4.9	24
1361	Eight new freshwater mussels (Unionidae) from tropical Asia. <i>Scientific Reports</i> , 2019 , 9, 12053	4.9	9
1360	Design Features in Multiple Generations of Electronic Cigarette Atomizers. 2019, 16,		38
1359	Development of an UPLC-MS/MS Method for the Analysis of Mycotoxins in Rumen Fluid with and without Maize Silage Emphasizes the Importance of Using Matrix-Matched Calibration. 2019 , 11,		9
1358	"Three-in-One" SERS Adhesive Tape for Rapid Sampling, Release, and Detection of Wound Infectious Pathogens. 2019 , 11, 36399-36408		16
1357	Nanobubble Liposome Complexes for Diagnostic Imaging and Ultrasound-Triggered Drug Delivery in Cancers: A Theranostic Approach. 2019 , 4, 15567-15580		43
1356	The use of qPCR in human Chagas disease: a systematic review. 2019 , 19, 875-894		4
1355	The Role of Attachment in Poly-Drug Use Disorder: An Overview of the Literature, Recent Findings and Clinical Implications. 2019 , 10, 579		11
1354	Structural and biochemical insights into an engineered high-redox potential laccase overproduced in Aspergillus. 2019 , 141, 855-867		9
1353	Individual variation in inter-ocular suppression and sensory eye dominance. 2019 , 163, 33-41		2
1352	Analyzing the Nanogranularity of Focused-Electron-Beam-Induced-Deposited Materials by Electron Tomography. 2019 , 2, 5356-5359		5
1351	Occurrence mechanism of lacustrine shale oil in the Paleogene Shahejie Formation of Jiyang Depression, Bohai Bay Basin, China. 2019 , 46, 833-846		31
1350	Complete Additively Manufactured (3D-Printed) Electrochemical Sensing Platform. 2019 , 91, 12844-128	51	85

1349	characterized by reduced virulence but enhanced proteolytic activity and biofilm formation. Scientific Reports, 2019 , 9, 13479	4.9	13	
1348	Dry period heat stress induces microstructural changes in the lactating mammary gland. 2019 , 14, e022	2120	18	
1347	Comparative analysis of the fecal microbiota from different species of domesticated and wild suids. <i>Scientific Reports</i> , 2019 , 9, 13616	4.9	12	
1346	Inhomogeneous strain and recrystallisation of a shot-peened Inconel 625 alloy after annealing. 2019 , 35, 1856-1863		5	
1345	Social Exclusion Shifts Personal Network Scope. 2019 , 10, 1619		4	
1344	Alumina-Doped Zirconia Submicro-Particles: Synthesis, Thermal Stability, and Microstructural Characterization. 2019 , 12,		10	
1343	Modeling cell-cell interactions in the brain using cerebral organoids. 2019 , 1724, 146458		7	
1342	Rattling Transport of Lithium Ion in the Cavities of Model Solid Electrolyte Interphase. 2019 , 123, 25015	5-2502	4 0	
1341	Role of protein conformation and weak interactions on Egliadin liquid-liquid phase separation. <i>Scientific Reports</i> , 2019 , 9, 13391	4.9	14	
1340	Hydrogel-Based Organic Subdural Electrode with High Conformability to Brain Surface. <i>Scientific Reports</i> , 2019 , 9, 13379	4.9	23	
1339	Mixing brain cerebrosides with brain ceramides, cholesterol and phospholipids. <i>Scientific Reports</i> , 2019 , 9, 13326	4.9	7	
1338	Bioactive Molecules in Plant Defense. 2019,		2	
1337	Cell-Autonomous and Non-cell-Autonomous Pathogenic Mechanisms in Huntington's Disease: Insights from In Vitro and In Vivo Models. 2019 , 16, 957-978		18	
1336	Assignment of unanchored scaffolds in genome of Brassica napus by RNA-seq analysis in a complete set of Brassica rapa-Brassica oleracea monosomic addition lines. 2019 , 18, 1541-1546		1	
1335	Rates of age- and amyloid		12	
1334	Neglected orbitozygomaticomaxillary fractures with complications: A case report. 2019 , 62, 35-39			
1333	Molecular approach indicates consumption of jellyfish by commercially important fish species in a coastal Mediterranean lagoon. 2019 , 152, 104787		5	
1332	Printing bone in a gel: using nanocomposite bioink to print functionalised bone scaffolds. 2019 , 4, 1000	28	31	

1331	Establishment of a stable sampling method to assay mercaptoalbumin/non-mercaptoalbumin and reference ranges. 2019 , 17, e00132		3
1330	Energy Effectiveness in Additive Manufacturing using Design for Property. 2019 , 80, 132-137		5
1329	Phytoliths, parasites, fibers, and feathers from dental calculus and sediment from Iron Age Luistari cemetery, Finland. 2019 , 222, 105888		6
1328	Refining of the egusi locus in watermelon using KASP assays. 2019 , 257, 108665		3
1327	Methodology of Kppen-Geiger-Photovoltaic climate classification and implications to worldwide mapping of PV system performance. 2019 , 191, 672-685		58
1326	Morphodynamics of sandy beaches under the influence of storm sequences: Current research status and future needs. 2019 , 12, 221-234		18
1325	The effects of mechanical constriction on the operation of sulfide based solid-state batteries. 2019 , 7, 23604-23627		32
1324	Hybrid Genome Assembly of a Neotropical Mutualistic Ant. 2019 , 11, 2306-2311		7
1323	Non-Coding RNAs in Pediatric Solid Tumors. 2019 , 10, 798		10
1322	Sulfonated graphene oxide incorporated thin film nanocomposite nanofiltration membrane to enhance permeation and antifouling properties. 2019 , 470, 114125		66
1321	Total synthesis of PGF2\(\text{\textbf{h}}\) nd 6,15-diketo-PGF1\(\text{\textbf{h}}\) nd formal synthesis of 6-keto-PGF1\(\text{\textbf{h}}\) ia three-component coupling. 2019 , 75, 130593		3
1320	Bisphenol A Analogues in Food and Their Hormonal and Obesogenic Effects: A Review. 2019 , 11,		58
1319	Combined effects of biochar and MgO expansive additive on the autogenous shrinkage, internal relative humidity and compressive strength of cement pastes. 2019 , 229, 116877		34
1318	Temperature and clone-dependent effects of microplastics on immunity and life history in Daphnia magna. 2019 , 255, 113178		20
1317	Nucleation dynamics of single crystal WS from droplet precursors uncovered by in-situ monitoring. <i>Scientific Reports</i> , 2019 , 9, 12958	4.9	4
1316	Unsupervised machine learning using an imaging mass spectrometry dataset automatically reassembles grey and white matter. <i>Scientific Reports</i> , 2019 , 9, 13213	4.9	7
1315	Chronic high fat feeding paradoxically attenuates cerebral capillary dysfunction and neurovascular inflammation in Senescence-Accelerated-Murine-Prone Strain 8 mice. 2021 , 24, 635-643		2
1314	Heart defibrillation: relationship between pacing threshold and defibrillation probability. 2019 , 18, 96		

1313	Endophyte Bacillus velezensis Isolated from Citrus spp. Controls Streptomycin-Resistant Xanthomonas citri subsp. citri That Causes Citrus Bacterial Canker. 2019 , 9, 470	18
1312	Effect of confinement on the adsorption behavior of inorganic and organic ions at aqueous-cyclohexane interfaces: a molecular dynamics study. <i>Physical Chemistry Chemical Physics</i> , 3.6 2019 , 21, 20770-20781	2
1311	Using evolved gas analysis Imass spectrometry to characterize adsorption on a nanoparticle surface. 2019 , 1, 2740-2747	3
1310	Does Blocking Facial Feedback Via Botulinum Toxin Injections Decrease Depression? A Critical Review and Meta-Analysis. 2019 , 11, 294-309	5
1309	New records and their associated DNA barcodes of the butterfly family Hesperiidae in Tibet, China. 2019 , 4674, zootaxa.4674.4.2	
1308	Functional aspects, phenotypic heterogeneity, and tissue immune response of macrophages in infectious diseases. 2019 , 12, 2589-2611	9
1307	Biological and demographic parameters of Tegolophus brunneus (Acari: Eriophyidae) in citrus. 2019 , 79, 35-46	1
1306	Insecticidal efficacy of three benzoate derivatives against Aphis gossypii and its predator Chrysoperla carnea. 2019 , 184, 109653	13
1305	Design of high shielding effectiveness magnetic shield for fiber optic gyroscope. 2019 , 198, 163160	1
1304	Thymoquinone (2-Isoprpyl-5-methyl-1, 4-benzoquinone) as a chemopreventive/anticancer agent: Chemistry and biological effects. 2019 , 27, 1113-1126	52
1303	PDR-like ABC systems in pathogenic fungi. 2019 , 170, 417-425	14
1302	A continuum-based multiphase DNS method for studying the Brownian dynamics of soot particles in a rarefied gas. 2019 , 210, 115229	4
1301	Are river protected areas sufficient for fish conservation? Implications from large-scale hydroacoustic surveys in the middle reach of the Yangtze River. 2019 , 19, 42	3
1300	Inclusion of enclosed hydration effects in the binding free energy estimation of dopamine D3 receptor complexes. 2019 , 14, e0222902	6
1299	Ensemble Machine Learning for Estimating Fetal Weight at Varying Gestational Age. 2019 , 33, 9522-9527	11
1298	Emerging medical applications based on non-ionizing electromagnetic fields from 0 Hz to 10 THz. 2019 , 12, 347-368	20
1297	Optical Molecular Imaging of Inflammatory Cells in Interventional Medicine-An Emerging Strategy. 2019 , 9, 882	5
1296	Tapered vs. Uniform Tube-Load Modeling of Blood Pressure Wave Propagation in Human Aorta. 2019 , 10, 974	2

1295	Challenges in Exosome Isolation and Analysis in Health and Disease. 2019 , 20,	146
1294	The Psychology of Micro-Targeted Election Campaigns. 2019,	4
1293	Vitellogenin and vitellogenin-like gene expression patterns in relation to caste and task in the ant Formica fusca. 2019 , 66, 519-531	10
1292	Characteristics and atomization behavior of Ti-6Al-4V powder produced by plasma rotating electrode process. 2019 , 30, 2330-2337	21
1291	Modeling and environmental evaluation of a system linking a fishmeal facility with a microalgae plant within a circular economy context. 2019 , 20, 356-364	3
1290	Environmental DNA Metabarcoding: A Promising Tool for Ballast Water Monitoring. 2019 , 53, 11849-11859	12
1289	Bacterial Candidates for Colonization and Degradation of Marine Plastic Debris. 2019 , 53, 11636-11643	89
1288	Fabrication of TiC-TiB2 composite ceramic tool and its cutting performance in turning austenitic stainless steel. 2019 , 118, 473-483	
1287	Quantitative Proteomic and Network Analysis of Differentially Expressed Proteins in PBMC of Friedreich's Ataxia (FRDA) Patients. 2019 , 13, 1054	7
1286	Kinetic Study on Alloying Element Transfer During an Electroslag Remelting Process. 2019 , 50, 3088-3102	6
1285	25 years of criticality in neuroscience - established results, open controversies, novel concepts. 2019 , 58, 105-111	36
1284	Effects of Model, Method of Collection, and Topography on Chemical Elements and Metals in the Aerosol of Tank-Style Electronic Cigarettes. <i>Scientific Reports</i> , 2019 , 9, 13969	16
1283	Genotoxic Strains Encoding Colibactin, Cytolethal Distending Toxin, and Cytotoxic Necrotizing Factor in Laboratory Rats. 2019 , 69, 103-113	6
1282	Inhibition of nSMase2 Reduces the Transfer of Oligomeric	20
1281	Leptin Promotes Expression of EMT-Related Transcription Factors and Invasion in a Src and FAK-Dependent Pathway in MCF10A Mammary Epithelial Cells. 2019 , 8,	20
1280	Verification of the Translocon and its Localization in the Chloroplast Membrane in Diatoms. 2019 , 20,	2
1279	Climate change impacts on renewable energy generation. A review of quantitative projections. 2019 , 116, 109415	84
1278	A fluoroimmunodiagnostic nanoplatform for thyroglobulin detection based on fluorescence quenching signal. 2019 , 300, 127052	10

1277 Management of Pest Insects and P	Plant Diseases by Non-Transformative RNAi. 2019 , 10, 1319	82
Epidemiology of Deltacoronavirus United States. 2019 , 11,	es (ECoV) and Gammacoronaviruses (ECoV) in Wild Birds in the	18
1275 Solid Solution Li(Ni,Mn,Co,Fe)O2 F	Homogeneity Range. 2019 , 40, 725-731	3
The muscular, hepatic and adipose between males and females. 2019	e tissues proteomes in muskox (Ovibos moschatus): Difference , 208, 103480	es 7
Extreme biomimetics: Preservation meshes laid down by sponges. 201	n of molecular detail in centimeter-scale samples of biological 1 9 , 5, eaax2805	38
1272 Pharmacokinetics and Pharmacody	ynamics of Morroniside: A Review. 2019 , 14, 1934578X198565	2 2
	d cingulum degradation and within-network decreases in nal Alzheimer's disease. 2019 , 14, e0222977	4
Transcription Factors Associated w Crops Improvement. 2019 , 10,	vith Abiotic and Biotic Stress Tolerance and Their Potential for	136
1269 Non-typhoidal salmonella: invasive	e, lethal, and on the loose. 2019 , 19, 1267-1269	2
Diverse sources of aeolian sediments modified Bayesian un-mixing mode	nt revealed in an arid landscape in southeastern Iran using a el. 2019 , 41, 100547	20
	circulating tumor cells in the blood using an electrochemical a lipid-bonded conducting polymer. 2019 , 146, 111746	22
Post-decorated surface fluoropho 2019 , 527, 110503	res enhance the photoluminescence of carbon quantum dots.	11
1265 V1 microcircuits underlying mouse	e visual behavior. 2019 , 58, 191-198	1
1264 Acupuncture for the Treatment of	Animal Pain. 2019 , 49, 1029-1039	5
1263 Metabolic crosstalk in the breast c	ancer microenvironment. 2019 , 121, 154-171	63
Field scale nitrogen load in surface 2019 , 249, 109327	e runoff: Impacts of management practices and changing clima	ate. 6
1261 Transient transfection of Babesia	ovis using heterologous promoters. 2019 , 10, 101279	5
Best Practices for Characterization 91, 14159-14169	n of Magnetic Nanoparticles for Biomedical Applications. 2019), 46

1259	Characterization of the Anti-Cancer Activity of the Probiotic Bacterium Using 2D vs. 3D Culture in Colorectal Cancer Cells. 2019 , 9,		23
1258	DNA Copy Number Variations as Markers of Mutagenic Impact. 2019 , 20,		9
1257	How Targeted Memory Reactivation Promotes the Selective Strengthening of Memories in Sleep. 2019 , 29, R906-R912		16
1256	Microstructure and properties of functional magnesium titanate ceramic joint brazed by bismuth-borate glass. 2019 , 39, 4901-4910		8
1255	Neural-network-enhanced torque estimation control of a soft wearable exoskeleton for elbow assistance. 2019 , 63, 102279		13
1254	Genetic Therapies for Hearing Loss: Accomplishments and Remaining Challenges. 2019 , 713, 134527		7
1253	Si-Based GeSn Photodetectors toward Mid-Infrared Imaging Applications. 2019 , 6, 2807-2815		65
1252	Oral Anti-Tumour Necrosis Factor Domain Antibody V565 Provides High Intestinal Concentrations, and Reduces Markers of Inflammation in Ulcerative Colitis Patients. <i>Scientific Reports</i> , 2019 , 9, 14042	4.9	11
1251	Radio-enhancement effects by radiolabeled nanoparticles. <i>Scientific Reports</i> , 2019 , 9, 14346	4.9	15
1250	Biochemical characterization of phosphoenolpyruvate carboxykinases from Arabidopsis thaliana. 2019 , 476, 2939-2952		3
1249	Geographic variation in morphology in the Mohave Rattlesnake (Crotalus scutulatus Kennicott 1861) (Serpentes: Viperidae): implications for species boundaries. 2019 , 4683, zootaxa.4683.1.7		4
1248	Nanopore sequencing of the pharmacogene allows simultaneous haplotyping and detection of duplications. 2019 , 20, 1033-1047		19
1247	Measuring Neural Mechanisms Underlying Sleep-Dependent Memory Consolidation During Naps in Early Childhood. 2019 ,		1
1246	Efficacy of alginate- and clay-encapsulated microorganisms on the growth of AraBoi seedlings (Eugenia stipitata). 2019 , 41, 43936		O
1245	Comprehensive coastal vulnerability assessment and adaptation for Cherating-Pekan coast, Pahang, Malaysia. 2019 , 182, 104948		12
1244	Optimization of ultrastructural preservation of human brain for transmission electron microscopy after long post-mortem intervals. 2019 , 7, 144		9
1243	Vegetation structure across fire edges in a Neotropical rain forest. 2019 , 453, 117587		6
1242	In vitro antibacterial effect analysis of stabilized PEGylated allicin-containing extract from Allium sativum in conjugation with other antibiotics. 2019 , 87, 221-231		5

1241	Overall supply level, not the relative supply of nitrogen and phosphorus, affects the plant community composition of a supratidal wetland in the Yellow River Delta. 2019 , 695, 133866		2	
1240	Wide-band Beam-scanning by Surface Wave Confinement on Leaky Wave Holograms. <i>Scientific Reports</i> , 2019 , 9, 13227	4.9	15	
1239	Haplotype-resolved genomes of geminivirus-resistant and geminivirus-susceptible African cassava cultivars. 2019 , 17, 75		25	
1238	Thermal tolerance in the urban heat island: thermal sensitivity varies ontogenetically and differs between embryos of two sympatric ectotherms. 2019 , 222,		11	
1237	LOW RCS MULTI-BIT CODING METASURFACE MODELING AND OPTIMIZATION: MOM-GEC METHOD IN CONJUNCTION WITH GENETIC ALGORITHM. 2019 , 84, 107-116			
1236	Characteristics of in Vivo Model Systems for Ovarian Cancer Studies. 2019 , 9,		15	
1235	Fungi and mycotoxin problems in the apple industry. 2019 , 29, 42-47		11	
1234	Uprooting defects to enable high-performance III-V optoelectronic devices on silicon. 2019 , 10, 4322		27	
1233	CPT1A plays a key role in the development and treatment of multiple sclerosis and experimental autoimmune encephalomyelitis. <i>Scientific Reports</i> , 2019 , 9, 13299	4.9	9	
1232	Using de novo transcriptome assembly and analysis to study RNAi in Phenacoccus solenopsis Tinsley (Hemiptera: Pseudococcidae). <i>Scientific Reports</i> , 2019 , 9, 13710	4.9	7	
1231	Age effects on sensorimotor predictions: What drives increased tactile suppression during reaching?. 2019 , 19, 9		9	
1230	Transcribing the heart: faithfully interpreting cardiac transcriptional insights. 2019 , 14, 805-810		1	
1229	Does Health Insurance Modify the Association Between Race and Cancer-Specific Survival in Patients with Urinary Bladder Malignancy in the U.S.?. 2019 , 16,		2	
1228	Reparative and Regenerative Effects of Mesenchymal Stromal Cells-Promising Potential for Kidney Transplantation?. 2019 , 20,		3	
1227	SnSe Quantum Dots: Facile Fabrication and Application in Highly Responsive UV-Detectors. 2019 , 9,		7	
1226	Stable Colloidal Quantum Dot Inks Enable Inkjet-Printed High-Sensitivity Infrared Photodetectors. 2019 , 13, 11988-11995		55	
1225	Effects from diet-induced gut microbiota dysbiosis and obesity can be ameliorated by fecal microbiota transplantation: A multiomics approach. 2019 , 14, e0218143		34	
1224	Microbiome Multi-Omics Network Analysis: Statistical Considerations, Limitations, and Opportunities. 2019 , 10, 995		42	

1223	Variation in regional risk of engineered nanoparticles: nanoTiO2 as a case study. 2019 , 6, 444-455	13
1222	A safe-by-design tool for functionalised nanomaterials through the Enalos Nanoinformatics Cloud platform. 2019 , 1, 706-718	24
1221	Low-temperature, high-speed reactive deposition of metal oxides for perovskite solar cells. 2019 , 7, 2283-2290	6
1220	Current status and future perspectives of gold nanoparticle vectors for siRNA delivery. 2019 , 7, 876-896	35
1219	Methylmercury's chemistry: From the environment to the mammalian brain. 2019 , 1863, 129284	40
1218	Satellite-derived PM concentration trends over Eastern China from 1998 to 2016: Relationships to emissions and meteorological parameters. 2019 , 247, 1125-1133	112
1217	Reassessing the role of grazing lands in carbon-balance estimations: Meta-analysis and review. 2019 , 661, 531-542	28
1216	A translational approach to assess the metabolomic impact of stabilized gold nanoparticles by NMR spectroscopy. 2019 , 144, 1265-1274	8
1215	Tunable biomaterials from synthetic, sequence-controlled polymers. 2019 , 7, 490-505	37
1214	Investigation on the structure and thermoelectric properties of CuTe binary compounds. 2019 , 48, 1040-1050	20
1213	Oak genotype and phenolic compounds differently affect the performance of two insect herbivores with contrasting diet breadth. 2019 , 39, 615-627	5
1212	Effect of milk feeding strategy and lactic acid probiotics on growth and behavior of dairy calves fed using an automated feeding system1. 2019 , 97, 1052-1065	8
1211	Development of Allergenicity and Toxicity Assessment Methods for Evaluating Transgenic Sugarcane Overexpressing Sucrose P hosphate Synthase. 2019 , 9, 23	
1210	Impact of topical anti-fibrotics on corneal nerve regeneration in vivo. 2019 , 181, 49-60	11
1209	Earth system impacts of the European arrival and Great Dying in the Americas after 1492. 2019 , 207, 13-36	169
1208	Comparative observations on the premolar root and pulp canal configurations of Middle Pleistocene Homo in China. 2019 , 168, 637-646	6
1207	Using recurrent neural networks with attention for detecting problematic slab shapes in steel rolling. 2019 , 70, 365-377	11
1206	5-Arylideneimidazolones with Amine at Position 3 as Potential Antibiotic Adjuvants against Multidrug Resistant Bacteria. 2019 , 24,	5

1205	Inorganic Nanomaterials. 2019 , 11, 6456-6462	3
1204	Interleukin-6 in juvenile idiopathic arthritis. 2019 , 29, 275-286	11
1203	The effect of biologging systems on reproduction, growth and survival of adult sea turtles. 2019 , 7, 2	5
1202	Recent advances of neoadjuvant chemoradiotherapy in rectal cancer: Future treatment perspectives. 2019 , 3, 24-33	2
1201	White matter has impaired resting oxygen delivery in sickle cell patients. 2019, 94, 467-474	22
1200	Tree species classification in tropical forests using visible to shortwave infrared WorldView-3 images and texture analysis. 2019 , 149, 119-131	74
1199	Electrochemical Synthesis of Highly Nitrogen Containing FeN0.13 and Fe3N1.51 in a Molten Salt System. 2019 , 2019, 730-734	4
1198	Identification and characterization of miRNAs during flag leaf senescence in rice by high-throughput sequencing. 2019 , 24, 1-14	2
1197	Evolution of tetrapyrrole pathway in eukaryotic phototrophs. 2019 , 90, 273-309	5
1196	Enhancement of electromagnetic shielding and piezoelectric properties of White Portland cement by hydration time. 2019 , 204, 20-27	5
1195	Enhanced photocatalytic hydrogen evolution of CdWO4 through polar organic molecule modification. 2019 , 44, 4754-4763	12
1194	The effect of boron content on the microstructure and mechanical properties of Fe50-XMn30Co10Cr10BX ($x = 0, 0.3, 0.6$ and 1.7 wt%) multi-component alloys prepared by arc-melting. 2019 , 748, 244-252	16
1193	Fully Printed Infrared Photodetectors from PbS Nanocrystals with Perovskite Ligands. 2019 , 13, 2389-2397	24
1192	Consistency of satellite-based precipitation products in space and over time compared with gauge observations and snow- hydrological modelling in the Lake Titicaca region. 2019 , 23, 595-619	41
1191	Electron-Driven In Situ Transmission Electron Microscopy of 2D Transition Metal Dichalcogenides and Their 2D Heterostructures. 2019 , 13, 978-995	42
1190	Morphological evolution and modularity of the caecilian skull. 2019 , 19, 30	40
1189	Using Life Cycle Thinking to Assess the Sustainability Benefits of Complex Valorization Pathways for Bauxite Residue. 2019 , 5, 69-84	10
1188	Efficacy of Salicylic Acid as a Cofactor for Ameliorating Effects of Water Stress and Enhancing Wheat Yield and Water Use Efficiency in Saline Soil. 2019 , 13, 163-176	17

1187	Thermosynechococcus as a thermophilic photosynthetic microbial cell factory for CO utilisation. 2019 , 278, 255-265	28
1186	A fluorescence study of the loading and time stability of doxorubicin in sodium cholate/PEO-PPO-PEO triblock copolymer mixed micelles. 2019 , 540, 593-601	18
1185	Reply to Sajja. 2019 , 56, 421-422	
1184	Simulation, Fabrication, and Characterization of a Sensitive SU-8-Based Fabry-Pfot MOEMS Accelerometer. 2019 , 37, 1893-1902	10
1183	The Contribution of Iron to Protein Aggregation Disorders in the Central Nervous System. 2019 , 13, 15	37
1182	Current Trends in Fabrication of Biomaterials for Bone and Cartilage Regeneration: Materials Modifications and Biophysical Stimulations. 2019 , 20,	44
1181	Adenine nucleotides as paracrine mediators and intracellular second messengers in immunity and inflammation. 2019 , 47, 329-337	10
1180	Thioguanine-based DENV-2 NS2B/NS3 protease inhibitors: Virtual screening, synthesis, biological evaluation and molecular modelling. 2019 , 14, e0210869	17
1179	Evolving complexity of MIF signaling. 2019 , 57, 76-88	66
1178	Musical creativity and the motor system. 2019 , 27, 146-153	10
1177	Ant colony optimization for Cuckoo Search algorithm for permutation flow shop scheduling problem. 2019 , 7, 20-27	12
1176	Developmental Neurotoxicity: An Update. 2019 , 31, 108-114	3
1175	Shaping Microbiota During the First 1000 Days of Life. 2019 , 1125, 3-24	27
1174	Pure hydrogen references synthesized by low energy ion implantation into amorphous silicon. 2019 , 442, 47-52	3
1173	Engineering of gradient osteochondral tissue: From nature to lab. 2019 , 87, 41-54	49
1172	Microstructure and properties of M2 high-speed steel cast by the gravity and vacuum investment casting. 2019 , 162, 183-198	16
1171	Drought and small-bodied herbivores modify nutrient cycling in the semi-arid shortgrass steppe. 2019 , 220, 227-239	2
1170	Design by optimization and comparative evaluation of vesicular gels of etodolac for transdermal delivery. 2019 , 45, 611-628	8

Healthy Aging Impairs Photon Absorption Efficiency of Cones. 2019 , 60, 544-551	7
A Boost in Mitochondrial Activity Underpins the Cholesterol-Lowering Effect of Annurca App Polyphenols on Hepatic Cells. 2019 , 11,	le 16
Quantification of controlled release leuprolide and triptorelin in rabbit plasma using electromembrane extraction coupled with HPLC-UV. 2019 , 40, 1074-1081	9
Trembling aspen root suckering and stump sprouting response to above ground disturbance reclaimed boreal oil sands site in Alberta, Canada. 2019 , 50, 771-784	on a 3
1165 Nanocarriers in Different Preclinical and Clinical Stages. 2019 , 685-731	8
Toward a highly selective artificial saliva sensor using printed hybrid field effect transistors. 2 285, 186-192	2019 , ₁₈
Fluorescence lifetime-activated droplet sorting in microfluidic chip systems. 2019 , 19, 403-40	09 25
Tunable graphene oxide inter-sheet distance to obtain graphene oxide&lilver nanoparticle hyl 2019 , 43, 1285-1290	brids.
Site-specific attraction dynamics of surface colloids driven by gradients of liquid crystalline distortions. 2019 , 15, 983-988	
$_{ m 1160}$ Proposal of a stable B3S nanosheet as an efficient hydrogen evolution catalyst. 2019 , 7, 3752	2-3756 22
The influence of female mice age on biodistribution and biocompatibility of citrate-coated magnetic nanoparticles. 2019 , 14, 3375-3388	3
$_{ m 1158}$ The impact of (mass) tourism on coastal dune pollination networks. 2019 , 236, 70-78	15
Combined high-precision 48 and 47 analysis of carbonates. 2019 , 522, 186-191	31
$_{ m 1156}$ Quantifying the Strength of a Salt Bridge by Neutron Scattering and Molecular Dynamics. 20 °	19 , 10, 3254-3259 ₁₁
A comprehensive analysis of the Lactuca sativa, L. transcriptome during different stages of the compatible interaction with Rhizoctonia solani. <i>Scientific Reports</i> , 2019 , 9, 7221	he 4.9 10
Descriptive osteology and patterns of limb loss of the European limbless skink Ophiomorus punctatissimus (Squamata, Scincidae). 2019 , 235, 313-345	6
1153 Kosten der Operationsverfahren des Pilonidalsinus. 2019 , 41, 127-130	1
The effect of different surface topographies of titanium implants on bacterial biofilm: a system review. 2019 , 1, 1	ematic 9

1151	Investigating the toxicities of different functionalized polystyrene nanoplastics on Daphnia magna. 2019 , 180, 509-516	54
1150	Thermal decomposition of CuProp2: In-situ analysis of film and powder pyrolysis. 2019 , 140, 312-320	9
1149	Discovering BuriedLehannels of the Palaeo-Yamuna river in NW India using geophysical evidence: Implications for major drainage reorganization and linkage to the Harappan Civilization. 2019 , 167, 128-139	11
1148	A high-order state-of-charge estimation model by cubature particle filter. 2019 , 146, 35-42	14
1147	Modeling of Mycobacterium tuberculosis dormancy in bacterial cultures. 2019 , 117, 7-17	6
1146	High-precision isotopic analysis sheds new light on mercury metabolism in long-finned pilot whales (Globicephala melas). <i>Scientific Reports</i> , 2019 , 9, 7262	23
1145	Encapsulation of complex solutions using droplet microfluidics towards the synthesis of artificial cells. 2019 , 29, 083001	13
1144	Development and application of a novel real-time polymerase chain reaction assay to detect illegal trade of the European eel (Anguilla anguilla). 2019 , 1, e39	7
1143	Effect of Collagen Cross-Link Deficiency on Incorporation of Grafted Bone. 2019, 7,	
1142	Glial Cell AMPA Receptors in Nervous System Health, Injury and Disease. 2019 , 20,	28
1141	Meaning and Attentional Guidance in Scenes: A Review of the Meaning Map Approach. 2019, 3,	18
1140	Time-dependent changes in cognitive flexibility performance during intermittent social stress: Relevance for motivation and reward-seeking behavior. 2019 , 370, 111972	1
1139	Zolmitriptan attenuates hepatocellular carcinoma via activation of caspase mediated apoptosis. 2019 , 308, 120-129	9
1138	Exfoliation level of aggregated graphitic nanoplatelets by oxidation followed by silanization on controlling mechanical and nanomechanical performance of hybrid CFRP composites. 2019 , 173, 106855	18
1137	Bioinspired oral insulin delivery system using yeast microcapsules. 2019 , 103, 109753	12
1136	Toward Axonal System Biology: Genome Wide Views of Local mRNA Translation. 2019 , 19, e1900054	5
1135	Prognostic significance of combining immunohistochemical markers for cancer-associated fibroblasts in lung adenocarcinoma tissue. 2019 , 475, 181-189	4
1134	Dynamic changing of soil water in artificial ryegrass land in the hilly regions of Sichuan Basin area. 2019 , 221, 99-108	О

1133	Photosynthesis by symbiotic sponges enhances their ability to erode calcium carbonate. 2019 , 516, 140-149	8
1132	Analyzing Microbial Population Heterogeneity-Expanding the Toolbox of Microfluidic Single-Cell Cultivations. 2019 , 431, 4569-4588	22
1131	Performance of restricted access copper-imprinted poly(allylthiourea) in an on-line preconcentration and sample clean-up FIA-FAAS system for copper determination in milk samples. 2019 , 202, 460-468	10
1130	PyRod: Tracing Water Molecules in Molecular Dynamics Simulations. 2019 , 59, 2818-2829	9
1129	Mechanism of miR-143-3p inhibiting proliferation, migration and invasion of osteosarcoma cells by targeting MAPK7. 2019 , 47, 2065-2071	18
1128	Von Uexk[] Revisited: Addressing Human Biases in the Study of Animal Perception. 2019 , 59, 1451-1462	15
1127	Preliminary phytochemical analysis and evaluation of in vitro antioxidant, antiproliferative, antidiabetic, and anticholinergics effects of endemic Gypsophila taxa from Turkey. 2019 , 43, e12908	17
1126	Arsenite Oxidation by a Newly Isolated Betaproteobacterium Possessing Genes and Diversity of the Gene Cluster in Bacterial Genomes. 2019 , 10, 1210	6
1125	Microbial fuel cells (MFCs) for bioelectrochemical treatment of different wastewater streams. 2019 , 254, 115526	109
1124	A Supramolecular Platform for the Introduction of Fc-Fusion Bioactive Proteins on Biomaterial Surfaces. 2019 , 1, 2044-2054	4
1123	Taking advantage of external mechanical work to reduce metabolic cost: the mechanics and energetics of split-belt treadmill walking. 2019 , 597, 4053-4068	29
1122	Changes in the gut microbiome and fermentation products concurrent with enhanced longevity in acarbose-treated mice. 2019 , 19, 130	98
1121	The intermittent administration of ethanol during the juvenile period produces changes in the expression of hippocampal genes and proteins and deterioration of spatial memory. 2019 , 372, 112033	9
1120	Pro-remodeling peptides modulate collagen #(I) promoter activity in rat cardiac myofibroblasts. 2019 , 515, 693-698	
1119	Scaling laws of cell-fate responses to transient stress. 2019 , 478, 14-25	3
1118	Investigating Eye Contact Effect on People's Name Retrieval in Normal Aging and in Alzheimer's Disease. 2019 , 10, 1218	2
1117	Determination of the metabolic index using the fluorescence lifetime of free and bound nicotinamide adenine dinucleotide using the phasor approach. 2019 , 12, e201900156	21
1116	The effect of global change on mosquito-borne disease. 2019 , 19, e302-e312	113

1115	Fabrication of carbon quantum dots/TiO2/Fe2O3 composites and enhancement of photocatalytic activity under visible light. 2019 , 730, 391-398	25
1114	Anion recognition in aqueous solution by cyclic dinuclear square cage-shaped coordination complexes. 2019 , 495, 118961	2
1113	Black carbon-doped TiO2 films: Synthesis, characterization and photocatalysis. 2019 , 382, 111941	56
1112	Three-dimensional kernel-based coda attenuation imaging of caldera structures controlling the 1982-84 Campi Flegrei unrest. 2019 , 381, 273-283	12
1111	The Impact of the Ketogenic Diet on Glial Cells Morphology. A Quantitative Morphological Analysis. 2019 , 413, 239-251	13
1110	Engineered Substrate for Cyclooxygenase-2: A Pentapeptide Isoconformational to Arachidonic Acid for Managing Inflammation. 2019 , 62, 6363-6376	4
1109	Disordered and Densely Packed ITO Nanorods as an Excellent Lithography-Free Optical Solar Reflector Metasurface. 2019 , 6, 1812-1822	36
1108	Molecular Imaging for Radiotherapy Planning and Response Assessment for Cervical Cancer. 2019 , 49, 493-500	11
1107	Herbal Formula Fo Shou San Attenuates Alzheimer's Disease-Related Pathologies via the Gut-Liver-Brain Axis in APP/PS1 Mouse Model of Alzheimer's Disease. 2019 , 2019, 8302950	11
1106	Tree Species Shape Soil Bacterial Community Structure and Function in Temperate Deciduous Forests. 2019 , 10, 1519	34
1105	Design of Rigidity and Breaking Strain for a Kirigami Structure with Non-Uniform Deformed Regions. 2019 , 10,	3
1104	Protection of the Marine Environment: The International and National Regulation of Deep Seabed Mining Activities. 2019 , 471-503	3
1103	Identification of a novel PRR15L-RSPO2 fusion transcript in a sigmoid colon cancer derived from superficially serrated adenoma. 2019 , 475, 659-663	4
1102	The feasibility of picture-based insurance (PBI): Smartphone pictures for affordable crop insurance. 2019 , 4, 100042	22
1101	Significance of Perylene for Source Allocation of Terrigenous Organic Matter in Aquatic Sediments. 2019 , 53, 8244-8251	16
1100	Nanoparticle Formation in Stable Microemulsions for Enhanced Oil Recovery Application. 2019 , 58, 120	664-126 <i>7</i> 57
1099	Visible-Light-Mediated Photodynamic Water Disinfection @ Bimetallic-Doped Hybrid Clay Nanocomposites. 2019 , 11, 25483-25494	17
1098	Diesel soot coated non-woven fabric for oil-water separation and adsorption applications. <i>Scientific Reports</i> , 2019 , 9, 8503	4.9 17

1097	Preventing fungal growth on heritage paper with antifungal and cellulase inhibiting magnesium oxide nanoparticles. 2019 , 7, 6412-6419	11
1096	A Novel Sex-Dependent Target for the Treatment of Postoperative Pain: The NLRP3 Inflammasome. 2019 , 10, 622	19
1095	Subsynaptic Domains in Super-Resolution Microscopy: The Treachery of Images. 2019 , 12, 161	13
1094	Effect of SLM Build Parameters on the Compressive Properties of 304L Stainless Steel. 2019 , 3, 43	5
1093	Towards clinical application of image mining: a systematic review on artificial intelligence and radiomics. 2019 , 46, 2656-2672	93
1092	Potential of Solanum viarum Dunal in use for phytoremediation of heavy metals to mining areas, southern Brazil. <i>Environmental Science and Pollution Research</i> , 2019 , 26, 24132-24142	13
1091	Surface Morphologies in Ultra-short Pulsed Laser Processing of Stainless-Steel at High Repetition Rate. 2019 , 20, 1465-1474	3
1090	Galectin-3 is associated with glomerular filtration rate and outcome in patients with stable decompensated cirrhosis. 2019 , 51, 1692-1697	3
1089	The oncogenic role of hepatitis delta virus in hepatocellular carcinoma. 2019 , 1, 120-130	19
1088	Nuclear magnetic resonance screening of changes in fatty acid and cholesterol content of ovine milk induced by ensiled olive cake inclusion in Chios sheep diets. 2019 , 177, 111-116	12
1087	Electrospun Hybrid Perovskite Fibers-Flexible Networks of One-Dimensional Semiconductors for Light-Harvesting Applications. 2019 , 11, 25163-25169	7
1086	Actinobacteria and Cyanobacteria Diversity in Terrestrial Antarctic Microenvironments Evaluated by Culture-Dependent and Independent Methods. 2019 , 10, 1018	22
1085	Large Scale Cardiovascular Model Personalisation for Mechanistic Analysis of Heart and Brain Interactions. 2019 , 285-293	2
1084	Iron homeostasis and iron-regulated ROS in cell death, senescence and human diseases. 2019 , 1863, 1398-1409	122
1083	Distinct brain representations of processed and unprocessed foods. 2019 , 50, 3389-3401	3
1082	Special issues for the 55th Inner Ear Biology Workshop 0608.09.2018 in Berlin: Basic research and clinical aspects-translational aspects of hearing research. 2019 , 67, 43-45	
1081	Association of elevated serum triglyceride levels with a more severe course of acute pancreatitis: Cohort analysis of 1457 patients. 2019 , 19, 623-629	17
1080	Evaluation of complete blood count parameters, cell ratios, and cell volume indices in mushroom poisonings. 2019 , 38, 1127-1131	1

1079	Automated characterization and classification of coronary atherosclerotic plaques for intravascular optical coherence tomography. 2019 , 39, 719-727	5
1078	The Relevance of Variants With Unknown Significance for Autism Spectrum Disorder Considering the Genotype-Phenotype Interrelationship. 2019 , 10, 409	6
1077	Myelinated axon physiology and regulation of neural circuit function. 2019 , 67, 2050-2062	32
1076	Small-molecule agents for the treatment of inflammatory bowel disease. 2019 , 29, 2034-2041	7
1075	Defining mEier for the Celtic Sea mixed fisheries: A multiannual international study of typology. 2019 , 219, 105310	8
1074	An experimental study on the oil-soluble surfactant-assisted cyclic mixed solvent injection process for heavy oil recovery after primary production. 2019 , 254, 115656	16
1073	Dietary exposure assessment of organochlorine pesticides in two commonly grown leafy vegetables in South-western Nigeria. 2019 , 5, e01895	20
1072	Photothermal versus photodynamic treatment for the inactivation of the bacteria Escherichia coli and Bacillus cereus: An in vitro study. 2019 , 27, 317-326	8
1071	Rethinking EBAD: Evolution of smart noninvasive detection of diabetes. 2019 , 118, 477-487	5
1070	Enhanced inertial focusing of microparticles and cells by integrating trapezoidal microchambers in spiral microfluidic channels 2019 , 9, 19197-19204	9
1069	Uncertainty analysis in structured laser illumination planar imaging (SLIPI) applied to non-linear signals: gas-phase phosphor thermometry. 2019 , 30, 084003	1
1068	Genome-wide association study identifies seven novel loci associating with circulating cytokines and cell adhesion molecules in Finns. 2019 , 56, 607-616	21
1067	In Situ 2D Perovskite Formation and the Impact of the 2D/3D Structures on Performance and Stability of Perovskite Solar Cells. 2019 , 3, 1900199	19
1066	From bone regeneration to three-dimensional in vitro models: tissue engineering of organized bone extracellular matrix. 2019 , 10, 107-115	21
1065	Testosterone administration increases social discounting in healthy males. 2019 , 108, 127-134	17
1064	Modification of membrane hydrophobicity in membrane contactors for environmental remediation. 2019 , 227, 115721	11
1063	Similarity in benthic habitat and fish assemblages in the upper mesophotic and shallow water reefs in the West Philippine Sea. 2019 , 99, 1507-1517	2
1062	A mass-customizable dermal patch with discrete colorimetric indicators for personalized sweat rate quantification. 2019 , 5, 29	14

1061	Coevolution of vocal signal characteristics and hearing sensitivity in forest mammals. 2019 , 10, 2778		13	
1060	Boiling Histotripsy-induced Partial Mechanical Ablation Modulates Tumour Microenvironment by Promoting Immunogenic Cell Death of Cancers. <i>Scientific Reports</i> , 2019 , 9, 9050	4.9	23	
1059	Activating KIRs on Educated NK Cells Support Downregulation of CD226 and Inefficient Tumor Immunosurveillance. 2019 , 7, 1307-1317		6	
1058	Modified MHD Radiative Mixed Convective Nanofluid Flow Model with Consideration of the Impact of Freezing Temperature and Molecular Diameter. 2019 , 11, 833		7	
1057	Small Molecule Targeting TDP-43's RNA Recognition Motifs Reduces Locomotor Defects in a Model of Amyotrophic Lateral Sclerosis (ALS). 2019 , 14, 2006-2013		26	
1056	Binary Silanization and Silver Nanoparticle Encapsulation to Create Superhydrophobic Cotton Fabrics with Antimicrobial Capability. <i>Scientific Reports</i> , 2019 , 9, 9172	4.9	14	
1055	The influence of progesterone on bovine uterine fluid energy, nucleotide, vitamin, cofactor, peptide, and xenobiotic composition during the conceptus elongation-initiation window. <i>Scientific Reports</i> , 2019 , 9, 7716	4.9	12	
1054	Deep expression analysis reveals distinct cold-response strategies in rubber tree (Hevea brasiliensis). 2019 , 20, 455		11	
1053	Serp-2, a virus-derived apoptosis and inflammasome inhibitor, attenuates liver ischemia-reperfusion injury in mice. 2019 , 16, 12		9	
1052	Solubility and solution-phase chemistry of isocyanic acid, methyl isocyanate, and cyanogen halides. 2019 , 19, 4419-4437		14	
1051	Sustainable Agriculture Reviews 36. 2019 ,		3	
1050	Analysis of the Pressure-Pulse Propagation in Rock: a New Approach to Simultaneously Determine Permeability, Porosity, and Adsorption Capacity. 2019 , 52, 4301-4317		22	
1049	Theoretical Spectroscopic Study on the Au, Ag, Au/Ag, and Ag/Au Nanosurfaces and Their Cytosine/Nanosurface Complexes: UV, IR, and Charge-Transfer SERS Spectra. 2019 , 123, 16345-16358		3	
1048	Graphene prevents neurostimulation-induced platinum dissolution in fractal microelectrodes. 2019 , 6, 035037		4	
1047	Design of Nano-Chitosans for Tissue Engineering and Molecular Release. 2019 , 315-334		3	
1046	Rapid manufacturing of copper components using 3D printing and ultrasonic assisted pressureless sintering: Experimental investigations and process optimization. 2019 , 43, 253-269		27	
1045	Can analysis of a small clod of soil help to solve a murder case?. 2019 , 59, 667-677		8	
1044	Parental Effects and Climate Change: Will Avian Incubation Behavior Shield Embryos from Increasing Environmental Temperatures?. 2019 , 59, 1068-1080		14	

1043	Holocene Ecohydrological Variability on the East Coast of Kamchatka. 2019 , 7,		1
1042	Current issues regarding the application of recombinant lactic acid bacteria to mucosal vaccine carriers. 2019 , 103, 5947-5955		8
1041	Swift heavy ion-irradiated multi-phase calcium borosilicates: implications to molybdenum incorporation, microstructure, and network topology. 2019 , 54, 11763-11783		4
1040	Epigenetic inheritance across multiple generations. 2019 , 401-420		1
1039	Comparison of ionic liquid electrolyte to aqueous electrolytes on carbon nanofibres supercapacitor electrode derived from oxygen-functionalized graphene. 2019 , 375, 121906		27
1038	Draft genome sequence of a multidrug-resistant bla-producing Acinetobacter baumannii L13 isolated from Tarim River sample in China. 2019 , 18, 145-147		4
1037	Erythromycin, Cethromycin and Solithromycin display similar binding affinities to the E. ´coli's ribosome: A molecular simulation study. 2019 , 91, 80-90		2
1036	Multimodal Wrist Biosensor for Wearable Cuff-less Blood Pressure Monitoring System. <i>Scientific Reports</i> , 2019 , 9, 7947	4.9	27
1035	Highly stable binder free CNTs/rGO aerogel electrode for decolouration of methylene blue & palm oil mill effluent electro-Fenton oxidation process 2019 , 9, 16472-16478		10
1034	Surface characterization of an organosilane-grafted moisture-crosslinked polyethylene compound treated by air atmospheric pressure non-equilibrium gliding arc plasma. 2019 , 490, 436-450		14
1033	Antibiotic microbial resistance (AMR) removal efficiencies by conventional and advanced wastewater treatment processes: A review. 2019 , 685, 596-608		101
1032	Efficient planar perovskite solar cells with low-temperature atomic layer deposited TiO2 electron transport layer and interfacial modifier. 2019 , 188, 239-246		16
1031	Immunodiagnosis of active tuberculosis. 2019 , 13, 521-532		3
1030	Heart Failure and Cancer: Mechanisms of Old and New Cardiotoxic Drugs in Cancer Patients. 2019 , 5, 112-118		27
1029	Single Fragment or Bulk Soil DNA Metabarcoding: Which is Better for Characterizing Biological Taxa Found in Surface Soils for Sample Separation?. 2019 , 10,		5
1028	Oxidation Behavior of Silicides. 2019 , 21, 127-156		2
1027	High brightness and precise adjustment of multicolor-tunable luminescence of Lu2GeO5:Tb3+, Eu3+ phosphors for white LEDs. 2019 , 19, 1052-1061		12
1026	An Overview of the Influence of Biodiesel, Alcohols, and Various Oxygenated Additives on the Particulate Matter Emissions from Diesel Engines. 2019 , 12, 1987		29

1025	Tunneling nanotubes: A bridge for heterogeneity in glioblastoma and a new therapeutic target?. 2019 , 2, e1185		11
1024	Ergodicity and spike rate for stochastic FitzHughNagumo neural model with periodic forcing. 2019 , 123, 383-399		2
1023	A simple process to tune wettability of pectin-modified silanized glass. 2019 , 577, 67-74		1
1022	In-depth characterization of congenital Zika syndrome in immunocompetent mice: Antibody-dependent enhancement and an antiviral peptide therapy. 2019 , 44, 516-529		20
1021	Photocatalytic study of some synthesized MWCNTs/TiO2 nanocomposites used in the treatment of industrial hazard materials. 2019 , 28, 247-252		18
1020	Skeletal-muscle-derived mesenchymal stem/stromal cells from patients with osteoarthritis show superior biological properties compared to bone-derived cells. 2019 , 38, 101465		13
1019	Aptamer-based Targeted Delivery of a G-quadruplex Ligand in Cervical Cancer Cells. <i>Scientific Reports</i> , 2019 , 9, 7945	4.9	40
1018	Microwave-assisted synthesis of carbon dots and their applications. 2019 , 7, 7175-7195		132
1017	Usnic Acid Potassium Salt: Evaluation of the Acute Toxicity and Antinociceptive Effect in Murine Model. 2019 , 24,		3
1016	Unravelling the links between heat stress, bleaching and disease: fate of tabular corals following a combined disease and bleaching event. 2019 , 38, 591-603		17
1015	Controlled atmosphere dependent tribological properties of thermally annealed ultrananocrystalline diamond films. 2019 , 97, 107437		8
1014	Simple and rapid method for synthesis of porous gold nanoparticles and its application in improving DNA loading capacity. 2019 , 103, 109795		9
1013	Dramatic Enhancement of Optoelectronic Properties of Electrophoretically Deposited C-Graphene Hybrids. 2019 , 11, 24349-24359		18
1012	Electrical Resistivity of Iron Phosphides at High-Pressure and High-Temperature Conditions With Implications for Lunar Core's Thermal Conductivity. 2019 , 124, 5544-5556		10
1011	Omics Approaches for Developing Abiotic Stress Tolerance in Wheat. 2019 , 443-463		3
1010	The Structural and Functional Diversity of Intrinsically Disordered Regions in Transmembrane Proteins. 2019 , 252, 273-292		8
1009	8.2 ka event North Sea hydrography determined by bivalve shell stable isotope geochemistry. <i>Scientific Reports</i> , 2019 , 9, 6753	4.9	7
1008	Extensive eccentric contractions in intact cardiac trabeculae: revealing compelling differences in contractile behaviour compared to skeletal muscles. 2019 , 286, 20190719		6

1007	CBLL1 is highly expressed in non-small cell lung cancer and promotes cell proliferation and invasion. 2019 , 10, 1479-1488		13
1006	Calibration of life history traits with epiphyseal closure, dental eruption and bone histology in captive and wild red deer. 2019 , 235, 205-216		19
1005	Nuclear Receptors Regulate Intestinal Inflammation in the Context of IBD. 2019 , 10, 1070		20
1004	Antimicrobial properties of ⊞AgWO rod-like microcrystals synthesized by sonochemistry and sonochemistry followed by hydrothermal conventional method. 2019 , 58, 104620		22
1003	Second generation of pepino mosaic virus vectors: improved stability in tomato and a wide range of reporter genes. 2019 , 15, 58		6
1002	Quantum dot therapeutics: a new class of radical therapies. 2019 , 13, 48		15
1001	Omega 3-DHA and Delta-Tocotrienol Modulate Lipid Droplet Biogenesis and Lipophagy in Breast Cancer Cells: the Impact in Cancer Aggressiveness. 2019 , 11,		11
1000	Automated metrology and geometric analysis of additively manufactured lattice structures. 2019 , 28, 535-545		19
999	Influence of annealing on properties of SILAR deposited nickel oxide films. 2019, 167, 189-194		20
998	Zone folding induced tunable topological interface states in one-dimensional phononic crystal plates. 2019 , 383, 2797-2801		14
997	Exploring biomarkers in the overactive bladder: Alterations in miRNA levels of a panel of genes in patients with OAB. 2019 , 38, 1571-1578		7
996	Lipid enhancement through nutrient starvation in Chlorella sp. and its fatty acid profiling for appropriate bioenergy feedstock. 2019 , 20, 101179		31
995	Time course images of cellular injury and recovery in murine brain with high-resolution GRIN lens system. <i>Scientific Reports</i> , 2019 , 9, 7946	4.9	10
994	Long-range depth imaging using a single-photon detector array and non-local data fusion. <i>Scientific Reports</i> , 2019 , 9, 8075	4.9	26
993	Deep learning-based electroencephalography analysis: a systematic review. 2019 , 16, 051001		339
992	Taking a Stab at Quantifying the Energetics of Biological Puncture. 2019 , 59, 1586-1596		6
991	Humans Are Animals, Too: Critical Commonalities and Differences Between Human and Wildlife Forensic Genetics. 2019 , 64, 1603-1621		12
990	Biochemical functionality of magnetic particles as nanosensors: how far away are we to implement them into clinical practice?. 2019 , 17, 73		14

989	Arthroscopically assisted reduction and internal fixation (ARIF) versus open reduction and internal fixation (ORIF) for lateral tibial plateau fractures: a comparative retrospective study. 2019 , 14, 155		16
988	Application of Graph Theory for Identifying Connectivity Patterns in Human Brain Networks: A Systematic Review. 2019 , 13, 585		150
987	Occurrence of and radioanalytical methods used to determine medical radionuclides in environmental and biological samples. A review. 2019 , 207, 37-52		5
986	Studying GPCR conformational dynamics by single molecule fluorescence. 2019 , 493, 110469		9
985	A novel defect ground structure for decoupling closely spaced E-plane microstrip antenna array. 2019 , 11, 1069-1074		4
984	Method for diagnosing neoplastic lesions by quantitative fluorescence value. <i>Scientific Reports</i> , 2019 , 9, 7833	4.9	6
983	Impact of the Stacking Order of HfOx and AlOx Dielectric Films on RRAM Switching Mechanisms to Behave Digital Resistive Switching and Synaptic Characteristics. 2019 , 1-1		20
982	The relationship between multidimensional economic well-being and children's mental health, physical health, and executive function development in South Africa. 2019 , 22, e12846		4
981	Niche models do not predict experimental demography but both suggest dispersal limitation across the northern range limit of the scarlet monkeyflower (Erythranthe cardinalis). 2019 , 46, 1316		10
980	Soil Memory: Theoretical Basics of the Concept, Its Current State, and Prospects for Development. 2019 , 52, 229-243		16
979	Results from a cross-sectional sexual and reproductive health study among school girls in Tanzania: high prevalence of bacterial vaginosis. 2019 , 95, 219-227		9
978	Ultra-thin Skin Electronics for High Quality and Continuous Skin-Sensor-Silicon Interfacing. 2019,		2
977	Role and exploitation of underground chemical signaling in plants. 2019 , 75, 2455-2463		10
976	Study of the green synthesis of silver nanoparticles using a natural extract of dark or white Salvia hispanica L. seeds and their antibacterial application. 2019 , 489, 952-961		52
975	Development of Theragnostic Tool Using NIR Fluorescence Probe Targeting Mitochondria in Glioma Cells. 2019 , 30, 1642-1648		2
974	Well-controlled foam-based solid coatings. 2019 , 15, 5084-5093		2
973	The heterogenous distribution of white etching matter (WEM) around subsurface cracks in bearing steels. 2019 , 174, 300-309		17
972	Assessment of scoring functions and in silico parameters for AChE-ligand interactions as a tool for predicting inhibition potency. 2019 , 308, 216-223		17

971	Interaction mechanism between Smllo magnets and glass coatings doped with mixed adherent oxides. 2019 , 45, 18291-18297		1
970	Dwarf eelgrass (Zostera noltii) leaf fatty acid profile during a natural restoration process: Physiological and ecological implications. 2019 , 106, 105452		6
969	Development and catalytic characterization of L-asparaginase nano-bioconjugates. 2019 , 135, 1142-1150	0	26
968	The multi-allelic APRR2 gene is associated with fruit pigment accumulation in melon and watermelon. 2019 , 70, 3781-3794		33
967	Muscle changes with high-intensity aerobic training in an animal model of renal disease. 2019 , 34, e2019	0050	32
966	Molecular characterization of antimicrobial-resistant Enterococcus faecalis and Enterococcus faecium isolated from layer parent stock. 2019 , 98, 5892-5899		14
965	Molecular Analysis of Protein-Protein Interactions in the Ethylene Pathway in the Different Ethylene Receptor Subfamilies. 2019 , 10, 726		10
964	DaimonDNA: A portable, low-cost loop-mediated isothermal amplification platform for naked-eye detection of genetically modified organisms in resource-limited settings. 2019 , 141, 111409		8
963	Aphicidal activity of Bacillus amyloliquefaciens strains in the peach-potato aphid (Myzus persicae). 2019 , 226, 41-47		4
962	Deformation and annealing behaviour of a low carbon high Mn TWIP steel microalloyed with Ti. 2019 , 99, 2487-2516		1
961	Supramolecular Detection of a Nerve Agent Simulant by Fluorescent Zn-Salen Oligomer Receptors. 2019 , 24,		14
960	No sitting on the fence: protecting wetlands from feral pig damage by exclusion fences requires effective fence maintenance. 2019 , 27, 581-585		3
959	Effects of Short-Time Tempering on Impact Toughness, Strength, and Phase Evolution of 4340 Steel Within the Tempered Martensite Embrittlement Regime. 2019 , 50, 3654-3662		9
958	Supplementation with polyalcohols and sequential mixotrophy dilution photoinduction strategy boost the accumulation of astaxanthin by Haematococcus pluvialis. 2019 , 511, 734225		13
957	Point-bar brink and channel thalweg trajectories depicting interaction between vertical and lateral shifts of microtidal channels in the Venice Lagoon (Italy). 2019 , 342, 37-50		10
956	Stimulus information supporting bilateral symmetry perception. 2019 , 161, 18-24		1
955	A rapid method for measuring serum oxidized albumin in a rat model of proteinuria and hypertension. <i>Scientific Reports</i> , 2019 , 9, 8620	4.9	2
954	Towards bioinspired models of intestinal mucus 2019 , 9, 15887-15899		11

953	Discovery of Alpha-Gal-Containing Antigens in North American Tick Species Believed to Induce Red Meat Allergy. 2019 , 10, 1056	65
952	Modeling the effect of microstructure on elastic wave propagation in platelet-reinforced composites and ceramics. 2019 , 224, 111105	5
951	Porous ZnV2O4 Nanowire for Stable and High-Rate Lithium-Ion Battery Anodes. 2019 , 2, 4247-4256	26
950	A Burn-onlMichler's ketoneBenzimidazole fluorescent probe for selective detection of serum albumins. 2019 , 43, 10859-10867	7
949	Comparative and functional analysis of the digital mucus glands and secretions of tree frogs. 2019 , 16, 19	8
948	Brain structure and cognitive ability in healthy aging: a review on longitudinal correlated change. 2019 , 31, 1-57	62
947	Stepwise Development of an Continuous Fermentation Model for the Murine Caecal Microbiota. 2019 , 10, 1166	12
946	Design and Implementation of an Ultra-Low Resource Electrodermal Activity Sensor for Wearable Applications. 2019 , 19,	10
945	Urinary exosomal proteins as (pan-)cancer biomarkers: insights from the proteome. 2019 , 593, 1580-1597	27
944	In vitro cyst formation of ADPKD cells. 2019 , 153, 93-111	5
943	Mitochondrial Stress Response in Neural Stem Cells Exposed to Electronic Cigarettes. 2019 , 16, 250-269	29
942	Functional imaging of rostrocaudal spinal activity during upper limb motor tasks. 2019 , 200, 590-600	6
941	Power generation and longevity improvement of renewable energy systems via slippery surfaces A review. 2019 , 143, 922-938	8
940	Characterizing the fluctuations of dynamic resting-state electrophysiological functional connectivity: reduced neuronal coupling variability in mild cognitive impairment and dementia due to Alzheimer's disease. 2019 , 16, 056030	19
939	Phylogenetic evidence of allopatric speciation of bradyrhizobia nodulating cowpea (Vigna unguiculata L. walp) in South African and Mozambican soils. 2019 , 95,	6
938	Effect of Powdered Activated Carbon as Advanced Step in Wastewater Treatments on Antibiotic Resistant Microorganisms. 2019 , 20, 63-75	7
937	Material Formation of Recombinant Spider Silks through Aqueous Solvation using Heat and Pressure. 2019 ,	
936	Deflecting mode-I cracks in anisotropic materials. 2019 , 136, 103060	7

935	Oxytocin: Potential to mitigate cardiovascular risk. 2019 , 117, 170089	10
934	Whereabouts of truckers: An empirical study of predictability. 2019 , 104, 184-195	5
933	Enhanced Radiative Recombination of Excitons and Free Charges Due to Local Deformations in the Band Structure of MAPbBr3 Perovskite Crystals. 2019 , 123, 13444-13450	4
932	Shape-Adaptable 2D Titanium Carbide (MXene) Heater. 2019 , 13, 6835-6844	99
931	Disorders of the Liver Excluding Hepatitis A, B, C, D, and E. 2019 , 37-90	
930	Organic and biodynamic wines quality and characteristics: A review. 2019 , 295, 334-340	26
929	Dispersion property of electromagnetic wave in 1D magnetized ferrites photonic crystals for TE mode in longitudinal magnetization configuration. 2019 , 35, 100706	1
928	A review on enhanced biogas production from anaerobic digestion of lignocellulosic biomass by different enhancement techniques. 2019 , 84, 81-90	94
927	Mechanical Properties of Ultraviolet-Assisted Paste Extrusion and Postextrusion Ultraviolet-Curing of Three-Dimensional Printed Biocomposites. 2019 , 6, 127-137	9
926	The Presence and Localization of G-Quadruplex Forming Sequences in the Domain of Bacteria. 2019 , 24,	39
925	Recent advances in constructed wetland-microbial fuel cells for simultaneous bioelectricity production and wastewater treatment: A review. 2019 , 43, 5106-5127	53
924	Optical coherence tomography to detect acute esophageal radiation-induced damage in mice: A validation study. 2019 , 12, e201800440	3
923	Nutrigenomics as a tool to study the impact of diet on aging and age-related diseases: the approach. 2019 , 14, 12	13
922	Meet Our Regional Editor. 2019 , 15, 1-3	
921	Evanescent absorption based fluoride fiber sensing enhancement led by doped graphened thermo-optic dispersion in NIR. 2019 , 51, 1	O
920	Source term estimation in the presence of nuisance signals. 2019 , 203, 220-225	3
919	Applications of high-throughput Dimics Idata in the study of frailty. 2019 , 3, 40-51	5
918	Novel approaches for biomolecule immobilization in microscale systems. 2019 , 144, 3912-3924	4

917	Low temperature epitaxy of tungstentelluride heterostructure films. 2019, 21, 3409-3414	4
916	Reproductive biology of thin sharpbelly, Toxabramis swinhonis Glīther, 1873 in a shallow lake (Biandantang Lake) along the middle reach of the Yangtze River basin (China): implications for fisheries management. 2019 , 55, 8	1
915	Molecular transport through primary human small intestinal monolayers by culture on a collagen scaffold with a gradient of chemical cross-linking. 2019 , 13, 36	15
914	Current Biomedical Applications of 3D Printing and Additive Manufacturing. 2019 , 9, 1713	120
913	Transcriptome Analysis of Yamame () in Normal Conditions after Heat Stress. 2019, 8,	1
912	Changes in the Anterior Lamina Cribrosa Morphology with Glaucoma Severity. <i>Scientific Reports</i> , 4.9	10
911	The importance of determining circadian parameters in pharmacological studies. 2019 , 176, 2827-2847	14
910	Learning Single-Cell Distances from Cytometry Data. 2019 , 95, 782-791	3
909	The Systems Biology of Lateral Root Formation: Connecting the Dots. 2019 , 12, 784-803	19
908	Quantification of Hidden Whole-Field Stress Inside Porous Geomaterials Via Three-Dimensional Printing and Photoelastic Testing Methods. 2019 , 124, 5408-5426	14
907	diffcyt: Differential discovery in high-dimensional cytometry via high-resolution clustering. 2019 , 2, 183	78
906	A Sentinel-1 based hot-spot analysis: landslide mapping in north-western Italy. 2019 , 40, 7898-7921	32
905	Ostracods as ecological and isotopic indicators of lake water salinity changes: the Lake Van example. 2019 , 16, 2095-2114	10
904	Computationally guided synthesis of (2D/3D/2D) rGO/Fe2O3/g-C3N4 nanostructure with improved charge separation and transportation efficiency for degradation of pharmaceutical molecules. 2019 , 255, 117758	59
903	Corrosion behavior of Ti-29Nb-13Ta-4.6Zr and commercially pure Ti under simulated inflammatory conditions Leomparative effect of grain refinement and non-toxic phase stabilizers. 2019 , 312, 369-379	21
902	Colour plasticity in the shells and pearls of animal graft model Pinctada margaritifera assessed by HSV colour quantification. <i>Scientific Reports</i> , 2019 , 9, 7520	7
901	Carbon conversion and stabilisation of date palm and high rate algal pond (microalgae) biomass through slow pyrolysis. 2019 , 43, 4403-4416	6
900	A Broad Family of Carbon Nanomaterials: Classification, Properties, Synthesis, and Emerging Applications. 2019 , 1-40	2

899	Physiological performance of ballan wrasse (Labrus bergylta) at different temperatures and its implication for cleaner fish usage in salmon aquaculture. 2019 , 135, 117-123	16
898	An integrative view of mammalian seasonal neuroendocrinology. 2019 , 31, e12729	44
897	Catch shares drive fleet consolidation and increased targeting but not spatial effort concentration nor changes in location choice in a multispecies trawl fishery. 2019 , 76, 2377-2389	3
896	A neural signature of metabolic syndrome. 2019 , 40, 3575-3588	10
895	Orthorexia nervosa: A review of psychosocial risk factors. 2019 , 140, 50-75	86
894	Pharmacological and transcriptomic characterization of the nitric oxide pathway in aortic rings isolated from the tortoise Chelonoidis carbonaria. 2019 , 222, 82-89	6
893	Expanding the applications of microneedles in dermatology. 2019 , 140, 121-140	38
892	An efficient model transfer approach to suppress biological variation in elastic modulus and firmness regression models using hyperspectral data. 2019 , 99, 140-151	2
891	Formation of graphene oxide from carbon rods of zinc-carbon battery wastes by audiosonic sonication assisted by commercial detergent. 2019 , 2, 89-94	6
890	Risk assessment of plastic pollution on marine diversity in the Mediterranean Sea. 2019 , 678, 188-196	58
889	An Autonomous Microfluidic Device for Generating Volume-Defined Dried Plasma Spots. 2019 , 91, 7125-7130	9
888	An Exonuclease I-Assisted Silver-Metallized Electrochemical Aptasensor for Ochratoxin A Detection. 2019 , 4, 1560-1568	33
887	Bilayer MSe (M´= Zr, Hf) as promising two-dimensional thermoelectric materials: a first-principles study 2019 , 9, 12394-12403	14
886	Prenatal liver stromal cells: Favorable feeder cells for long-term culture of hepatic progenitor cells. 2019 , 120, 16624-16633	3
885	Facile deposition and characterization of large area highly conducting and transparent Sb-doped SnO2 thin film. 2019 , 487, 1385-1393	31
884	Starfish-like C/CoNiO2 heterostructure derived from ZIF-67 with tunable microwave absorption properties. 2019 , 373, 122-130	85
883	A 3D imaging textural characterization of pyroclastic products from the 1538 AD Monte Nuovo eruption (Campi Flegrei, Italy). 2019 , 340-341, 316-331	12
882	Cancer and cancer survival modulates brain and behavior in a time-of-day-dependent manner in mice. <i>Scientific Reports</i> , 2019 , 9, 6497	7

881	Testing relationship recognition in wild jackdaws (Corvus monedula). Scientific Reports, 2019, 9, 6710	4.9	4
880	Understanding and Managing SocialEcological Tipping Points in Primary Industries. 2019, 69, 335-347		12
879	Hydrogen-Bond Structure and Dynamics of TADDOL Asymmetric Organocatalysts Correlate with Catalytic Activity. 2019 , 25, 9984-9990		2
878	Unveiling the Mechanisms of Aquaglyceroporin-3 Water and Glycerol Permeation by Metadynamics. 2019 , 25, 8713-8718		9
877	Technical applications of plasma treatments: current state and perspectives. 2019 , 103, 5117-5129		52
876	Desired soy sauce characteristics and autolysis of induced by low temperature conditions during initial fermentation. 2019 , 56, 2888-2898		8
875	Emergence of shallow energy levels in B-doped Q-carbon: A high-temperature superconductor. 2019 , 174, 153-159		7
874	Effects of moisture and electrode material on AlN-based resistive random access memory. 2019 , 45, 16311-16316		9
873	Antimicrobial activity and carbohydrate metabolism in the bacterial metagenome of the soil-living invertebrate Folsomia candida. <i>Scientific Reports</i> , 2019 , 9, 7308	4.9	9
872	Detection of Yellow Fever Virus in Sylvatic Mosquitoes during Disease Outbreaks of 2017?2018 in Minas Gerais State, Brazil. 2019 , 10,		15
871	HIV and GI Tract Complications. 2019,		
870	Facile and cost-effective strategy for fabrication of polyamide 6 wrapped multi-walled carbon nanotube via anionic melt polymerization of Etaprolactam. 2019 , 373, 251-258		15
869	Insights into the metabolism of membrane lipid fatty acids associated with chilling injury in post-harvest bell peppers. 2019 , 295, 26-35		30
868	Prioritizing global genetic capacity building assistance to implement CITES shark and ray listings. 2019 , 106, 103544		4
867	Mineral and organic fertilization alters the microbiome of a soil nematode Dorylaimus stagnalis and its resistome. 2019 , 680, 70-78		20
866	Electrostriction, Electroresistance, and Electromigration in Epitaxial BaTiO3-Based Heterostructures: Role of Interfaces and Electric Poling. 2019 , 2, 3556-3569		2
865	Defining Cell Cluster Size by Dielectrophoretic Capture at an Array of Wireless Electrodes of Several Distinct Lengths. 2019 , 10,		5

863	Resolution and scale controls on the accuracy of atoll island shorelines interpreted from satellite imagery. 2019 , 11, 339-352	3
862	Synergistic effects of low-/medium-vacuum carbonization on physico-chemical properties and stability characteristics of biochars. 2019 , 373, 44-57	20
861	Extreme Pedology: Elements of Theory and Methodological Approaches. 2019 , 52, 1-13	15
860	Soybean Seed Yield Response to Plant Density by Yield Environment in North America. 2019 , 111, 1923-1932	28
859	Facilitation of neuropathic pain by the NPY Y1 receptor-expressing subpopulation of excitatory interneurons in the dorsal horn. <i>Scientific Reports</i> , 2019 , 9, 7248	27
858	Brine Recycling from Industrial Textile Wastewater Treated by Ozone. By-Products Accumulation. Part 1: Multi Recycling Loop. 2019 , 11, 460	5
857	An insight into the first stages of the Ferrar magmatism: ultramafic cumulates from Harrow Peaks, northern Victoria Land, Antarctica. 2019 , 174, 1	2
856	Effects of Cu on conformational change and aggregation of hPrP180-192 with a V180I mutation of the prion protein. 2019 , 514, 798-802	1
855	Species distribution models with field validation, a key approach for successful selection of receptor sites in conservation translocations. 2019 , 19, e00653	6
854	Additive manufacturing of TiBAlBV parts through laser metal deposition (LMD): Process, microstructure, and mechanical properties. 2019 , 804, 163-191	118
853	An innovative catalyst of nickel-palladium alloy nanocrystals embedded nitrogen-doped graphene for efficient oxygen reduction reaction. 2019 , 797, 314-324	12
852	Hybrid dynamics in a paired rhythmic synchronizationBontinuation task. 2019 , 524, 625-638	1
851	Defining optimal electron transfer partners for light-driven cytochrome P450 reactions. 2019 , 55, 33-43	12
850	Glial cells as therapeutic targets in progressive multiple sclerosis. 2019 , 19, 481-494	7
849	Nanotechnology in Plant Science: To Make a Long Story Short. 2019 , 7, 120	133
848	Microwave-assisted extraction of chitosan from Rhizopus oryzae NRRL 1526 biomass. 2019 , 219, 431-440	22
847	Modifying the Organ Matrix Pre-engraftment: A New Transplant Paradigm?. 2019, 25, 626-639	3
846	Cu/ZnSOD always responded stronger and rapider than MnSOD in Lymantria dispar larvae under the avermectin stress. 2019 , 156, 72-79	7

(2021-2019)

845	CB2 receptor deletion on myeloid cells enhanced mechanical allodynia in a mouse model of neuropathic pain. <i>Scientific Reports</i> , 2019 , 9, 7468	.9	18
844	Interaction of synthesized nitrogen enriched graphene quantum dots with novel anti-Alzheimer's drugs: spectroscopic insights. 2020 , 38, 1822-1837		10
843	Indium Zinc Oxide Thin-Film Transistors with Ultraviolet Post-Annealing Treatment. 2019 , 19, 6170-6173		
842	The need for mathematical modelling of spatial drug distribution within the brain. 2019, 16, 12		39
841	Informational Structures and Informational Fields as a Prototype for the Description of Postulates of the Integrated Information Theory. 2019 , 21,		4
840	Urban Ecosystem Services Quantification through Remote Sensing Approach: A Systematic Review. 2019 , 6, 51		11
839	The Effect of Hot-Mounting on the Microstructure of an As-Quenched Auto-Tempered Low-Carbon Martensitic Steel. 2019 , 9, 550		8
838	Solvent-free, one-pot synthesis of nitrogen-tailored alkali-activated microporous carbons with an efficient CO2 adsorption. 2021 , 172, 71-82		71
837	Cu2ZnSnS4 nanoparticles synthesized via reaction media with glycine. 2021 , 47, 5071-5078		1
836	High efficiency removal of heavy metals using tire-derived activated carbon vs commercial activated carbon: Insights into the adsorption mechanisms. 2021 , 264, 128455		87
835	Ultrasound assisted synthesis of magnetic Fe3O4/?-MnO2 nanocomposite for photodegradation of organic dye. 2021 , 609, 125720		14
834	Review on major fruit flies (Diptera: Tephritidae) in North Africa: Bio-ecological traits and future trends. 2021 , 140, 105416		7
833	Meta-analysis of small for gestational age births and disinfection byproduct exposures. 2021 , 196, 110280)	7
832	A positive relationship between body height and the testosterone response to physical exercise. 2021 , 42, 179-185		3
831	Plastome evolution and phylogenetic relationships among Malvaceae subfamilies. 2021 , 765, 145103		12
830	Design and manufacturing of monodisperse and malleable phytantriol-based cubosomes for drug delivery applications. 2021 , 61, 102149		2
829	Folate-targeted nanomicelles containing silibinin as an active drug delivery system for liver cancer therapy. 2021 , 61, 102157		11
828	Interactions between microplastics and oil dispersion in the marine environment. 2021, 403, 123944		19

827	Main nitric oxide (NO) hallmarks to relieve arsenic stress in higher plants. 2021, 406, 124289	22
826	Adversarial brain multiplex prediction from a single brain network with application to gender fingerprinting. 2021 , 67, 101843	2
825	Plant survival under drought stress: Implications, adaptive responses, and integrated rhizosphere management strategy for stress mitigation. 2021 , 242, 126626	56
824	The effect of annealing on the selective laser melting of 2205 duplex stainless steel: Microstructure, grain orientation, and manufacturing challenges. 2021 , 134, 106643	17
823	Variation in \$\mathbb{1}\$5N from shell-associated organic matter in bivalves: Implications for studies of modern and fossil ecosystems. 2021 , 562, 110076	3
822	Wideband graphene-based near-infrared solar absorber using C-shaped rectangular sawtooth metasurface. 2021 , 126, 114493	18
821	Grain boundary character distribution in an additively manufactured austenitic stainless steel. 2021 , 192, 115-119	14
820	Quantitative mass spectrometry-based analysis of proteins related to cattle and their products - Focus on cows' milk beta-casein proteoforms. 2021 , 186, 112-118	4
819	Evidence and speculations: vaccines and therapeutic options for COVID-19 pandemic. 2021 , 17, 1113-1121	4
818	A Single-Center Prospective Comparative Study of Two Single-Use Flexible Ureteroscopes: LithoVue (Boston Scientific, USA) and Uscope PU3022a (Zhuhai Pusen, China). 2021 , 35, 274-278	1
817	Wing: A suitable nonlethal tissue type for repeatable and rapid telomere length estimates in bats. 2021 , 21, 421-432	4
816	Are we ready to track climate-driven shifts in marine species across international boundaries? - A global survey of scientific bottom trawl data. 2021 , 27, 220-236	19
815	Comparative analysis and antibacterial properties of thermally sintered apatites with varied processing conditions. 2021 , 104, 1023-1039	2
814	Altered dynamics of lipid metabolism in muscle cells from patients with idiopathic inflammatory myopathy is ameliorated by 6 months of training. 2021 , 599, 207-229	2
813	ADMA (asymmetric dimethylarginine) and angiogenic potential in patients with type 2 diabetes and prediabetes. 2021 , 246, 153-162	1
812	Cardiovascular 3D Printing. 2021 ,	O
811	Improving memory performance of PVA:ZnO nanocomposite: The experimental and theoretical approaches. 2021 , 537, 148000	2
810	Remote estimation of pulse wave features related to arterial stiffness and blood pressure using a camera. 2021 , 64, 102242	9

(2021-2021)

809	Flupyradifurone reduces nectar consumption and foraging but does not alter honey bee recruitment dancing. 2021 , 207, 111268	8
808	DNA meta-barcoding revealed that sika deer foraging strategies vary with season in a forest with degraded understory vegetation. 2021 , 484, 118637	6
807	Modelling the effects of twinning and dislocation induced strengthening in orthogonal micro and macro cutting of commercially pure titanium. 2021 , 190, 106045	7
806	A Dual-Mode Microwave Resonator for Liquid Chromatography Applications. 2021 , 21, 1222-1228	2
805	Downy mildew resistance is genetically mediated by prophylactic production of phenylpropanoids in hop. 2021 , 44, 323-338	4
804	A review of the role of genetic factors in Guillain-Barrြsyndrome. 2021 , 71, 902-920	8
803	Phosphorus Diffusion and Agronomic Efficiency of Chicken Litter Organomineral Fertilizers Improved with Binder Materials. 2021 , 12, 3765-3772	1
802	Synthesis of thermogel modified with biomaterials as carrier for hUSSCs differentiation into cardiac cells: Physicomechanical and biological assessment. 2021 , 119, 111517	2
801	Genetically Modified Crops. 2021 ,	O
800	Study of the effect of the different parts of Morinda citrifolia L. (noni) on the green synthesis of silver nanoparticles and their antibacterial activity. 2021 , 537, 147855	22
799		4
	silver nanoparticles and their antibacterial activity. 2021 , 537, 147855 Frailty syndrome and risk of cardiovascular disease: Analysis from the International Mobility in	
799	silver nanoparticles and their antibacterial activity. 2021, 537, 147855 Frailty syndrome and risk of cardiovascular disease: Analysis from the International Mobility in Aging Study. 2021, 92, 104279 A comprehensive review of the effect of different kinetic promoters on methane hydrate	4
799 798	silver nanoparticles and their antibacterial activity. 2021, 537, 147855 Frailty syndrome and risk of cardiovascular disease: Analysis from the International Mobility in Aging Study. 2021, 92, 104279 A comprehensive review of the effect of different kinetic promoters on methane hydrate formation. 2021, 32, 1-16 Microfluidic fabrication of berberine-loaded nanoparticles for cancer treatment applications. 2021,	3
799 798 797	Frailty syndrome and risk of cardiovascular disease: Analysis from the International Mobility in Aging Study. 2021, 92, 104279 A comprehensive review of the effect of different kinetic promoters on methane hydrate formation. 2021, 32, 1-16 Microfluidic fabrication of berberine-loaded nanoparticles for cancer treatment applications. 2021, 61, 102134 Biochar applications combined with paddy-upland rotation cropping systems benefit the safe use	4 3 5
799 798 797 796	Frailty syndrome and risk of cardiovascular disease: Analysis from the International Mobility in Aging Study. 2021, 92, 104279 A comprehensive review of the effect of different kinetic promoters on methane hydrate formation. 2021, 32, 1-16 Microfluidic fabrication of berberine-loaded nanoparticles for cancer treatment applications. 2021, 61, 102134 Biochar applications combined with paddy-upland rotation cropping systems benefit the safe use of PAH-contaminated soils: From risk assessment to microbial ecology. 2021, 404, 124123 How fluorine minimizes density fluctuations of silica glass: Molecular dynamics study with	4357
799 798 797 796 795	Frailty syndrome and risk of cardiovascular disease: Analysis from the International Mobility in Aging Study. 2021, 92, 104279 A comprehensive review of the effect of different kinetic promoters on methane hydrate formation. 2021, 32, 1-16 Microfluidic fabrication of berberine-loaded nanoparticles for cancer treatment applications. 2021, 61, 102134 Biochar applications combined with paddy-upland rotation cropping systems benefit the safe use of PAH-contaminated soils: From risk assessment to microbial ecology. 2021, 404, 124123 How fluorine minimizes density fluctuations of silica glass: Molecular dynamics study with machine-learning assisted force-matching potential. 2021, 197, 109210 Non-rhythmic temporal prediction involves phase resets of low-frequency delta oscillations. 2021,	 4 3 5 7 6

791	Coronary computed tomography angiography versus invasive coronary angiography: medical staff perceptions and diagnostic interest in Gaza-Palestine. 2021 , 190, 567-575	1
790	Actin networks regulate the cell membrane permeability during electroporation. 2021 , 1863, 183468	13
789	Localization of prostaglandin E2 synthases and E-prostanoid receptors in the spinal cord in a rat model of neuropathic pain. 2021 , 1750, 147153	1
788	Bimetallic chalcogenide nanocrystallites as efficient electrocatalyst for overall water splitting. 2021 , 852, 156736	8
787	Zero-valent palladium dissolution using NaCl/CuCl solutions. 2021, 404, 124184	2
786	Knowing what you need to know in advance: The neural processes underpinning flexible semantic retrieval of thematic and taxonomic relations. 2021 , 224, 117405	8
785	Cortico-spinal imaging to study pain. 2021 , 224, 117439	8
784	Marine microorganisms as an untapped source of bioactive compounds. 2021 , 28, 224-231	25
783	Systematic identification of safe harbor regions in the CHO genome through a comprehensive epigenome analysis. 2021 , 118, 659-675	5
782	Alkaloids derived from the genus Daphniphyllum. 2021 , 30, 1-14	2
781	A systematic evaluation of biomethane production from sugarcane trash pretreated by different methods. 2021 , 319, 124137	3
780	An overview of beneficiary aspects of zinc oxide nanoparticles on performance of cement composites. 2021 , 43, 892-898	7
779	Dissecting Alzheimer's disease pathogenesis in human 2D and 3D models. 2021 , 110, 103568	10
778	Polydopamine nanoparticles-assisted impedimetric sensor towards label-free lung cancer cell detection. 2021 , 119, 111549	7
777	Modeling the spread of multiple contagions on multilayer networks. 2021 , 563, 125410	1
776	Cardiac computational modelling. 2021 , 74, 65-71	1
775	Screening for Viruses and Lemur-Associated Filara in Wild-Caught Mosquitoes From Madagascar. 2021 , 58, 983-989	1
774	Phylogenomics of Piranhas and Pacus (Serrasalmidae) Uncovers How Dietary Convergence and Parallelism Obfuscate Traditional Morphological Taxonomy. 2021 , 70, 576-592	10

Clinical Oral Disorders in Adults Screening Protocol (CODA-SP) from the 2019 Vancouver IADR 773 Consensus Symposium. 2021, 38, 5-16 Functional characterization and expression profiling of glyoxalase III genes in date palm grown 772 under abiotic stresses. 2021, 172, 780-794 Ensemble coding of crowd speed using biological motion. 2021, 83, 1014-1035 771 \circ Impact of the March Arctic Oscillation on the South China Sea summer monsoon onset. 2021, 41, E3239 770 6 Potential role of viral metagenomics as a surveillance tool for the early detection of emerging 769 3 novel pathogens. 2021, 203, 865-872 Activated carbon loaded with Ni-Co-S nanoparticle for superior adsorption capacity of antibiotics 768 23 and dye from wastewater: Kinetics and isotherms. 2021, 611, 125868 Core-shell cadmium sulphide @ silver sulphide nanowires surface architecture: Design towards 767 15 photoelectrochemical solar cells. 2021, 587, 715-726 How honey bees dip nectar: Dynamic spacing of tongue hairs facilitates to collect nectar of various 766 viscosities. 2021, 512, 110538 Unraveling salt responsive metabolites and metabolic pathways using non-targeted metabolomics approach and elucidation of salt tolerance mechanisms in the xero-halophyte Haloxylon 765 14 salicornicum. 2021, 158, 284-296 Can shifts in metabolic scaling predict coevolution between diet quality and body size?. 2021, 75, 141-148 764 Brain micro-vasculature imaging: An unsupervised deep learning algorithm for segmenting mouse 763 O brain volume probed by high-resolution phase-contrast X-ray tomography. 2021, 31, 1211-1220 Emerging cellular and molecular determinants of idiopathic pulmonary fibrosis. 2021, 78, 2031-2057 762 40 761 MOFs-Based Nitric Oxide Therapy for Tendon Regeneration. 2020, 13, 23 8 Serum phospholipidomics reveals altered lipid profile and promising biomarkers in multiple 760 9 sclerosis. 2021, 697, 108672 Lauric acid ameliorates lipopolysaccharide (LPS)-induced liver inflammation by mediating 6 759 TLR4/MyD88 pathway in Sprague Dawley (SD) rats. 2021, 265, 118750 Krppel-like factor 6 promotes odontoblastic differentiation through regulating the expression of 758 dentine sialophosphoprotein and dentine matrix protein 1 genes. 2021, 54, 572-584 Little parallelism in genomic signatures of local adaptation in two sympatric, cryptic sister species. 1 757 2021, 34, 937-952 A role for calcium-dependent protein kinases in differential CO - and ABA-controlled stomatal 756 7 closing and low CO -induced stomatal opening in Arabidopsis. 2021, 229, 2765-2779

755	CRISPR-based enrichment strategies for targeted sequencing. 2021 , 46, 107672	5
754	Extrusion bioprinting: Recent progress, challenges, and future opportunities. 2021 , 21, e00116	15
753	Nanocomposite powders of hydroxyapatite-graphene oxide for biological applications. 2021 , 47, 7653-7665	6
75²	Estimating charge-transport properties of fuel-cell and electrolyzer catalyst layers via electrochemical impedance spectroscopy. 2021 , 367, 137521	9
75 ¹	The effect of activated carbon additives on lead sulphide thin film for solar cell applications. 2021 , 864, 158117	1
75°	Review of aquatic toxicity of pharmaceuticals and personal care products to algae. 2021 , 410, 124619	18
749	Mass spectrometric studies on the peptide integrity of substance P and related human tachykinins in human biofluids. 2021 , 136, 170458	
748	Ameliorative role of Bacillus subtilis FBL-10 and silicon against lead induced stress in Solanum melongena. 2021 , 158, 486-496	12
747	Temporally Distinct Roles for the Zinc Finger Transcription Factor Sp8 in the Generation and Migration of Dorsal Lateral Ganglionic Eminence (dLGE)-Derived Neuronal Subtypes in the Mouse. 2021 , 31, 1744-1762	1
746	Discriminating lineages of Batrachochytrium dendrobatidis using quantitative PCR. 2021 , 21, 1452-1459	1
745	Comparative effects of ascobin and glutathione on copper homeostasis and oxidative stress metabolism in mitigation of copper toxicity in rice. 2021 , 23 Suppl 1, 162-169	5
744	The Therapeutic Potential of Regulatory T Cells: Challenges and Opportunities. 2020 , 11, 585819	5
743	CPAS: the UK's national machine learning-based hospital capacity planning system for COVID-19. 2020 , 110, 1-21	10
742	Biosynthetic, biomimetic, and self-assembled vascularized Organ-on-a-Chip systems. 2021 , 268, 120556	9
741	The transcriptomic response of adult salmon lice (Lepeophtheirus salmonis) to reduced salinity. 2021 , 37, 100778	2
740	Numerical analysis of the pulsating heat source effects in a tumor tissue. 2021 , 200, 105887	7
739	Monitoring the quality of honey: South African case study. 2021 , 343, 128527	5
738	Elastic Foundation Induced Wide Bandgaps for Actively-tuned Topologically Protected Wave Propagation in Phononic Crystal Beams. 2021 , 194, 106215	15

737	Cell aggregation on nanorough surfaces. 2021 , 115, 110134	3
736	Nanoscale optical voltage sensing in biological systems. 2021 , 230, 117719	3
735	Evidence of recent flood deposits within a distal shelf depocenter and implications for terrestrial carbon preservation in non-deltaic shelf settings. 2021 , 431, 106376	1
734	Three-dimensional chromatin organization in cardiac development and disease. 2021 , 151, 89-105	4
733	Unique genomic traits for cold adaptation in Naganishia vishniacii, a polyextremophile yeast isolated from Antarctica. 2021 , 21,	3
732	Fluctuations in pelagic fish density linked to ambient conditions. 2021 , 98, 756-767	
731	The Entner-Doudoroff Pathway Is an Essential Metabolic Route for Methylotuvimicrobium buryatense 5GB1C. 2021 , 87,	3
730	A single fed wideband mode-reconfigurable OAM metasurface CP antenna array with simple feeding scheme. 2021 , 31, e22499	4
729	Comparison of in vivo and in situ detection of hippocampal metabolites in mouse brain using H-MRS. 2021 , 34, e4451	3
728	Surface preparation for 10% efficient CZTSe solar cells. 2021 , 29, 188-199	3
727	Interferon-inducer antivirals: Potential candidates to combat COVID-19. 2021 , 91, 107245	17
726	Parental RNA interference as a tool to study genes involved in rostrum development in the Neotropical brown stink bug, Euschistus heros. 2021 , 128, 104161	3
725	Mind the gap: A mechanobiological hypothesis for the role of gap junctions in the mechanical properties of injured brain tissue. 2021 , 115, 104240	O
724	Pinna nobilis in suboptimal environments are more tolerant to disease but more vulnerable to severe weather phenomena. 2021 , 163, 105220	10
723	Pathophysiological implications of neuroinflammation mediated HPA axis dysregulation in the prognosis of cancer and depression. 2021 , 520, 111093	12
722	Nanomaterials for Parkinson disease: Recent progress. 2021 , 1231, 129698	12
721	Unveiling Fourier Ptychography via Fisher Information. 2021 , 483, 126642	1
720	Toward complete rational control over protein structure and function through computational design. 2021 , 66, 170-177	5

719	Quantitative proteomic analysis of MDCK cell adhesion. 2021 , 17, 121-129	3
718	Increased burning in a warming climate reduces carbon uptake in the Greater Yellowstone Ecosystem despite productivity gains. 2021 , 109, 1148-1169	2
717	Model adequacy tests for probabilistic models of chromosome-number evolution. 2021 , 229, 3602-3613	4
716	How Does Fearful Emotion Affect Visual Attention?. 2020 , 11, 584412	1
715	Fabrication of zeolitic imidazolate frameworks based mixed matrix membranes and mass transfer properties of C4H6 and N2 in membrane separation. 2021 , 67, e17114	1
714	Impact of Taguchi design to prepare wool composite system based on CS/PEG/SiO2NPs to promote wool dyeability of acid dyeing. 2021 , 29, 1099-1111	
713	Clustering-based anomaly detection in multivariate time series data. 2021 , 100, 106919	21
712	Affinity-triggered hydrogels: Developments and prospects in biomaterials science. 2021 , 268, 120563	1
711	Inhibition of macrophage migration in zebrafish larvae demonstrates in vivo efficacy of human CCR2 inhibitors. 2021 , 116, 103932	1
710	Recent advances for assessment of the condensed phase heat of formation of high-energy content organic compounds and ionic liquids (or salts) to introduce a new computer code for design of desirable compounds. 2021 , 533, 112913	1
709	Multiparametric EEG analysis of brain network dynamics during neonatal seizures. 2021, 348, 109003	8
708	Human attachments shape interbrain synchrony toward efficient performance of social goals. 2021 , 226, 117600	16
707	The prefrontal cortex as a target for atypical antipsychotics in schizophrenia, lessons of neurodevelopmental animal models. 2021 , 199, 101967	8
706	Diagnostic approaches for the rapid detection of Zika virus review. 2021 , 101, 156-168	9
705	COVID-19 lockdown impact on cognitions and emotions experienced during sexual intercourse. 2021 , 30, e9-e21	5
704	Mildly acidic pH and room temperature triggered peroxidase-mimics of rGOftu3(OH)2(MoO4)2 cuboidal nanostructures: an effective colorimetric detection of neurotransmitter dopamine in blood serum and urine samples. 2021 , 23, 599-616	8
703	Drying methods and structure-activity relationships of hydroxycinnamic acid derivatives in Maxim. Leaves. 2021 , 12, 1651-1661	1
702	A promising technology for wound healing; and evaluation of chitosan nano-biocomposite films containing gentamicin. 2021 , 38, 100-107	4

701	Mesocrystal aggregation of biological apatite nanocrystals. 2021 , 4, e10155	О
700	Whispering-gallery mode resonance-assisted plasmonic sensing and switching in subwavelength nanostructures. 2021 , 56, 4716-4726	1
699	Toward asynchronous EEG-based BCI: Detecting imagined words segments in continuous EEG signals. 2021 , 65, 102351	3
698	Studies toward the comprehension of fungal-macroalgae interaction in cold marine regions from a biotechnological perspective. 2021 , 125, 218-230	6
697	The role of the chromosomal rearrangements in the evolution and speciation of Elopiformes fishes (Teleostei; Elopomorpha). 2021 , 290, 40-48	1
696	A state-of-the-art review on the application of natural surfactants in enhanced oil recovery. 2021 , 321, 114888	21
695	Mechanosensation in traumatic brain injury. 2021 , 148, 105210	13
694	Dust mitigation by rolling water droplets from hydrophobic surfaces. 2021 , 22, 100825	3
693	Lipoprotein Lipase and Its Regulators: An Unfolding Story. 2021 , 32, 48-61	21
692	The galloyl moiety enhances the inhibitory activity of catechins and theaflavins against Eglucosidase by increasing the polyphenol-enzyme binding interactions. 2021 , 12, 215-229	11
691	Beneficial bacteria associated with Mimosa pudica and potential to sustain plant growth-promoting traits under heavy metals stress. 2021 , 25, 1-21	4
690	SARS-CoV-2 variants evolved during the early stage of the pandemic and effects of mutations on adaptation in Wuhan populations. 2021 , 17, 97-106	22
689	Point-of-Care Pathogen Detection with CRISPR-based Programmable Nucleic Acid Binding Proteins. 2021 , 16, 1566-1575	2
688	Spatial-temporal distribution of climate suitability of winter wheat in North China Plain for current and future climate scenarios. 2021 , 143, 915-930	O
687	Silver nanowire-network-film-coated soft substrates with wrinkled surfaces for use as stretchable surface enhanced Raman scattering sensors. 2021 , 859, 157862	8
686	Universal sensing of ammonia gas by family of lead halide perovskites based on paper sensors: Experiment and molecular dynamics. 2021 , 136, 111142	10
685	Use of black soldier fly and house fly in feed to promote sustainable poultry production. 2021 , 7, 761-780	24
684	Crop Breeding. 2021,	O

683	Melatonin levels and microRNA (miRNA) relative expression profile in the follicular ambient microenvironment in patients undergoing in vitro fertilization process. 2021 , 38, 443-459	5
682	Methods matter: An examination of factors that moderate predictions of the capability model concerning the relationship of frontal asymmetry to trait measures. 2021 , 158, 107993	5
681	Allelic diversity and forensic estimations of the Beijing Hans: Comparative data on sequence-based and length-based STRs. 2021 , 51, 102424	4
680	Morphologically engineered metal oxides for the enhanced removal of multiple pollutants from water with degradation mechanism. 2021 , 9, 104852	6
679	On the stability of rotating pipes conveying fluid in annular liquid medium. 2021 , 494, 115891	7
678	Geometallurgy of cobalt ores: A review. 2021 , 160, 106656	31
677	Structure-function coupling in the human connectome: A machine learning approach. 2021 , 226, 117609	18
676	Research progress of nanoplastics in freshwater. 2021 , 757, 143791	15
675	Animal- free skin permeation analysis using mass spectrometry imaging. 2021 , 71, 105062	О
674	UV-Resonant Al Nanocrystals: Synthesis, Silica Coating, and Broadband Photothermal Response. 2021 , 21, 536-542	10
673	The hole transporting behaviour of Cu2AgInS4 and Cu2AgInSe4 for a carbon electrode-based perovskite solar cell. 2021 , 45, 423-430	5
672	Bacteriophages for ESKAPE: role in pathogenicity and measures of control. 2021 , 19, 845-865	5
671	Evaluating the anticancer properties and real-time electrochemical extracellular bio-speciation of bis (1,10-phenanthroline) silver (I) acetate monohydrate in the presence of A549 lung cancer cells. 2021 , 175, 112876	3
670	Surface velocity fields of active rock glaciers and ice-debris complexes in the Central Andes of Argentina. 2021 , 46, 504-522	5
669	The role of caveolin-1 in the biofate and efficacy of anti-tumor drugs and their nano-drug delivery systems. 2021 , 11, 961-977	7
668	Synthesis, design, and assessment of novel morpholine-derived Mannich bases as multifunctional agents for the potential enzyme inhibitory properties including docking study. 2021 , 107, 104524	5
667	Reactive fungal wearable. 2021 , 199, 104304	15
666	Computational study of elastic, structural stability and dynamics properties of penta-graphene membrane. 2021 , 542, 111052	9

665	The impact of chimerism on DNA-based human identification from skin surface cells of post-allogenic hematopoietic stem cell transplantation (HCST) patients. 2021 , 318, 110636	
664	ZnO-Al2O3-SiO2 glass ceramics: Influence of composition on crystal phases, crystallite size and appearance. 2021 , 553, 120481	5
663	Targeting Conservation Actions at Species Threat Response Thresholds. 2021, 36, 216-226	1
662	In situ anodic dissolutionDathodic deposition route for preparation of the PtBiW11Co/SiW11CoINP/GC electrode: application as an efficient electrode for the hydrogen evolution reaction. 2021 , 11, 1098-1109	1
661	MRGPRX2 activation in mast cells by neuromuscular blocking agents and other agonists: Modulation by sugammadex. 2021 , 51, 685-695	11
660	Evidence of no horizontal or vertical transmission of tomato severe rugose virus by Bemisia tabaci MEAM1. 2021 , 70, 987-993	
659	Osmoregulation and its actions during the drought stress in plants. 2021 , 172, 1321-1335	40
658	Structure of the Bacterial Cellulose Ribbon and Its Assembly-Guiding Cytoskeleton by Electron Cryotomography. 2021 , 203,	9
657	Molecular insights into symbiosis-mapping sterols in a marine flatworm-algae-system using high spatial resolution MALDI-2-MS imaging with ion mobility separation. 2021 , 413, 2767-2777	10
656	Recent progress on transition metal oxides and carbon-supported transition metal oxides as catalysts for thermal decomposition of ammonium perchlorate. 2021 , 17, 1471-1485	10
655	Gut microbiota modulation by both Lactobacillus fermentum MSK 408 and ketogenic diet in a murine model of pentylenetetrazole-induced acute seizure. 2021 , 169, 106506	10
654	Biofilm formation on cat claws by Sporothrix species: An ex vivo model. 2021 , 150, 104670	2
653	Extended regorafenib treatment can be linked with mitochondrial damage leading to cardiotoxicity. 2021 , 336, 39-49	8
652	Pattern recognition: An effective tool for quality assessment of herbal medicine based on chemical information. 2021 , 35, e3305	1
651	Physical exercise stimulates hippocampal mTORC1 and FNDC5/irisin signaling pathway in mice: Possible implication for its antidepressant effect. 2021 , 400, 113040	4
650	Biosorption of iron ions through microalgae from wastewater and soil: Optimization and comparative study. 2021 , 265, 129172	2
649	Engineering approaches for effective therapeutic applications based on extracellular vesicles. 2021 , 330, 15-30	19
648	Squeezing through the microcirculation: survival adaptations of circulating tumour cells to seed metastasis. 2021 , 124, 58-65	9

647	Revisiting gene delivery to the brain: silencing and editing. 2021 , 9, 1065-1087	5
646	Dietary tributyrin modifies intestinal function by altering morphology, gene expression and microbiota profile in common carp (Cyprinus carpio) fed all-plant diets. 2021 , 27, 439-453	7
645	Polarization insensitive multilayered broadband absorber for L and S bands of the radar spectrum. 2021 , 63, 1229-1235	3
644	Tracking exogenous intracellular casp-3 using split GFP. 2021 , 30, 366-380	3
643	Perinatal COVID-19: review of current evidence and practical approach towards prevention and management. 2021 , 180, 1009-1031	18
642	Effect of treatments on seed dormancy breaking, seedling growth, and seedling antioxidant potential of Agrimonia eupatoria L 2021 , 20, 100282	4
641	Nitrogen-fixing trees in mixed forest systems regulate the ecology of fungal community and phosphorus cycling. 2021 , 758, 143711	7
640	Highly antifouling and chlorine resistance polyamide reverse osmosis membranes with g-C3N4 nanosheets as nanofiller. 2021 , 258, 117980	14
639	Emerging therapeutic targets for schizophrenia: a framework for novel treatment strategies for psychosis. 2021 , 25, 15-26	4
638	An S-ribonuclease binding protein EBS1 and brassinolide signaling are specifically required for Arabidopsis tolerance to bicarbonate. 2021 , 72, 1449-1459	4
637	Genetic predisposition to the development of congenital heart diseases: Role of xenobiotic biotransformation genes. 2021 , 113, 579-588	1
636	GSDME and its role in cancer: From behind the scenes to the front of the stage. 2021 , 148, 2872-2883	16
635	Delayed urea differential enhancement CEST (dudeCEST)-MRI with T correction for monitoring renal urea handling. 2021 , 85, 2791-2804	O
634	Reduced Graphene Oxide Thin Film with Strong Optical Nonlinearity. 2021 , 258, 2000397	3
633	Investigations on interactions between vortex flow and the induced string cavitation characteristics in real-size diesel tapered-hole nozzles. 2021 , 287, 119535	3
632	Additive manufacturing of high entropy alloys: A practical review. 2021 , 77, 131-162	69
631	Widespread occurrence of methane seeps in deep-water regions of Krishna-Godavari basin, Bay of Bengal. 2021 , 124, 104783	8
630	Linking Cognitive Impairment to Neuroinflammation in Multiple Sclerosis using neuroimaging tools. 2021 , 47, 102622	1

629	Porous bioactive glass micro- and nanospheres with controlled morphology: developments, properties and emerging biomedical applications. 2021 , 8, 300-335	21	
628	Enhancing ductility and fatigue strength of additively manufactured metallic materials by preheating the build platform. 2021 , 44, 257-270	6	
627	Structural and Functional Diversity of Resistance-Nodulation-Cell Division Transporters. 2021 , 121, 5378	3-5416 16	
626	Macrophage metabolic reprogramming during chronic lung disease. 2021, 14, 282-295	28	
625	Beyond the neural correlates of consciousness: using brain stimulation to elucidate causal mechanisms underlying conscious states and contents. 2021 , 51, 143-170	O	
624	Organ-specific toxicity of magnetic iron oxide-based nanoparticles. 2021 , 15, 167-204	12	
623	The interplay between executive control, behavioural variability and mind wandering: Insights from a high-definition transcranial direct-current stimulation study. 2021 , 53, 1498-1516	1	
622	Automatic counting methods in aquaculture: A review. 2021 , 52, 269-283	8	
621	Advances and clinical challenges for translating nerve conduit technology from bench to bed side for peripheral nerve repair. 2021 , 383, 617-644	15	
620	Non-spike timing-dependent plasticity learning mechanism for memristive neural networks. 2021 , 51, 3684-3695	4	
619	Methane and nitrous oxide emission characteristics of high-yielding rice field. <i>Environmental Science and Pollution Research</i> , 2021 , 28, 15021-15031	5.1 0	
618	Haematological, biochemical and immunological biomarkers, antibacterial activity, and survival in Nile tilapia Oreochromis niloticus after treatment using antimicrobial peptide LL-37 against Streptococcus agalactiae. 2021 , 533, 736181	8	
617	Progress in layered cathode and anode nanoarchitectures for charge storage devices: Challenges and future perspective. 2021 , 35, 443-469	18	
616	Role of extreme weather events and El Nië Southern Oscillation on incidence of Enteric Fever in Ahmedabad and Surat, Gujarat, India. 2021 , 196, 110417	2	
615	Extended-spectrum beta-lactamase-producing Escherichia coli and antimicrobial resistance in municipal and hospital wastewaters in Czech Republic: Culture-based and metagenomic approaches. 2021 , 193, 110487	6	
614	Doxycycline reverses cognitive impairment, neuroinflammation and oxidative imbalance induced by D-amphetamine mania model in mice: A promising drug repurposing for bipolar disorder treatment?. 2021 , 42, 57-74	2	
613	Damage or benefit? How future scenarios of climate change may affect the distribution of small pelagic fishes in the coastal seas of the Americas. 2021 , 234, 105815	2	
612	Thermochronology of South America passive margin between Uruguay and southern Brazil: A lengthy and complex cooling history based on (UIIh)/He and fission tracks. 2021 , 106, 103019	0	

611	Localization of multiple diffusion sources based on overlapping community detection. 2021, 226, 106613	1
610	A review on recent near infrared spectroscopic measurement setups and their challenges. 2021 , 171, 108732	3
609	Tunable control of electromagnetically induced transparency effect in a double slot terahertz waveguide. 2021 , 483, 126632	3
608	A Polar outlook: Potential interactions of micro- and nano-plastic with other anthropogenic stressors. 2021 , 754, 142379	11
607	Revisiting the role of factor H in age-related macular degeneration: Insights from complement-mediated renal disease and rare genetic variants. 2021 , 66, 378-401	7
606	Influence of interference effects on the spectral quality and histological classification by FT-IR imaging in transflection geometry. 2021 , 146, 646-654	2
605	The fungal and archaeal community within plant rhizosphere: a review on their contribution to crop safety. 2021 , 44, 600-618	6
604	Corrosion behaviours of arc-sprayed AlSi-based amorphous/nanocrystalline coating. 2021, 37, 606-617	3
603	Impacts of variable nutrient stoichiometry (N, Si and P) on a coastal phytoplankton community from the SW Bay of Bengal, India. 2021 , 56, 273-288	1
602	Phase plates in the transmission electron microscope: operating principles and applications. 2021 , 70, 75-115	8
601	The ameliorative effects of Lactobacillus coagulans and Lactobacillus casei probiotics on CCl4-induced testicular toxicity based on biochemical, histological and molecular analyses in rat. 2021 , 53, e13908	6
600	RAB5A is associated with genes involved in exosome secretion: Integration of bioinformatics analysis and experimental validation. 2021 , 122, 425-441	7
599	Evolutionary study of COVID-19, severe acute respiratory syndrome coronavirus 2 (SARS-CoV-2) as an emerging coronavirus: Phylogenetic analysis and literature review. 2021 , 7, 559-571	9
598	Role of Exosomes in Biological Communication Systems. 2021,	2
597	Trends and variability of ocean waves under RCP8.5 emission scenario in the Mediterranean Sea. 2021 , 71, 97-117	12
596	A photo-crosslinkable cartilage-derived extracellular matrix bioink for auricular cartilage tissue engineering. 2021 , 121, 193-203	27
595	Surface composite engineering of polyimide to create amine functionalities for autocatalytic metallization. 2021 , 541, 148500	3
594	Ultrasensitive detection of interleukin 1 sing 3-phosphonopropionic acid modified FTO surface as an effective platform for disposable biosensor fabrication. 2021 , 138, 107698	3

593	Membrane tension may define the deadliest virus infection. 2021 , 40, 100338	1
592	The impact of pre- and post-image processing techniques on deep learning frameworks: A comprehensive review for digital pathology image analysis. 2021 , 128, 104129	37
591	A review of the impact of xenobiotics from dietary sources on infant health: Early life exposures and the role of the microbiota. 2021 , 269, 115994	4
590	Bactericidal materials prepared via conjugation of responsive polymers to cysteine. <i>Materials Today Communications</i> , 2021 , 26, 101813	2
589	Climate change versus land-use change-What affects the ecosystem services more in the forest-steppe ecotone?. 2021 , 759, 143525	20
588	Phase evolution in novel Y2O3 dispersed CrCuFeNiZn nanocrystalline multicomponent alloy prepared by mechanical alloying. 2021 , 184, 109802	2
587	Chronic 4-Na/K-ATPase inhibition reverses the elongation of the axon initial segment of the hippocampal CA1 pyramidal neurons in Angelman syndrome model mice. 2021 , 46, 654-664	2
586	A comparative study of antimicrobial activity of differently-synthesized chitosan nanoparticles against bovine mastitis pathogens. 2021 , 17, 694-703	3
585	Proportion optimization of grouting materials for roadways with soft surrounding mass. 2021 , 18, 203-218	2
584	Characterisation of sperm piRNAs and their correlation with semen quality traits in swine. 2021 , 52, 114-120	4
583	High responsiveness of auditory neurons to specific combination of acoustic features in female songbirds. 2021 , 53, 1412-1427	0
582	The evolutionary history of the human oral microbiota and its implications for modern health. 2021 , 85, 90-100	7
581	Lactic Acid Bacteria in Wine: Technological Advances and Evaluation of Their Functional Role. 2020 , 11, 612118	23
580	Assessing the impact of taxon resolution on network structure. 2021 , 102, e03256	1
579	Prefusion spike protein stabilization through computational mutagenesis. 2021 , 89, 399-408	1
578	Nucleolin regulates 14-3-3[mRNA and promotes cofilin phosphorylation to induce tunneling nanotube formation. 2021 , 35, e21199	3
577	Oceanic dispersal barriers in a holoplanktonic gastropod. 2021 , 34, 224-240	6
576	International consensus statement on allergy and rhinology: rhinosinusitis 2021. 2021 , 11, 213-739	97

575	Quantifying energetic and fitness consequences of seasonal heterothermy in an Arctic ungulate. 2021 , 11, 338-351	6
574	Timing of Foliar Calcium Sprays Improves Fruit Firmness and Antioxidants in 🛭 iberty 🗷 lueberries. 2021 , 21, 426-436	4
573	Deployment of wild relatives for genetic improvement in rice (Oryza sativa). 2021, 140, 23-52	5
572	The role of 3D printing during COVID-19 pandemic: a review. 2021 , 6, 19-37	26
571	Frequency of bovine viral diarrhea virus (BVDV) in Argentinean bovine herds and comparison of diagnostic tests for BVDV detection in bovine serum samples: a preliminary study. 2021 , 52, 467-475	O
570	ATN incorporating cerebrospinal fluid neurofilament light chain detects frontotemporal lobar degeneration. 2021 , 17, 822-830	9
569	Nanoscience and nanotechnology in fabrication of scaffolds for tissue regeneration. 2021 , 11, 1-23	
568	Electrochemical performance of composites made of rGO with Zn-MOF and PANI as electrodes for supercapacitors. 2021 , 367, 137563	12
567	Nanosized Co3O4MoS2 heterostructure electrodes for improving the oxygen evolution reaction in an alkaline medium. 2021 , 853, 156946	14
566	Micro- and nano-plastic pollution: Behavior, microbial ecology, and remediation technologies. 2021 , 291, 125240	23
565	A state-of-the-art review on WWTP associated bioaerosols: Microbial diversity, potential emission stages, dispersion factors, and control strategies. 2021 , 410, 124686	9
564	genomC: A Database to Explore the Association between Genetic Variation (SNPs) and CpG Methylation in the Human Genome. 2021 , 433, 166709	O
563	Comparative study of the immune responses to the HMS-based fusion protein and capsule-based conjugated molecules as vaccine candidates in a mouse model of Staphylococcus aureus systemic infection. 2021 , 150, 104656	
562	Ferroelectric polarization-enhanced charge separation in quantum dots sensitized semiconductor hybrid for photoelectrochemical hydrogen production. 2021 , 81, 105626	9
561	HOX transcript antisense RNA: An oncogenic lncRNA in diverse malignancies. 2021, 118, 104578	4
560	Relevant Physicochemical Methods to Functionalize, Purify, and Characterize Surface-Decorated Lipid-Based Nanocarriers. 2021 , 18, 44-64	2
559	Mutational drivers of cancer cell migration and invasion. 2021 , 124, 102-114	22
558	Triggering factors and threshold analysis of baishuihe landslide based on the data mining methods. 2021 , 105, 2677-2696	8

(2021-2021)

557	Environmental prevalence, fate, impacts, and mitigation of microplastics-a critical review on present understanding and future research scope. <i>Environmental Science and Pollution Research</i> , 5.1 2021 , 28, 4951-4974	12
556	The Network Ontogeny of the Parrot: Altriciality, Dynamic Skeletal Assemblages, and the Avian Body Plan. 2021 , 48, 41-53	2
555	Expanding Materials Selection Via Transfer Learning for High-Temperature Oxide Selection. 2021 , 73, 103-115	2
554	Genome-Wide Analysis of Heat Shock Transcription Factors in Ziziphus jujuba Identifies Potential Candidates for Crop Improvement Under Abiotic Stress. 2021 , 193, 1023-1041	2
553	Genome-wide analysis of Hsp70 and Hsp100 gene families in Ziziphus jujuba. 2021 , 26, 341-353	4
552	Colorimetric Sensors for Toxic and Hazardous Gas Detection: A Review. 2021 , 17, 1-17	19
551	In vitro calcification studies on bioprosthetic and decellularized heart valves under quasi-physiological flow conditions. 2021 , 4, 10-21	О
550	Potential regional declines in species richness of tomato pollinators in North America under climate change. 2021 , 31, e02259	О
549	Metabarcoding as a tool to enhance marine surveillance of nonindigenous species in tropical harbors: A case study in Tahiti. 2021 , 3, 173-189	6
548	Multidisciplinary Treatment of Colorectal Cancer. 2021 ,	O
548 547	Multidisciplinary Treatment of Colorectal Cancer. 2021, Challenges and possible solutions to mitigate the problems of single-use plastics used for packaging food items: a review. 2021, 58, 3251-3269	12
	Challenges and possible solutions to mitigate the problems of single-use plastics used for	
547	Challenges and possible solutions to mitigate the problems of single-use plastics used for packaging food items: a review. 2021 , 58, 3251-3269 The relationship of cortical activity induced by pain stimulation with clinical and cognitive features	12
547 546	Challenges and possible solutions to mitigate the problems of single-use plastics used for packaging food items: a review. 2021 , 58, 3251-3269 The relationship of cortical activity induced by pain stimulation with clinical and cognitive features of somatic symptom disorder: A controlled functional near infrared spectroscopy study. 2021 , 140, 110300	12
547 546 545	Challenges and possible solutions to mitigate the problems of single-use plastics used for packaging food items: a review. 2021 , 58, 3251-3269 The relationship of cortical activity induced by pain stimulation with clinical and cognitive features of somatic symptom disorder: A controlled functional near infrared spectroscopy study. 2021 , 140, 110300 Behaviour moderates the impacts of food-web structure on species coexistence. 2021 , 24, 298-309	12
547 546 545	Challenges and possible solutions to mitigate the problems of single-use plastics used for packaging food items: a review. 2021, 58, 3251-3269 The relationship of cortical activity induced by pain stimulation with clinical and cognitive features of somatic symptom disorder: A controlled functional near infrared spectroscopy study. 2021, 140, 110300 Behaviour moderates the impacts of food-web structure on species coexistence. 2021, 24, 298-309 Scaffold-free biofabrication of adipocyte structures with magnetic levitation. 2021, 118, 1127-1140	12 1 2
547 546 545 544 543	Challenges and possible solutions to mitigate the problems of single-use plastics used for packaging food items: a review. 2021, 58, 3251-3269 The relationship of cortical activity induced by pain stimulation with clinical and cognitive features of somatic symptom disorder: A controlled functional near infrared spectroscopy study. 2021, 140, 110300 Behaviour moderates the impacts of food-web structure on species coexistence. 2021, 24, 298-309 Scaffold-free biofabrication of adipocyte structures with magnetic levitation. 2021, 118, 1127-1140 Functional analysis of CD44 variants and xCT in canine tumours. 2021, 7, 577-585 Dissecting the non-neuronal cell contribution to Parkinson's disease pathogenesis using induced	12 1 2 5

539	Nephroprotective effect of ethanol extract and fractions of a sea lettuce, Ulva fasciata against cisplatin-induced kidney injury in rats. <i>Environmental Science and Pollution Research</i> , 2021 , 28, 9448-9461 ^{5.1}	7
538	Introduction. 2021 , 1-17	
537	Advances in phycobiliproteins research: innovations and commercialization. 2021, 57-81	3
536	Detection of a novel glycodelin biomarker using electrochemical immunosensor for endometriosis. 2021 , 1146, 146-154	2
535	Characterization of a novel endo-levanase from Azotobacter chroococcum DSM 2286 and its application for the production of prebiotic fructooligosaccharides. 2021 , 255, 117384	2
534	Advances in generation of three-dimensional skin equivalents: pre-clinical studies to clinical therapies. 2021 , 23, 1-9	7
533	Environmental impacts of solar photovoltaic systems: A critical review of recent progress and future outlook. 2021 , 759, 143528	59
532	Biochemical and histopathological responses in peripubertal male rats exposed to agrochemicals isolated or in combination: A multivariate data analysis study. 2021 , 447, 152636	2
531	Therapeutic Ultrasound Parameter Optimization for Drug Delivery Applied to a Murine Model of Hepatocellular Carcinoma. 2021 , 47, 309-322	5
530	Peculiar relationships among morphology, burrowing performance and sand type in two fossorial microteiid lizards. 2021 , 144, 125880	O
529	Opportunities for the application of real-time bacterial cell analysis using flow cytometry for the advancement of sterilization microbiology. <i>Journal of Applied Microbiology</i> , 2021 , 130, 1794-1812	6
528	miR-146a regulates insulin sensitivity via NPR3. 2021 , 78, 2987-3003	5
527	Carbon dots Beparative techniques: Tools-objective towards green analytical nanometrology focused on bioanalysis. 2021 , 161, 105773	3
526	Characterization of novel human intragenic antimicrobial peptides, incorporation and release studies from ureasil-polyether hybrid matrix. 2021 , 119, 111581	4
525	Effective anticorrosive performance of benzo-imidazo-pyrimidine-g-graphene oxide composite coating for copper in natural and artificial sea water. 2021 , 22, 100828	4
524	Metabolic design for selective production of nicotinamide mononucleotide from glucose and nicotinamide. 2021 , 65, 167-177	8
523	Diversification of Fungal Chitinases and Their Functional Differentiation in Histoplasma capsulatum. 2021 , 38, 1339-1355	3
522	Thymol-Loaded Biogenic Silica Nanoparticles in an Aquatic Environment: The Impact of Particle Aggregation on Ecotoxicity. 2021 , 40, 333-341	O

(2021-2021)

521	Silver nanoparticles improved the plant growth and reduced the sodium and chlorine accumulation in pearl millet: a life cycle study. <i>Environmental Science and Pollution Research</i> , 2021 , 28, 13712-13724	1 17
520	The Interplay Between Adolescent Friendship Quality and Resilient Functioning Following Childhood and Adolescent Adversity. 2021 , 2, 37-50	5
519	Electrospun PGS/PCL, PLLA/PCL, PLGA/PCL and pure PCL scaffolds for retinal progenitor cell cultivation. 2021 , 166, 107846	12
518	Carboxymethyl cellulose nanocomposite beads as super-efficient catalyst for the reduction of organic and inorganic pollutants. 2021 , 167, 101-116	15
517	The Earth's magnetic field of the last centuries from the perspective of the Jequitinhonha and Mucuri river valleys: A natural observatory of the South Atlantic Anomaly in Brazil. 2021 , 108, 102984	O
516	Organoids and organ chips in ophthalmology. 2021 , 19, 1-15	16
515	Effect of steam velocity during dropwise condensation. 2021 , 165, 120624	6
514	The Role of the Establishment of Causal Connections and the Modality of Presentation of Discourse in the Generation of Emotion Inferences by Argentine College Students. 2021 , 42, 22-41	1
513	Optimal Target Control of Complex Networks With Selectable Inputs. 2021 , 8, 212-221	2
512	Glass: The carrier of lightPart IIA brief look into the future of optical fiber. 2021 , 12, 3-24	5
511	Population genomics for wildlife conservation and management. 2021, 30, 62-82	51
510	The "cheerleader effect" in facial and bodily attractiveness: A result of memory bias and not perceptual encoding. 2021 , 74, 972-980	2
509	Factors influencing the acquisition and eradication of early Pseudomonas aeruginosa infection in cystic fibrosis. 2021 , 20, 8-16	7
508	Mild and large-scale synthesis of nanoscale metal-organic framework used as a potential adenine-based drug nanocarrier. 2021 , 61, 102135	7
507	Comparison of different MyotonPRO probes for skin stiffness evaluation in young women. 2021 , 27, 332-339	1
506	Surface receptor-mediated targeted drug delivery systems for enhanced cancer treatment: A state-of-the-art review. 2021 , 82, 309-340	14
505	Assessment of pulmonary toxicity of potential antioxidant drug PEGylated nanoceria after intratracheal instillation in rats. 2021 , 41, 941-952	2
504	Current Trends in Microbial Biotechnology for Agricultural Sustainability: Conclusion and Future Challenges. 2021 , 555-572	34

503	Rational design of novel CrZrOx catalysts for efficient low temperature SCR of NOx. 2021 , 413, 127554	7
502	A data science approach for advanced solid polymer electrolyte design. 2021 , 187, 110108	2
501	Improved green biosynthesis of chitosan decorated Ag- and CoO-nanoparticles: A relationship between surface morphology, photocatalytic and biomedical applications. 2021 , 32, 102331	14
500	An update on the association between traumatic brain injury and Alzheimer's disease: Focus on Tau pathology and synaptic dysfunction. 2021 , 120, 372-386	7
499	The Musashi proteins MSI1 and MSI2 are required for photoreceptor morphogenesis and vision in mice. 2021 , 296, 100048	6
498	Transcription factors as key molecular target to strengthen the drought stress tolerance in plants. 2021 , 172, 847-868	26
497	A systematic review of the label accuracy of cannabinoid-based products in regulated markets: is what's on the label what's in the product?. 2021 , 29, 88-96	1
496	Unnatural trend of global land long-term surface air temperature change. 2021 , 41, 2330-2341	2
495	Use of alternative protein sources for fishmeal replacement in the diet of largemouth bass (Micropterus salmoides). Part I: effects of poultry by-product meal and soybean meal on growth, feed utilization, and health. 2021 , 53, 33-47	18
494	The transcriptome of anterior regeneration in earthworm Eudrilus eugeniae. 2021 , 48, 259-283	2
493	Ultra-efficient reconstruction of 3D microstructure and distribution of properties of random heterogeneous materials containing multiple phases. 2021 , 204, 116526	12
492	Deep learning model for predicting phase diagrams of block copolymers. 2021 , 188, 110224	11
491	Gene expression profiling of corona virus microarray datasets to identify crucial targets in COVID-19 patients. 2021 , 22, 100980	6
490	Droplet stretching between hydrophobic and hydrophilic plates: Droplet fluid heating. 2021 , 120, 105010	
489	Deciphering indigenous bacteria in compacted bentonite through a novel and efficient DNA extraction method: Insights into biogeochemical processes within the Deep Geological Disposal of nuclear waste concept. 2021 , 408, 124600	6
488	An in vitro investigation into the release of fugitive medical aerosols into the environment during manual ventilation. 2021 , 108, 135-141	2
487	Antifungal immune responses in mosquitoes (Diptera: Culicidae): A review. 2021 , 178, 107505	5
486	NF- B -mediated effects on behavior and cartilage pathology in a non-invasive loading model of post-traumatic osteoarthritis. 2021 , 29, 248-256	7

485	Enhanced precipitation strengthening of multi-principal element alloys by 🛭 and B2-phases. 2021 , 198, 109315	4
484	Osteogenic differentiation cues of the bone morphogenetic protein-9 (BMP-9) and its recent advances in bone tissue regeneration. 2021 , 120, 111748	9
483	Simultaneous doxorubicin encapsulation and in-situ microfluidic micellization of bio-targeted polymeric nanohybrids using dichalcogenide monolayers: A molecular in-silico study. <i>Materials Today Communications</i> , 2021 , 26, 101948	12
482	Neural and phenotypic representation under the free-energy principle. 2021 , 120, 109-122	4
481	Dissociable neural indices for time and space estimates during virtual distance reproduction. 2021 , 226, 117607	3
480	Transglutaminase 2 as a novel target in chronic kidney disease - Methods, mechanisms and pharmacological inhibition. 2021 , 222, 107787	3
479	The effects of chromium supplementation on lipidprofile in humans: A systematic review and meta-analysis ofrandomized controlled trials. 2021 , 164, 105308	1
478	CRISPR/Cas genome editing to optimize pharmacologically active plant natural products. 2021 , 164, 105359	8
477	Measuring salivary markers of inflammation in health research: A review of methodological considerations and best practices. 2021 , 124, 105069	9
476	Ectoparasites reduce scope for growth in a rocky-shore mussel (Perna perna) by raising maintenance costs. 2021 , 753, 142020	4
475	An overview of methods of fine and ultrafine particle collection for physicochemical characterisation and toxicity assessments. 2021 , 756, 143553	15
474	The effects of land use on spatial pattern of urban green spaces and their cooling ability. 2021 , 35, 100743	18
473	Drop squeezing between arbitrary smooth obstacles. 2021 , 908,	2
472	Oxygen Isotopic Signatures of Major Climate Modes and Implications for Detectability in Speleothems. 2021 , 48,	4
471	Relationship Between C 4 Biomass and C 4 Agriculture During the Holocene and its Implications for Millet Domestication in Northeast China. 2021 , 48,	1
470	Tandem solar cells efficiency prediction and optimization deep learning. <i>Physical Chemistry Chemical Physics</i> , 2021 , 23, 2991-2998	2
469	Power-dependent upconversion luminescence properties of self-sensitized ErWO phosphor. 2021 , 50, 229-239	9
468	Surface modifications of carbon nanodots reveal the chemical source of their bright fluorescence. 2021 , 3, 716-724	7

467	Ex vivo binding studies of the anti-cancer drug noscapine with human hemoglobin: a spectroscopic and molecular docking study. 2021 , 45, 1525-1534		1
466	Fungi and their secondary metabolites in water-damaged indoors after a major flood event in eastern Croatia. 2021 , 31, 730-744		5
465	Evidence-based point-of-care technology development during the COVID-19 pandemic. 2021 , 70, 58-67		6
464	Ridge-furrow rainfall harvesting planting and its effect on soil erosion and soil quality in sloping farmland. 2021 , 113, 863-877		2
463	Automated plankton classification from holographic imagery with deep convolutional neural networks. 2021 , 19, 21-36		9
462	Role of Dietary Micronutrients on Gut Microbial Dysbiosis and Modulation in Inflammatory Bowel Disease. 2021 , 65, 1901271		3
461	Development of temperature-assisted solidification of floating organic droplet-based dispersive liquid incroextraction performed during centrifugation for extraction of organochlorine pesticide residues in cocoa powder prior to GC-ECD. <i>Chemical Papers</i> , 2021 , 75, 1691-1700	1.9	2
460	Economic loss due to diseases in Indian shrimp farming with special reference to Enterocytozoon hepatopenaei (EHP) and white spot syndrome virus (WSSV). 2021 , 533, 736231		20
459	Alter macrophage adhesion and modulate their response on hydrophobically modified hydrogels. 2021 , 165, 107821		5
458	Gated temporal convolutional neural network and expert features for diagnosing and explaining physiological time series: A case study on heart rates. 2021 , 200, 105847		3
457	Comparison of segmentation algorithms for FIB-SEM tomography of porous polymers: Importance of image contrast for machine learning segmentation. 2021 , 171, 110806		1
456	A multiscale modeling of damage accumulation and permeability variation in shale rocks under mechanical loading. 2021 , 198, 108123		3
455	Occurrence, predictors and hazards of elevated groundwater arsenic across India through field observations and regional-scale AI-based modeling. 2021 , 759, 143511		26
454	Wearable and Biodegradable Sensors for Clinical and Environmental Applications. 2021 , 3, 68-100		20
453	Effect of Auricularia auricula fermentation broth on the liver and stomach of mice with acute alcoholism. 2021 , 12, 191-202		4
45 ²	Nanoparticle-mediated gene therapy strategies for mitigating inflammatory bowel disease. 2021 , 9, 1481-1502		5
451	Zingiber zerumbet L. essential oil-based chitosan nanoemulsion as an efficient green preservative against fungi and aflatoxin B contamination. 2021 , 86, 149-160		7
450	Variation in the management of Kawasaki disease in Australia and New Zealand: A survey of paediatricians. 2021 , 57, 646-652		

449	The zero-shear-rate limiting rheological behaviors of ideally conductive particles suspended in concentrated dispersions under an electric field. 2021 , 65, 13-26	1
448	The Effects of Soil Depth on the Structure of Microbial Communities in Agricultural Soils in Iowa, USA. 2020 ,	16
447	Anaerobic wastewater treatment and reuse enabled by thermophilic bioprocessing integrated with a bioelectrochemical/ultrafiltration module. 2021 , 321, 124406	6
446	Large Sensitivity of Simulated Indian Summer Monsoon Rainfall (ISMR) to Global Warming: Implications of ISMR Projections. 2021 , 126,	3
445	Surface contacts strongly influence the elasticity and thermal conductivity of silica nanoparticle fibers. <i>Physical Chemistry Chemical Physics</i> , 2021 , 23, 3707-3715	2
444	Mental health consequences of infections by coronaviruses including severe acute respiratory syndrome coronavirus 2 (SARS-CoV-2). 2021 , 11, e01901	6
443	Diffusion-PEPTIDE: Distortion- and blurring-free diffusion imaging with self-navigated motion-correction and relaxometry capabilities. 2021 , 85, 2417-2433	3
442	The Response of Growth and Yield of Canola Genotypes to Humic Acid Application in Different Plant Densities. 2021 , 73, 17-27	5
441	How Wheat Pericarp Alter Fungal Growth and Toxigenicity Profiles. 2021, 46, 5299-5306	
440	Improved self-healing performance of polymeric nanocomposites reinforced with talc nanoparticles (TNPs) and urea-formaldehyde microcapsules (UFMCs). <i>Arabian Journal of Chemistry</i> , 5.9 2021 , 14, 102926	15
439	Cryogel/hydrogel biomaterials and acupuncture combined to promote diabetic skin wound healing through immunomodulation. 2021 , 269, 120608	34
438	Electrochemical performance of polymer-derived SiOC and SiTiOC ceramic electrodes for artificial cardiac pacemaker applications. 2021 , 47, 7593-7601	2
437	Forensic taphonomy: Characterization of the gravesoil chemistry using a multivariate approach combining chemical and volatile analyses. 2021 , 318, 110569	2
436	Experimental/computational assessments of steel in HCl medium containing aminocarbonitrile-incorporated polyhydroxy-functionalized pyrido[2,3-d]pyrimidine as a green corrosion inhibitor. 2021 , 321, 114902	6
435	Comprehensive assessment of amino acid substitutions in the trimeric RNA polymerase complex of influenza A virus detected in clinical trials of baloxavir marboxil. 2021 , 15, 389-395	11
434	Aerosol-deposited Al2O3/PTFE hydrophobic coatings with adjustable transparency. 2021 , 104, 1716-1725	3
433	Loss of Arabidopsis matrix metalloproteinase-5 affects root development and root bacterial communities during drought stress. 2021 , 172, 1045-1058	2
432	Is there evidence that periodontal diseases are risk factors for coronary arterial disease?-Scoping review. 2021 , 41, 66-77	

431	The Impact of Experimentally Induced Limb Ischemia on the Rubber Hand Illusion. 2021, 50, 88-96	4
430	The Role of Pathogen Dynamics and Immune Gene Expression in the Survival of Feral Honey Bees. 2021 , 8,	3
429	The dysregulation of metabolic pathways and induction of the pentose phosphate pathway in renal ischaemia-reperfusion injury. 2021 , 253, 404-414	5
428	Analysis of lipopolysaccharides by coupling microscale solid-phase extraction with capillary electrophoresis-laser induced fluorescence. 2021 , 161, 105771	4
427	Comparison of Short- and Long-Term Toxicity of Microplastics with Different Chemical Constituents on Button Polyps. (Protopalythoa sp.). 2021 , 5, 12-22	6
426	Perovskite quantum dots integrated with vertically aligned graphene toward ambipolar multifunctional photodetectors. 2021 , 9, 609-619	8
425	Petroleum waste hydrocarbon resin as a carbon source modified on a Si composite as a superior anode material in lithium ion batteries. 2021 , 259, 124011	7
424	Towards a point-of-care SERS sensor for biomedical and agri-food analysis applications: a review of recent advancements. 2021 , 13, 553-580	40
423	Organic composition of three different size ranges of aerosol particles over the Southern Ocean. 2021 , 55, 268-288	3
422	Predator preferences shape the diets of arthropodivorous bats more than quantitative local prey abundance. 2021 , 30, 855-873	7
421	Age-related changes in gaze behaviour during social interaction: An eye-tracking study with an embodied conversational agent. 2021 , 74, 1128-1139	0
420	Dynamic functional networks in idiopathic normal pressure hydrocephalus: Alterations and reversibility by CSF tap test. 2021 , 42, 1485-1502	4
419	Antifungal properties of natural products from Pterocarya tonkinensis against phytopathogenic fungi. 2021 , 77, 1864-1872	3
418	Substrate stoichiometry changes during pulsed laser deposition: a case study on SrTiO3. 2021 , 203, 116461	9
417	3D culture models to study SARS-CoV-2 infectivity and antiviral candidates: From spheroids to bioprinting. 2021 , 44, 31-42	11
416	Estimation of missing values in aggregate level spatial data. 2021 , 9, 304-309	2
415	The impact of family environment on the life satisfaction among young adults with personality as a mediator. 2021 , 120, 105653	6
414	High-temperature synthesis in activated powder mixtures under conditions of linear heating: NiAl system. 2021 , 223, 88-97	6

413	Stress corrosion cracking behavior of selected stainless steels in saturated potash brine solution at different temperatures. 2021 , 178, 109025	3
412	Relationship of arsenic and chromium availability with carbon functional groups, aluminum and iron in Little Washita River Experimental Watershed Reservoirs, Oklahoma, USA. 2021 , 207, 111468	1
411	Variations in rifampicin and isoniazid resistance associated genetic mutations among drug nalle and recurrence cases of pulmonary tuberculosis. 2021 , 103, 56-61	2
410	Assessing tree diversity and carbon density of a riparian zone within a protected area in southern Philippines. 2021 , 14, 78-86	O
409	Characterization method for calculating diffusion coefficient of drug from polylactic acid (PLA) microneedles into the skin. 2021 , 61, 102192	10
408	Peptide-assisted pre-bonding remineralization of dentin to improve bonding. 2021 , 113, 104119	5
407	Void shrinkage in 21Cr32Ni austenitic model alloy during in-situ ion irradiation. 2021 , 543, 152636	Ο
406	Tumor associated tissue eosinophilia in oral squamous cell carcinoma: A systematic review and meta-analysis. 2021 , 11, 33-39	Ο
405	Preoperative brain MRI features and occurrence of postoperative delirium. 2021, 140, 110301	4
404	POEMS (POLYMERIC OPTO-ELECTRO-MECHANICAL SYSTEMS) FOR ADVANCED NEURAL INTERFACES. 2021 , 285,	3
403	Evaluation of microwave acid baking on Indian red mud sample. 2021 , 160, 106686	5
402	Solubilisation of salicylate in F127 micelles: Effect of pH and temperature on morphology and interactions with cyclodextrin. 2021 , 322, 114892	3
401	The cellular boundary with high density of dislocations governed the strengthening mechanism in selective laser melted 316L stainless steel. 2021 , 799, 140279	23
400	Anatoxin-a degradation by using titanium dioxide. 2021 , 756, 143590	1
399	What the dingo says about dog domestication. 2021 , 304, 19-30	7
398	Effects of anthropogenic habitat disturbance and infection on a sentinel species' gut bacteria. 2021 , 11, 45-57	2
397	Comparing environmental DNA metabarcoding and underwater visual census to monitor tropical reef fishes. 2021 , 3, 142-156	16
396	Detecting fish assemblages with environmental DNA: Does protocol matter? Testing eDNA metabarcoding method robustness. 2021 , 3, 619-630	2

395	Lateral and longitudinal fish environmental DNA distribution in dynamic riverine habitats. 2021 , 3, 305-318	9
394	Fisetin: An anticancer perspective. 2021 , 9, 3-16	24
393	Extended-amygdala intrinsic functional connectivity networks: A population study. 2021 , 42, 1594-1616	3
392	Vitamin D and Clinical Cancer Outcomes: A Review of Meta-Analyses. 2021 , 5, e10420	10
391	Research on improved wavelet convolutional wavelet neural networks. 2021 , 51, 4106-4126	9
390	Subtilisin like proteins in the war between Grapevine and Plasmopara viticola isolates with contrasting aggressiveness. 2021 , 159, 433-439	1
389	Patching Hele-Shaw Cells to Investigate the Flow at Low Reynolds Number in Fracture Networks. 2021 , 136, 147-163	2
388	Dominant drivers of plant community assembly vary by soil type and time in reclaimed forests. 2021 , 222, 159-171	4
387	Educators reflecting on sleep and rest time dilemmas in ECEC: where is the Britical In reflective practices?. 2021 , 48, 697-719	
386	Symbiotic fungi in nature Finnish peat moss promote vegetative growth in rabbiteye blueberry cuttings. 2021 , 62, 191-198	3
385	In Vitro Anti-diabetic Activity of Free Amino Acid and Protein Amino Acid Extracts from Four Iranian Medicinal Plants. 2021 , 45, 443-454	1
384	Breaking Deadlocks: Reward Probability and Spontaneous Preference Shape Voluntary Decisions and Electrophysiological Signals in Humans. 2021 , 4, 191-212	1
383	Spatio-temporal changes in water-related ecosystem services provision and trade-offs with food production. 2021 , 286, 125316	8
382	Microneedles for painless transdermal immunotherapeutic applications. 2021 , 330, 185-217	64
381	Characterization of Adult and Neonatal Articular Cartilage From the Equine Stifle. 2021, 96, 103294	
380	Static interaction between colloidal carbon nano-dots and aniline: A novel platform for ultrasensitive detection of aniline in aqueous media. 2021 , 134, 111119	8
379	Effect of rare earth elements on coatings developed by thermal spraying processes (TSP) [A brief review. 2021 , 44, 4053-4058	4
378	A Clearinghouse for Genome-Edited Crops and Field Testing. 2021 , 14, 3-5	2

377	Lanthanum doped dicalcium phosphate bone cements for potential use as filler for bone defects. <i>Materials Today Communications</i> , 2021 , 26, 101774	2.5	4
376	An integrated strategic framework for large-scale crop planning: sustainable climate-smart crop planning and agri-food supply chain management. 2021 , 26, 709-732		7
375	Effect of melting time on volatility, OH in glass in microwave processing. 2021, 36, 426-434		1
374	Oil field microorganisms cause highly localized corrosion on chemically inhibited carbon steel. 2021 , 14, 171-185		5
373	Directly converted astrocytes retain the ageing features of the donor fibroblasts and elucidate the astrocytic contribution to human CNS health and disease. 2021 , 20, e13281		10
372	Exploring views on alcohol consumption and digital support for alcohol reduction in UK-based Punjabi-Sikh men: A think aloud and interview study. 2020 , 40, 231		1
371	Association of beta-hydroxybutyrate with development of heart failure: Sex differences in a Dutch population cohort. 2021 , 51, e13468		8
370	Modulation of binocular rivalry with rapid monocular visual stimulation. 2021 , 53, 1008-1018		
369	Globally consistent reef size spectra integrating fishes and invertebrates. 2021, 24, 572-579		5
368	Evolutionary responses of marine organisms to urbanized seascapes. 2021 , 14, 210-232		8
367	Suppressing evolution in genetically engineered systems through repeated supplementation. 2021 , 14, 348-359		
366	Dominant wintertime surface air temperature modes in the Northern Hemisphere extratropics. 2021 , 56, 687-698		2
365	Auditory and Visual Tasks Influence the Temporal Dynamics of EEG Microstates During Post-encoding Rest. 2021 , 34, 19-28		4
364	Synthesize optimization, characterization, and application of ZIF-8 adsorbent for elimination of olive oil from aqueous solution. <i>Environmental Science and Pollution Research</i> , 2021 , 28, 12725-12739	5.1	4
363	Microbial Inactivation by Non-equilibrium Short-Pulsed Atmospheric Pressure Dielectric Barrier Discharge (Cold Plasma): Numerical and Experimental Studies. 2021 , 13, 136-147		5
362	Use of compost and phosphate-solubilizing bacteria affect sugarcane mineral nutrition, phosphorus availability, and the soil bacterial community. <i>Applied Soil Ecology</i> , 2021 , 157, 103760	5	27
361	Automatic diagnosis of cardiovascular disorders by sub images of the ECG signal using multi-feature extraction methods and randomized neural network. 2021 , 64, 102260		7
360	Low velocity impact response of 3D printed structures formed by cellular metamaterials and stiffening plates: PLA vs. PETg. 2021 , 256, 113128		13

359	Targeting Atg4B for cancer therapy: Chemical mediators. 2021 , 209, 112917	4
358	Landscape composition is more important than local vegetation structure for understory birds in cocoa agroforestry systems. 2021 , 481, 118704	9
357	Mo2C nanospheres anchored on nickel foam as self-supported electrode for high-performance hydrogen production. 2021 , 294, 121825	2
356	Discovery of the Paleocene-Eocene Thermal Maximum in shallow-marine sediments of the Xigaze forearc basin, Tibet: A record of enhanced extreme precipitation and siliciclastic sediment flux. 2021 , 562, 110095	8
355	The dynamic nature of the Mre11-Rad50 DNA break repair complex. 2021 , 163, 14-22	O
354	Climate-induced denudational changes during the Little Ice Age inferred from 10Be (meteoric)/9Be ratio: A case study from the core monsoon zone of India. 2021 , 599-600, 107-116	5
353	Substance P blocks	1
352	Circular Polarization Selective Metamaterial Absorber in Terahertz Frequency Range. 2021 , 27, 1-6	4
351	Smartphone ophthalmoscopy: a potential way forward for non-ophthalmology medics in the COVID-19 era. 2021 , 7, 237-239	O
350	Dry powder inhalers: a concise summary of the electronic monitoring devices. 2021 , 12, 1-6	8
350 349	Dry powder inhalers: a concise summary of the electronic monitoring devices. 2021 , 12, 1-6 Covid-19 pandemic in the lens of food safety and security. 2021 , 193, 110405	24
349	Covid-19 pandemic in the lens of food safety and security. 2021 , 193, 110405 Rhizoremediation of Heavy Metal- and Xenobiotic-Contaminated Soil: An Eco-Friendly Approach.	24
349 348	Covid-19 pandemic in the lens of food safety and security. 2021 , 193, 110405 Rhizoremediation of Heavy Metal- and Xenobiotic-Contaminated Soil: An Eco-Friendly Approach. 2021 , 95-113 Production and characterization of bacterial cellulose scaffold and its modification with hyaluronic	24 6
349 348 347	Covid-19 pandemic in the lens of food safety and security. 2021 , 193, 110405 Rhizoremediation of Heavy Metal- and Xenobiotic-Contaminated Soil: An Eco-Friendly Approach. 2021 , 95-113 Production and characterization of bacterial cellulose scaffold and its modification with hyaluronic acid and gelatin for glioblastoma cell culture. 2021 , 28, 117-132 Paleolimnology in support of archeology: a review of past investigations and a proposed	24 6 5
349 348 347 346	Covid-19 pandemic in the lens of food safety and security. 2021, 193, 110405 Rhizoremediation of Heavy Metal- and Xenobiotic-Contaminated Soil: An Eco-Friendly Approach. 2021, 95-113 Production and characterization of bacterial cellulose scaffold and its modification with hyaluronic acid and gelatin for glioblastoma cell culture. 2021, 28, 117-132 Paleolimnology in support of archeology: a review of past investigations and a proposed framework for future study design. 2021, 65, 1-32 Protein Enrichment of Cassava-Based Dried Distiller® Grain by Solid State Fermentation Using	24651
349 348 347 346 345	Covid-19 pandemic in the lens of food safety and security. 2021, 193, 110405 Rhizoremediation of Heavy Metal- and Xenobiotic-Contaminated Soil: An Eco-Friendly Approach. 2021, 95-113 Production and characterization of bacterial cellulose scaffold and its modification with hyaluronic acid and gelatin for glioblastoma cell culture. 2021, 28, 117-132 Paleolimnology in support of archeology: a review of past investigations and a proposed framework for future study design. 2021, 65, 1-32 Protein Enrichment of Cassava-Based Dried Distiller Grain by Solid State Fermentation Using Trichoderma Harzianum and Yarrowia Lipolytica for Feed Ingredients. 2021, 12, 3875-3888	24 6 5 1

341	Surface interactions with the metal oxide surface control Ru nanoparticle formation and catalytic performance. 2021 , 610, 125722	3
340	The gut microbiota in anxiety and depression - A systematic review. 2021 , 83, 101943	81
339	BiFeO3-Thiourea/Carbon heterostructure based self-powered white light photodetector. 2021 , 284, 128906	5
338	Modulation of nonlinear optical properties in CdS based core shell nanocolloids fostered by metal nanoparticles. 2021 , 134, 106626	4
337	RUVBL1-RUVBL2 AAA-ATPase: a versatile scaffold for multiple complexes and functions. 2021 , 67, 78-85	6
336	The bifunctional role of copper nanoparticles in tomato: Effective treatment for Fusarium wilt and plant growth promoter. 2021 , 277, 109810	19
335	Extraction strategies for tackling complete hair metabolome using LC-HRMS-based analysis. 2021 , 223, 121708	4
334	Integrated correction of optical distortions for global HR-EBSD techniques. 2021 , 221, 113158	8
333	A review of the methods for studying biotic interactions in phenological analyses. 2021 , 12, 227-244	2
332	Hemangiol in infantile haemangioma: A paediatric post-marketing surveillance drug study. 2021 , 87, 1970-1980	2
331	Remove or retain: ecosystem effects of woody encroachment and removal are linked to plant structural and functional traits. 2021 , 229, 2637-2646	7
330	Forecasting monthly fluctuations of lake surface areas using remote sensing techniques and novel machine learning methods. 2021 , 143, 713-735	8
329	Response of ammonia-oxidizing archaea and bacteria to sulfadiazine and copper and their interaction in black soils. <i>Environmental Science and Pollution Research</i> , 2021 , 28, 11357-11368	1
328	Thermoregulation and energetics. 2021 , 237-260	O
327	Changes in fine root decomposition of primary Pinus koraiensis forest after clear cutting and restoration succession into secondary broad-leaved forest. <i>Applied Soil Ecology</i> , 2021 , 158, 103785	6
326	Niosomal virosome derived by vesicular stomatitis virus glycoprotein as a new gene carrier. 2021 , 534, 980-987	7
325	Influence of reduced graphene oxide (rGO) on phase development and porosity of SiOC/rGO ceramic composites. 2021 , 47, 6030-6040	3
324	Unravelling high-affinity binding compounds towards transmembrane protease serine 2 enzyme in treating SARS-CoV-2 infection using molecular modelling and docking studies. 2021 , 890, 173688	16

323	Estimation of laryngeal closure duration during swallowing without invasive X-rays. 2021 , 115, 610-618	8
322	Nickel decorated MoO3 single crystal microflakes with multi-site functionality for enhanced hydrogen evolution reaction. 2021 , 46, 1945-1954	4
321	A novel hybrid quantum-PSO and credal decision tree ensemble for tropical cyclone induced flash flood susceptibility mapping with geospatial data. 2021 , 596, 125682	11
320	SARS-CoV-2 variants lacking a functional ORF8 may reduce accuracy of serological testing. 2021 , 488, 112906	10
319	Intercellular Communication in the Heart: Therapeutic Opportunities for Cardiac Ischemia. 2021 , 27, 248-262	18
318	Altered behaviour, dopamine and norepinephrine regulation in stressed mice heterozygous in TPH2 gene. 2021 , 108, 110155	2
317	Application of laser induced breakdown spectroscopy for direct and quick determination of fuel property of woody biomass pellets. 2021 , 164, 1204-1214	2
316	Microbial decomposition of soil organic matter determined by edaphic characteristics of mangrove forests in East Asia. 2021 , 763, 142972	5
315	Detection of microbial contamination based on uracil-selective synthetic receptors. 2021 , 224, 121813	3
314	Molecular and morphological diversity in species of Kronichthys (Teleostei, Loricariidae) from Atlantic coastal rivers of Brazil. 2021 , 98, 668-679	1
313	Bacillus thuringiensis Cry1Ab Domain III 即 6 Is Involved in Binding to Prohibitin, Which Correlates with Toxicity against Helicoverpa armigera (Lepidoptera: Noctuidae). 2021 , 87,	1
312	AG490 protects cerebral ischemia/reperfusion injury via inhibiting the JAK2/3 signaling pathway. 2021 , 11, e01911	2
311	Large colloidal probes for atomic force microscopy: Fabrication and calibration issues. 2021 , 34, e2879	4
310	Fe3O4 Nanoparticles Capped with PEG Induce Apoptosis in Breast Cancer AMJ13 Cells Via Mitochondrial Damage and Reduction of NF-B Translocation. 2021 , 31, 1241-1259	25
309	Assessment of Aerosol optical depth under background and polluted conditions using AERONET and VIIRS datasets. <i>Atmospheric Environment</i> , 2021 , 245, 117994	2
308	On the association between high outdoor thermo-hygrometric comfort index and severe ground-level ozone: A first investigation. 2021 , 195, 110306	3
307	Mixed halide CsPb(Br1-xlx)3 nanocrystals for green, orange, and red light-emitting diodes. 2021 , 858, 157643	2
306	Fabrication of nanocomposites mediated from aluminium nanoparticles/Moringa oleifera gum activated carbon for effective photocatalytic removal of nitrate and phosphate in aqueous solution. 2021 , 281, 124553	18

305	Investigating the True Effect of Psychological Variables Measured Prior to Arthroplastic Surgery on Postsurgical Outcomes: A P-Curve Analysis. 2021 , 22, 400-414	О
304	Facile preparation of a novel biomass-derived H3PO4 and Mn(NOMactivated carbon from citrus bergamia peels for high-performance supercapacitors. <i>Materials Today Communications</i> , 2021 , 26, 1017795	3
303	Photocatalytic treatment of natural waters. Reality or hype? The case of cyanotoxins remediation. 2021 , 188, 116543	35
302	The role of the cerebellum in creativity and expert stone knapping. 2021 , 29, 217-229	O
301	Multifunctional sodium alginate fabric based on reduced graphene oxide and polypyrrole for wearable closed-loop point-of-care application. 2021 , 406, 126778	12
300	Association between dietary factors and brown adipose tissue volume/F-FDG uptake in young adults. 2021 , 40, 1997-2008	2
299	Non-targeted metabolomics reveal the impact of phenanthrene stress on root exudates of ten urban greening tree species. 2021 , 196, 110370	6
298	Numerical investigation of wideband L-shaped metasurface based solar absorber for visible and ultraviolet region. 2021 , 601, 412503	19
297	Beyond synchrony: the capacity of fMRI hyperscanning for the study of human social interaction. 2021 , 16, 84-92	16
296	Accurate whole-mount bone and cartilage staining requires acid-free conditions. 2021 , 304, 958-960	O
295	Establishing the allosteric mechanism in CRISPR-Cas9. 2021 , 11, e1503	12
294	Employing geochemistry and geochronology to unravel genesis and tectonic setting of iron oxide-apatite deposits of the Bafq-Saghand metallogenic belt, Central Iran. 2021 , 110, 127-164	3
293	An anatomically detailed and personalizable head injury model: Significance of brain and white matter tract morphological variability on strain. 2021 , 20, 403-431	27
292	Atomistic simulation of martensitic transformations induced by deformation of 臣e single crystal during the mode-I fracture. 2021 , 56, 2275-2295	2
291	Microwave Processing of Low-Grade Banded Iron Ore with Different Reductants. 2021 , 38, 151-160	1
290	Effect of binary zinc-magnesium oxides on polyphenylsulfone/cellulose acetate derivatives hollow fiber membranes for the decontamination of arsenic from drinking water. 2021 , 405, 126809	9
289	3D printed bioceramics fabricated using negative thermoresponsive hydrogels and silicone oil sealing to promote bone formation in calvarial defects. 2021 , 47, 5464-5476	2
288	Nanostructured Biomaterials for Models of Bone Metastasis Cancer. 2021 , 17,	3

287	Folic acid based carbon dot functionalized stearic acid-g-polyethyleneimine amphiphilic nanomicelle: Targeted drug delivery and imaging for triple negative breast cancer. 2021 , 197, 111382	14
286	Deep and machine learning techniques for medical imaging-based breast cancer: A comprehensive review. 2021 , 167, 114161	52
285	Physiological and oral parameters contribute prediction of retronasal aroma release in an elderly cohort. 2021 , 342, 128355	14
284	Diagnostic value of digital droplet polymerase chain reaction and digital multiplexed detection of single-nucleotide variants in pancreatic cytology specimens collected by EUS-guided FNA. 2021 , 93, 1142-115	51. <mark>ē</mark> 2
283	Nanoparticles in sustainable agriculture: An emerging opportunity. 2021 , 329, 1234-1248	60
282	Material composition and associated toxicological impact assessment of mobile phones. 2021 , 9, 104603	4
281	Effect of magnetic-field-induced restructuring on the elastic properties of magnetoactive elastomers. 2021 , 517, 167392	2
280	Corneal stromal wound healing: Major regulators and therapeutic targets. 2021 , 19, 290-306	14
279	Understanding Host-Pathogen-Vector Interactions with Chronic Asymptomatic Malaria Infections. 2021 , 37, 195-204	1
278	Race against the Machine: can deep learning recognize microstructures as well as the trained human eye?. 2021 , 193, 33-37	8
277	Machine learning based surrogate modeling approach for mapping crystal deformation in three dimensions. 2021 , 193, 1-5	16
276	HDL and cancer - causality still needs to be confirmed? Update 2020. 2021 , 73, 169-177	7
275	Stem lodging resistance in hulless barley: Transcriptome and metabolome analysis of lignin biosynthesis pathways in contrasting genotypes. 2021 , 113, 935-943	2
274	Recent progress in extrusion 3D bioprinting of hydrogel biomaterials for tissue regeneration: a comprehensive review with focus on advanced fabrication techniques. 2021 , 9, 535-573	89
273	Breakdown of the superplastic deformation behavior of heterogeneous nanomaterials at small length scales. 2021 , 9, 41-49	2
272	A walk on the dirt: soil microbial forensics from ecological theory to the crime lab. 2021 , 45,	1
271	Device architectures for low voltage and ultrafast graphene integrated phase modulators. 2021 , 27, 1-9	10
270	Who inhabits the world deepest crater lake? A taxonomic review of Corbicula (Bivalvia: Cyrenidae) clams from Lake Toba, North Sumatra, Indonesia. 2021 , 59, 400-410	O

269	Machine Learning Enables Selection of Epistatic Enzyme Mutants for Stability Against Unfolding and Detrimental Aggregation. 2021 , 22, 904-914	7
268	Comprehensive Phenotyping of Dendritic Cells in Cancer Patients by Flow Cytometry. 2021 , 99, 218-230	2
267	Photocatalytic performance improvement by utilizing GO_MWCNTs hybrid solution on sand/ZnO/TiO-based photocatalysts to degrade methylene blue dye. <i>Environmental Science and Pollution Research</i> , 2021 , 28, 6966-6979	5
266	Detection of major depressive disorder using vocal acoustic analysis and machine learning In exploratory study. 2021 , 37, 53-64	6
265	Multi-omics integration in biomedical research - A metabolomics-centric review. 2021 , 1141, 144-162	31
264	Effects of burning harvested residues on the archaeal and bacterial communities of Eucalyptus urophylla substituting native vegetation. <i>Applied Soil Ecology</i> , 2021 , 158, 103796	6
263	Prolidase - A protein with many faces. 2021 , 183, 3-12	3
262	Lattice-Boltzmann simulation of dissolution of carbonate rock during CO2-saturated brine injection. 2021 , 408, 127235	10
261	A simple and sustainable beamhouse by the recycling of waste-water from KCl-dispase synergistic unhairing in leather making. 2021 , 282, 124535	7
260	Imprint of Kairei and Pelagia deep-sea hydrothermal systems (Indian Ocean) on marine dissolved organic matter. 2021 , 152, 104141	3
259	Optical coherence tomography angiography in diabetic retinopathy: an updated review. 2021 , 35, 149-161	26
258	Genetic and genomic resources for finger millet improvement: opportunities for advancing climate-smart agriculture. 2021 , 35, 204-233	9
257	Synergistic effect of ZnO nanoparticles with organic compound as corrosion inhibition. 2021 , 16, 429-435	5
256	The conserved brassinosteroid-related transcription factor BIM1a negatively regulates fruit growth in tomato. 2021 , 72, 1181-1197	2
255	Gender differences in mothers' spatial language use and children's mental rotation abilities in Preschool and Kindergarten. 2021 , 24, e13037	4
254	Artificial nightlight alters the predatorBrey dynamics of an apex carnivore. 2021 , 44, 149-161	13
253	Fractal analysis of the infiltration curve and soil particle size in a semi-humid watershed. 2021 , 72, 1373-1394	2
252	Role of Nature of Rare Earth Ion Dopants on Structural, Spectral, and Magnetic Properties in Spinel Ferrites. 2021 , 34, 1745-1751	2

251	EEG power spectral density in locked-in and completely locked-in state patients: a longitudinal study. 2021 , 15, 473-480	4
250	Evaluation and prediction of the biogenic amines in Chinese traditional broad bean paste. 2021 , 58, 2734-274	80
249	Impact of a Nature-Inspired Engineered Soil Structure on Microbial Diversity and Community Composition in the Bulk Soil and Rhizosphere of Tomato Grown Under Saline Irrigation Water. 2021 , 21, 173-186	О
248	Enhancing soil water holding capacity and provision of a potassium source via optimization of the pyrolysis of bamboo biochar. 2021 , 3, 51-61	10
247	An upwelling area as a hot spot for mercury biomonitoring in a climate change scenario: A case study with large demersal fishes from Southeast Atlantic (SE-Brazil). 2021 , 269, 128718	1
246	Supplementation of ram's semen extender with Mito-TEMPO I: Improvement in quality parameters and reproductive performance of cooled-stored semen. 2021 , 98, 215-218	5
245	An ecological approach to climate change-informed tree species selection for reforestation. 2021 , 481, 118705	7
244	Peptide conjugation enhances the cellular co-localization, but not endosomal escape, of modular poly(acrylamide-co-methacrylic acid) nanogels. 2021 , 329, 1162-1171	4
243	Measuring network rationality and simulating information diffusion based on network structure. 2021 , 564, 125501	4
242	Characterization of MXenes at every step, from their precursors to single flakes and assembled films. 2021 , 120, 100757	80
241	Long-range mechanical signaling in biological systems. 2021 , 17, 241-253	7
240	A Discreet Wearable IoT Sensor for Continuous Transdermal Alcohol Monitoring - Challenges and Opportunities. 2021 , 21, 5322-5330	6
239	Highly Sensitive Electrochemical Impedance- Based Biosensor for Label-Free and Wide Range Detection of Fibrinogen Using Hydrothermally Grown AlFeO3 Nanospheres Modified Electrode. 2021 , 21, 4160-4166	2
238	Expanding the molecular spectrum and the neurological phenotype related to CAMTA1 variants. 2021 , 99, 259-268	1
237	Multisensory action effects facilitate the performance of motor sequences. 2021 , 83, 475-483	2
236	Bioaerosol measurements over a fattening period in a pig barn focused on the presence of Staphylococcus spp 2021 , 37, 1-12	2
235	Active-screen plasma multi-functionalization of graphene oxide for supercapacitor application. 2021 , 56, 3296-3311	5
234	Effects of Land Use Patterns on the Bacterial Community Structure and Diversity of Wetland Soils in the Sanjiang Plain. 2021 , 21, 1-12	5

233	Identifying high-priority conservation areas for endangered waterbirds using a flagship species in the Korean DMZ. 2021 , 159, 106080	3
232	Organic sulfones in the brine of Lake Vida, East Antarctica. 2021 , 292, 409-426	
231	Cardiovascular imaging modalities in the diagnosis and management of rheumatic heart disease. 2021 , 325, 176-185	3
230	Optoelectronic and material properties of solution-processed Earth-abundant Cu2BaSn(S, Se)4 films for solar cell applications. 2021 , 80, 105556	12
229	Tumor-infiltrating lymphocytes in the immunotherapy era. 2021 , 18, 842-859	89
228	SleepPoseNet: Multi-View Learning for Sleep Postural Transition Recognition Using UWB. 2021 , 25, 1305-131	417
227	Highly Sensitive Phase Variation Sensors Based on Step-Impedance Coplanar Waveguide (CPW) Transmission Lines. 2021 , 21, 2864-2872	13
226	A 16-Channel Dense Array for In Vivo Animal Cortical MRI/fMRI on 7T Human Scanners. 2021 , 68, 1611-1618	2
225	Recovery disparity between coral cover and the physical functionality of reefs with impaired coral assemblages. 2021 , 27, 640-651	12
224	Anticoagulation in hemodialysis: A narrative review. 2021 , 34, 103-115	7
223	The role of naps in memory and executive functioning in early childhood. 2021 , 60, 139-158	1
223	The role of naps in memory and executive functioning in early childhood. 2021 , 60, 139-158 Inclusion of low cost activated carbon for improving hydrogen production performance of TiO2 nanoparticles under natural solar light irradiation. 2021 , 47, 10216-10225	5
	Inclusion of low cost activated carbon for improving hydrogen production performance of TiO2	
222	Inclusion of low cost activated carbon for improving hydrogen production performance of TiO2 nanoparticles under natural solar light irradiation. 2021 , 47, 10216-10225	5
222	Inclusion of low cost activated carbon for improving hydrogen production performance of TiO2 nanoparticles under natural solar light irradiation. 2021 , 47, 10216-10225 Fast 4D elastic group-wise image registration. Convolutional interpolation revisited. 2021 , 200, 105812 Lithium polyacrylate polymer coating enhances the performance of graphite/silicon/carbon	2
222	Inclusion of low cost activated carbon for improving hydrogen production performance of TiO2 nanoparticles under natural solar light irradiation. 2021, 47, 10216-10225 Fast 4D elastic group-wise image registration. Convolutional interpolation revisited. 2021, 200, 105812 Lithium polyacrylate polymer coating enhances the performance of graphite/silicon/carbon composite anodes. 2021, 365, 137387	5 2 3
222 221 220 219	Inclusion of low cost activated carbon for improving hydrogen production performance of TiO2 nanoparticles under natural solar light irradiation. 2021, 47, 10216-10225 Fast 4D elastic group-wise image registration. Convolutional interpolation revisited. 2021, 200, 105812 Lithium polyacrylate polymer coating enhances the performance of graphite/silicon/carbon composite anodes. 2021, 365, 137387 Applications of M2ZrO2 (M = Li, Na, K) composite as a catalyst for biodiesel production. 2021, 286, 119392 Application of a new bio-ASP for enhancement of oil recovery: Mechanism study and core	5 2 3

215	Multi-Regression based supervised sample selection for predicting baby connectome evolution trajectory from neonatal timepoint. 2021 , 68, 101853	4
214	Review on Metamaterial Perfect Absorbers and Their Applications to IoT. 2021, 8, 4105-4131	15
213	CNN-Based Multistage Gated Average Fusion (MGAF) for Human Action Recognition Using Depth and Inertial Sensors. 2021 , 21, 3623-3634	6
212	DeepEcho: Echoacoustic Recognition of Materials using Returning Echoes with Deep Neural Networks. 2021 , 1-1	1
211	The Protective Effects of Perindopril Against Acute Kidney Damage Caused by Septic Shock. 2021 , 44, 148-159	3
210	Analysis of continuous neuronal activity evoked by natural speech with computational corpus linguistics methods. 2021 , 36, 167-186	1
209	d-Amino acids in antimicrobial peptides: a potential approach to treat and combat antimicrobial resistance. 2021 , 67, 119-137	7
208	Production of phenolic compounds and antioxidant activity via bioconversion of wheat straw by Inonotus obliquus under submerged fermentation with the aid of a surfactant. 2021 , 101, 1021-1029	4
207	Hydrological regulation of Vibrio dynamics in a tropical monsoonal estuary: a classification and regression tree approach. <i>Environmental Science and Pollution Research</i> , 2021 , 28, 724-737	2
206	. 2021 , 21, 1635-1643	15
206	. 2021 , 21, 1635-1643 A Full Bayesian Approach to Sparse Network Inference Using Heterogeneous Datasets. 2021 , 66, 3282-3288	15
205	A Full Bayesian Approach to Sparse Network Inference Using Heterogeneous Datasets. 2021 , 66, 3282-3288 Chronic nicotine impairs sparse motor learning via striatal fast-spiking parvalbumin interneurons.	1
205	A Full Bayesian Approach to Sparse Network Inference Using Heterogeneous Datasets. 2021 , 66, 3282-3288 Chronic nicotine impairs sparse motor learning via striatal fast-spiking parvalbumin interneurons. 2021 , 26, e12956 Nobiletin ameliorates nonylphenol-induced testicular damage by improving biochemical,	2
205	A Full Bayesian Approach to Sparse Network Inference Using Heterogeneous Datasets. 2021, 66, 3282-3288 Chronic nicotine impairs sparse motor learning via striatal fast-spiking parvalbumin interneurons. 2021, 26, e12956 Nobiletin ameliorates nonylphenol-induced testicular damage by improving biochemical, steroidogenic, hormonal, spermatogenic, apoptotic and histological profile. 2021, 40, 403-416	2 8
205 204 203 202	A Full Bayesian Approach to Sparse Network Inference Using Heterogeneous Datasets. 2021, 66, 3282-3288 Chronic nicotine impairs sparse motor learning via striatal fast-spiking parvalbumin interneurons. 2021, 26, e12956 Nobiletin ameliorates nonylphenol-induced testicular damage by improving biochemical, steroidogenic, hormonal, spermatogenic, apoptotic and histological profile. 2021, 40, 403-416 Future Interior Concepts. 2021,	1 2 8
205 204 203 202 201	A Full Bayesian Approach to Sparse Network Inference Using Heterogeneous Datasets. 2021, 66, 3282-3288 Chronic nicotine impairs sparse motor learning via striatal fast-spiking parvalbumin interneurons. 2021, 26, e12956 Nobiletin ameliorates nonylphenol-induced testicular damage by improving biochemical, steroidogenic, hormonal, spermatogenic, apoptotic and histological profile. 2021, 40, 403-416 Future Interior Concepts. 2021, Structural basis of SARS-CoV-2 spike protein induced by ACE2. 2021, 37, 929-936 Knowledge creation practices at organizational boundaries: the role of ICT in sickle-cell care for	1 2 8 O 11

197	Functions and mechanisms of RNA tailing by metazoan terminal nucleotidyltransferases. 2021, 12, e1622	9
196	GWAS Analysis of 17,019 Korean Women Identifies the Variants Associated with Facial Pigmented Spots. 2021 , 141, 555-562	5
195	Spray solution pH and soybean injury as influenced by synthetic auxin formulation and spray additives. 2021 , 35, 113-127	5
194	Pollen Collected by Stingless Bees in a Reforested Urban Area of Rio de Janeiro City. 2021 , 98, 23-26	1
193	Ultra-broadband Near-Unity Light Absorption by Disjunct Scattering Resonances of Disordered Nanounits Created with Atomic Scale Shadowing Effect. 2021 , 16, 83-90	1
192	On farm interventions to minimise spp. contamination in chicken. 2021 , 62, 53-67	5
191	Perspective: The Role of Human Breast-Milk Extracellular Vesicles in Child Health and Disease. 2021 , 12, 59-70	9
190	Towards multi-omics characterization of tumor heterogeneity: a comprehensive review of statistical and machine learning approaches. 2021 , 22,	4
189	A Pragmatic Guide to Enrichment Strategies for Mass Spectrometry-Based Glycoproteomics. 2020 , 20, 100029	44
188	Phylogenomic Data Reveal Widespread Introgression Across the Range of an Alpine and Arctic Specialist. 2021 , 70, 527-541	1
187	A Graphical-User-Interface-Based Azimuth-Collection Method in Autonomous Auditory Localization of Real and Virtual Sound Sources. 2021 , 25, 988-996	
186	Bayesian Optimization With Improved Scalability and Derivative Information for Efficient Design of Nanophotonic Structures. 2021 , 39, 167-177	4
185	. 2021 , 27, 1-7	1
184	Influence of Montmorillonite and Clinoptilolite on the Properties of Starch/Minerals Biocomposites and Their Effect on Aquatic Environments. 2021 , 29, 382-391	1
183	Portrait of visual cortical circuits for generating neural oscillation dynamics. 2021 , 15, 3-16	
182	Feature selection for improved classification accuracy targeting riverine sand mapping. 2021 , 29, 389-404	
181	Deep amplicon sequencing for culture-free prediction of susceptibility or resistance to 13 anti-tuberculous drugs. 2021 , 57,	19
180	A review on fundamentals and strategy of epoxy-resin-based anticorrosive coating materials. 2021 , 60, 601-625	4

179	Citizen science versus professional data collection: Comparison of approaches to mosquito monitoring in Germany. 2021 , 58, 214-223	15
178	Nudging Charitable Giving: What (If Anything) Is Wrong With It?. 2021 , 50, 353-371	O
177	An apoplastic fluid extraction method for the characterization of grapevine leaves proteome and metabolome from a single sample. 2021 , 171, 343-357	5
176	Computational Radiology in Breast Cancer Screening and Diagnosis Using Artificial Intelligence. 2021 , 72, 98-108	6
175	Endothelial-to-Mesenchymal Transition: Role in Cardiac Fibrosis. 2021 , 26, 3-11	4
174	For safe and compliant interaction: an outlook of soft underwater manipulators. 2021 , 235, 3-14	2
173	Quantification of Macrophage-Driven Inflammation During Myocardial Infarction with F-LW223, a Novel TSPO Radiotracer with Binding Independent of the rs6971 Human Polymorphism. 2021 , 62, 536-544	13
172	Structural analysis of the N-acetyltransferase Eis1 from Mycobacterium abscessus reveals the molecular determinants of its incapacity to modify aminoglycosides. 2020 ,	О
171	Anatomy and histology of the foramen of ovarian bursa opening to the peritoneal cavity and its changes in autoimmune disease-prone mice. 2021 , 238, 73-85	2
170	Large-scale assessment of intra- and inter-annual breeding success using a remote camera network. 2021 , 7, 97-108	3
169	Molecular and cellular responses to short exposure to bisphenols A, F, and S and eluates of microplastics in C. elegans. <i>Environmental Science and Pollution Research</i> , 2021 , 28, 805-818	9
168	Glaucoma Home Monitoring Using a Tablet-Based Visual Field Test (Eyecatcher): An Assessment of Accuracy and Adherence Over 6 Months. 2021 , 223, 42-52	10
167	Modeling brain, symptom, and behavior in the winds of change. 2021 , 46, 20-32	7
166	Multivariate model for cooperation: bridging social physiological compliance and hyperscanning. 2021 , 16, 193-209	3
165	Pathogenesis of necrotising enterocolitis: The impact of the altered gut microbiota and antibiotic exposure in preterm infants. 2021 , 110, 433-440	5
164	Enhancement of mechanical properties and chemical durability of Soda-lime silicate glasses treated by DC gas discharges. 2021 , 104, 157-166	1
163	The evaluation of surface topography changes in nanoscaled 2,6-diphenyl anthracene thin films by atomic force microscopy. 2021 , 84, 89-100	1
162	Enhanced resistance of Trichoderma harzianum LZDX-32-08 to hygromycin B induced by sea salt. 2021 , 43, 213-222	

161 Sustainable Development for Energy, Power, and Propulsion. 2021,

160	To hunt or to rest: prey depletion induces a novel starvation survival strategy in bacterial predators. 2021 , 15, 109-123	6
159	Hypoxia-driven secretion of extracellular matrix proteins in the exosomes reflects the asymptomatic pathology of rotator cuff tendinopathies. 2021 , 99, 224-230	1
158	Gut microbiota in human metabolic health and disease. 2021 , 19, 55-71	487
157	Cobalt-containing bioactive glass mimics vascular endothelial growth factor A and hypoxia inducible factor 1 function. 2021 , 109, 1051-1064	5
156	A systematic review of interventions to mitigate radiotherapy-induced oral mucositis in head and neck cancer patients. 2021 , 29, 2187-2202	6
155	The quest for absolute abundance: The use of internal standards for DNA-based community ecology. 2021 , 21, 30-43	12
154	Macromolecular crystallization: basics and advanced methodologies. 2021 , 18, 543-565	
153	Microengineered systems with iPSC-derived cardiac and hepatic cells to evaluate drug adverse effects. 2021 , 246, 317-331	5
152	Impact of DNA damage repair defects and aggressive variant features on response to carboplatin-based chemotherapy in metastatic castration-resistant prostate cancer. 2021 , 148, 385-395	13
151	Traditional Chinese medicine may be further explored as candidate drugs for pancreatic cancer: A review. 2021 , 35, 603-628	9
150	Data acquisition and imaging using wavelet transform: a new path for high speed transient force microscopy. 2021 , 3, 383-398	2
149	Investigation of mode interaction for a gyrotron with dense mode spectrum. 2021 , 35, 19-26	3
148	Microplastics and their potential effects on the aquaculture systems: a critical review. 2021 , 13, 719-733	25
147	Coronaviruses in farm animals: Epidemiology and public health implications. 2021 , 7, 322-347	10
146	Environmental Remediation Through Carbon Based Nano Composites. 2021 ,	3
145	Annual Research Review: Reading disorders revisited - the critical importance of oral language. 2021 , 62, 635-653	20
144	Functional morphology, diversity, and evolution of yolk processing specializations in embryonic reptiles and birds. 2021 , 282, 995-1014	3

143	Rhenium substitutional doping for enhanced photoresponse of n-SnSe2/p-Si heterojunction based tunable and high-performance visible-light photodetector. 2021 , 536, 147739	11
142	Maternal antenatal stress and mental and behavioral disorders in their children. 2021 , 278, 57-65	9
141	Gold nanoparticles coated with polyvinylpyrrolidone and sea urchin extracellular molecules induce transient immune activation. 2021 , 402, 123793	12
140	Artificial Intelligence and Machine Learning in Nuclear Medicine: Future Perspectives. 2021 , 51, 170-177	13
139	Optical Fiber Technologies for Nanomanipulation and Biodetection: A Review. 2021 , 39, 251-262	12
138	A New Capacitive Sensor for Histomorphometry Evaluation of Dental Implants. 2021 , 21, 14515-14521	2
137	Hormone manipulation to overcome a major barrier in male catfish spawning: The role of oxytocin augmentation in inducing voluntary captive spawning. 2021 , 52, 51-64	O
136	Optical coherence tomography angiography in diabetes: focus on microaneurysms. 2021 , 35, 142-148	2
135	Contrasting the Water Quality and Bacterial Community Patterns in Shallow and Deep Lakes: Manyas vs. Iznik. 2021 , 67, 506-512	5
134	Analysis of low-frequency vibration-assisted bone drilling in reducing thermal injury. 2021 , 36, 27-38	2
133	Environmental covariates for modelling the distribution and abundance of breeding ducks in northern North America: a review. 2021 , 28, 33-52	1
132	Cognitive Correlates of Math Performance in School-Aged Children with Sickle Cell Disease and Silent Cerebral Infarcts. 2021 , 36, 465-474	O
131	Comprehensive Analysis of Long-Range Connectivity from and to the Posterior Parietal Cortex of the Mouse. 2021 , 31, 356-378	1
130	Bacteriophages as drivers of bacterial virulence and their potential for biotechnological exploitation. 2021 , 45,	16
129	Can N O emissions offset the benefits from soil organic carbon storage?. 2021 , 27, 237-256	54
128	An Efficient and Robust Method for Selective Conversion of Aniline to Azobenzene Using nano-TiO -P25-SO H, under Visible Light Irradiation. 2021 , 97, 278-288	
127	ACE2: Its potential role and regulation in severe acute respiratory syndrome and COVID-19. 2021 , 236, 2430-2442	18
126	Studies of 2D Bulk and Nanoribbon Band Structures in MoxW1\(\mathbb{U}\)S2 Alloy System Using Full sp3d5 Tight-Binding Model. 2021 , 258, 2000375	

(2021-2021)

125	Building health monitoring in the old town of Madrid: applicability of SAR Imagery to the monitoring of underground works through classification indexes. 2021 , 14, 271-287	2
124	EpiDope: a deep neural network for linear B-cell epitope prediction. 2021, 37, 448-455	5
123	Memristor-Based Variation-Enabled Differentially Private Learning Systems for Edge Computing in IoT. 2021 , 8, 9672-9682	3
122	Comparative pharmacokinetics of Ding-Zhi-Xiao-Wan preparation and its single herbs in rats by using a putative multiple-reaction monitoring UPLC-MS/MS method. 2021 , 32, 362-374	1
121	Deep Learning for Cancer Diagnosis. 2021,	7
120	Partial rewarding during clicker training does not improve nalle dogs' learning speed and induces a pessimistic-like affective state. 2021 , 24, 107-119	2
119	. 2021 , 59, 3607-3622	2
118	Extracellular vesicles derived from inflamed murine colorectal tissue induce fibroblast proliferation via epidermal growth factor receptor. 2021 , 288, 1906-1917	1
117	Beta diversity patterns in zooplankton assemblages from a semiarid river ecosystem. 2021 , 106, 29-40	4
116	Organization of the Pluripotent Genome. 2021 , 13,	3
115	Concentration-dependent emission of nitrogen-doped carbon dots and its use in hazardous metal-ion detection. 2021 , 31, 523-536	2
114	Facile Stereoselective Reduction of Prochiral Ketones by using an F-dependent Alcohol Dehydrogenase. 2021 , 22, 156-159	4
113	Probing hepatic metabolism of [2-C]dihydroxyacetone in vivo with H-decoupled hyperpolarized C-MR. 2021 , 34, 49-56	5
112	Factors Affecting Bacterial Adhesion on Selected Textile Fibres. 2021 , 61, 31-37	5
111	Shigella sonnei: virulence and antibiotic resistance. 2021 , 203, 45-58	8
110	Joint liability and adaptation to climate change: evidence from Burkinabe cooperatives. 2021 , 48, 502-537	1
109	A cross-sectional study of factors predicting readmission in Thais with coronary artery disease 2021 , 26, 293-304	4
108	Sterile inflammation drives multiple programmed cell death pathways in the gut. 2021 , 109, 211-221	2

107	Resonance Analysis of a Surface Plasmon-Polariton Wave in a Prismatic Structure with a Limited Cross Section of a Test Beam. 2021 , 16, 131-138	1
106	Experimental Warming Enhances Effects of Eelgrass Genetic Diversity Via Temperature-Induced Niche Differentiation. 2021 , 44, 545-557	2
105	Functionalization of conducting polymers and their applications in optoelectronics. 2021, 60, 465-487	10
104	Applications of digital imaging and analysis in seabird monitoring and research. 2021, 163, 317-337	10
103	Neutrophils produce proinflammatory or anti-inflammatory extracellular vesicles depending on the environmental conditions. 2021 , 109, 793-806	15
102	Analysis of Putative Epitope Candidates of Against Pakistani Human Leukocyte Antigen Background: An Immunoinformatic Study for the Development of Future Vaccine. 2020 , 27, 1-18	3
101	Building a Culture of Prevention: Tasks for Multi-Taskers. 2021 , 22, 91-93	
100	Calcium Oscillatory Patterns and Oocyte Activation During Fertilization: a Possible Mechanism for Total Fertilization Failure (TFF) in Human In Vitro Fertilization?. 2021 , 28, 639-648	7
99	Using a coupled LES aerosol-radiation model to investigate the importance of aerosol-boundary layer feedback in a Beijing haze episode. 2021 , 226, 173-190	2
98	Fo and Ni Relations in Olivine Differentiate between Crystallization and Diffusion Trends. 2021 , 61,	3
97	Microfluidic devices for detection of RNA viruses. 2021 , 31, 1-11	48
96	Hemodynamics mediated epigenetic regulators in the pathogenesis of vascular diseases. 2021 , 476, 125-143	4
95	Wettability Distribution on the Surface Treated by Plasma Jet at Different Flow Rates for Microfluidic Applications. 2021 , 49, 168-176	2
94	Anthropogenic injuries disrupt social associations of common bottlenose dolphins (Tursiops truncatus) in Sarasota Bay, Florida. 2021 , 37, 29-44	5
93	Micromechanics-based damage model for liquid-assisted healing. 2021 , 30, 123-144	3
92	Long-term changes in Italian mountain forests detected by resurvey of historical vegetation data. 2021 , 32,	1
91	Chemical Ecology in Insect-microbe Interactions in the Neotropics. 2021 , 87, 38-48	4
90	Relating pollen representation to an evolving Amazonian landscape between the last glacial maximum and Late Holocene. 2021 , 99, 63-79	2

89	Legal cannabis-what's in it?. 2021 , 116, 231-232	3
88	Isolation, growth kinetics, and immunophenotypic characterization of adult human cardiac progenitor cells. 2021 , 236, 1840-1853	
87	Microwave diamond devices technology: Field-effect transistors and modeling. 2021, 34,	1
86	Anticancer and therapeutic potential of Delonix regia extract and silver nanoparticles (AgNPs) against pancreatic (Panc-1) and breast (MCF-7) cancer cell. 2021 , 13, 45-56	4
85	Dense lamellar scaffold, biomimetically inspired, for reverse cardiac remodeling: Effect of proanthocyanidins and glutaraldehyde. 2021 , 42, 248-261	O
84	Robust Self-Regulated Rectifier for Parallel-Resonant Rx Coil in Multiple-Receiver Wireless Power Transmission System. 2021 , 9, 3812-3821	3
83	Mindfulness, Moral Reasoning and Responsibility: Towards Virtue in Ethical Decision-Making. 2021 , 169, 103-117	13
82	Synthesis and Biological Activity Evaluation of 3,4,7,8-Tetrahydro-3,3-Dimethyl-11-Aryl-2H-Pyridazino[1,2-a]Indazole-1,6,9(11H)-Triones by Using an Acidic Ionic Liquid 1-Methylimidazolium Trinitromethanide {[HMIM]C(NO2)3} as a Green Catalyst.	1
81	Price and product variation in Washington's recreational cannabis market. 2021 , 91, 102547	15
80	DNA G-quadruplexes: functional significance in plant and farm animal science. 2021 , 32, 262-271	2
79	Remediation of Thorium (IV) from Wastewater: Current Status and Way Forward. 2021, 50, 177-202	17
78	Effects of an extreme drought on the endangered pearl mussel Margaritifera margaritifera: a before/after assessment. 2021 , 848, 3003-3013	2
77	A Comparison of Training Modality and Total Genotype Scores to Enhance Sport-Specific Biomotor Abilities in Under 19 Male Soccer Players. 2021 , 35, 154-161	1
76	Evolution and Evaluation of GC Columns. 2021 , 51, 150-173	5
75	A Single Laboratory Validation for the Analysis of Underivatized 卧-Methylamino-L-Alanine (BMAA). 2021 , 39, 49-71	6
74	Destination Events, Stability, and Turning Points of Development. 2021 , 60, 172-183	6
73	Social reinforcement learning as a predictor of real-life experiences in individuals with high and low depressive symptomatology. 2021 , 51, 408-415	4
72	New perspectives on the nature and imaging of active site in small metallic particles: I. Geometric effects. 2021 , 208, 89-109	

71	Aspirin and N-acetylcysteine co-administration markedly inhibit chronic ethanol intake and block relapse binge drinking: Role of neuroinflammation-oxidative stress self-perpetuation. 2021 , 26, e12853	3	16
70	Disaster City Digital Twin: A vision for integrating artificial and human intelligence for disaster management. 2021 , 56, 102049		68
69	Microbiomics to Define Wine Terroir. 2021 , 438-451		4
68	Glycosyltransformation of ginsenoside Rh2 into two novel ginsenosides using recombinant glycosyltransferase from and its applications. 2021 , 45, 48-57		5
67	Microarrays: A Road Map to Uncover Host Pathogen Interactions. 2021 , 125-137		
66	Visualization of microwave near-field distribution in sodium chloride and glucose aqueous solutions by a thermo-elastic optical indicator microscope. <i>Scientific Reports</i> , 2021 , 11, 2589	4.9	7
65	Measurement and modelling solubility of amino acids and peptides in aqueous 2-propanol solutions. <i>Physical Chemistry Chemical Physics</i> , 2021 , 23, 10852-10863	3.6	3
64	Preclinical Evaluation of Safety, Pharmacokinetics, Efficacy, and Mechanism of Radioprotective Agent HL-003. 2021 , 2021, 6683836		О
63	Uncovering genomic regions controlling plant architectural traits in hexaploid wheat using different GWAS models. <i>Scientific Reports</i> , 2021 , 11, 6767	4.9	7
62	Self-Healable, Recyclable, and Ultrastrong Adhesive Ionogel for Multifunctional Strain Sensor. 2021 , 13, 20653-20661		20
61	Synthesis and radioprotective effects of novel hybrid compounds containing edaravone analogue and 3-n-butylphthalide ring-opening derivatives. 2021 , 25, 5470-5485		2
60	Towards sustainable production and utilization of plant-biomass-based nanomaterials: a review and analysis of recent developments. 2021 , 14, 114		22
59	Effect of Cu doping on the photocatalytic activity of InVO for hazardous dye photodegradation under LED light and its mechanism. 2021 , 84, 576-595		2
58	Interactions between polyphenolic antioxidants quercetin and naringenin dictate the distinctive redox-related chemical and biological behaviour of their mixtures. <i>Scientific Reports</i> , 2021 , 11, 12282	4.9	6
57	Anticancer activity of Helicobacter pylori ribosomal protein (HPRP) with iRGD in treatment of colon cancer. 2021 , 147, 2851-2865		1
56	Evaluation of the immunomodulatory effects of cobalt, copper and magnesium ions in a pro inflammatory environment. <i>Scientific Reports</i> , 2021 , 11, 11707	4.9	3
55	Congenital Anomalies of the Tracheobronchial Tree: A Meta-Analysis and Clinical Considerations. 2021 , 112, 315-325		2
54	Integrated computational and experimental pipeline for quantifying local cell-matrix interactions. <i>Scientific Reports</i> , 2021 , 11, 16465	4.9	О

53	Enhanced catalytic performance of Cu2ZnSnS4/MoS2 nanocomposites based counter electrode for Pt-free dye-sensitized solar cells. 2021 , 894, 162166		2
52	Ultra-narrow, highly efficient power splitters and waveguides that exploit the TE Mie-resonant bandgap. <i>Optics Express</i> , 2021 , 29, 32951-32965	3.3	1
51	Soil K forms and K budget in integrated crop-livestock systems in subtropical paddy fields. 2021 , 213, 105070		0
50	Assessment of air quality in the Aburr Valley (Colombia) using composite indices: Towards comprehensive sustainable development planning. 2021 , 39, 100942		2
49	Influence of non-thermal microwaveradiationon emulsifying properties of sunflower protein. 2022 , 372, 131275		O
48	Colorimetric ammonia (NH) sensor based on an alginate-methylcellulose blend hydrogel and the potential opportunity for the development of a minced pork spoilage indicator. 2021 , 362, 130151		13
47	The effect of heat treatment parameters on the microstructure and torque response of a 13 wt% Cr steel. 2022 , 541, 168543		
46	Differential organization of open field behavior in mice following acute or chronic simulated GCR exposure. 2022 , 416, 113577		2
45	Effectiveness of deep cryogenic treatment on carbide precipitation. 2020, 9, 13014-13026		17
44	Physiological models to study the effect of molecular crowding on multi-drug bound proteins: insights from SARS-CoV-2 main protease. 2021 , 1-17		2
43	Comparative evaluation of gliadins from four extraction protocols using advanced analytical techniques. 2021 ,		О
42	Comparative evaluation of amino acid composition and protein profile of gliadin from different extraction protocols. 2022 , 99, 194		O
41	Radiotherapy-Induced Digestive Injury: Diagnosis, Treatment and Mechanisms. 2021, 11, 757973		2
40	Characterization of gliadin, secalin and hordein fractions using analytical techniques. <i>Scientific Reports</i> , 2021 , 11, 23135	4.9	2
39	S-nitrosothiols signaling in cystic fibrosis airways. 2021 , 46, 1		0
38	Tight-binding Model in First and Second Quantization for Band Structure Calculations. <i>Brazilian Journal of Physics</i> , 2022 , 52, 1	1.2	1
37	The boosted activity of AgI/BiOI nanocatalyst: a RSM study towards Eriochrome Black T photodegradation <i>Environmental Science and Pollution Research</i> , 2022 , 1	5.1	О
36	Fertilization effects on soil microbial composition and nutrient availability in integrated rice-livestock production systems. <i>Applied Soil Ecology</i> , 2022 , 174, 104420	5	O

35	All-dielectric magnetophotonic gratings for maximum TMOKE enhancement <i>Physical Chemistry Chemical Physics</i> , 2022 ,	3.6	2
34	Room-temperature growth optimization and PL characteristic of polytype h/\textsup MoO3 thin films by chemical precipitation method. <i>Physica Scripta</i> , 2022 , 97, 045811	2.6	O
33	Strategies for enhancing immunity against avian influenza virus in chickens: A review <i>Avian Pathology</i> , 2022 , 1-86	2.4	1
32	Management of abiotic stresses by microbiome-based engineering of the rhizosphere <i>Journal of Applied Microbiology</i> , 2022 ,	4.7	1
31	Inertial separation of microparticles suspended in shear-thinning fluids. Chemical Papers, 1	1.9	1
30	Modulation of radiation-induced intestinal injury by radioprotective agents: a cellular and molecular perspectives <i>Reviews on Environmental Health</i> , 2022 ,	3.8	1
29	Optimized assay for transposase-accessible chromatin by sequencing (ATAC-seq) library preparation from adult Drosophila melanogaster neurons <i>Scientific Reports</i> , 2022 , 12, 6043	4.9	O
28	Nanogenerators-Based Self-Powered Sensors. <i>Advanced Materials Technologies</i> , 2200282	6.8	2
27	Evaluation of nutrient characteristics and bacterial community in agricultural soil groups for sustainable land management <i>Scientific Reports</i> , 2022 , 12, 7368	4.9	1
26	Anticancer Potential of Thymoquinone: A Novel Bioactive Natural Compound from Nigella sativa L <i>Anti-Cancer Agents in Medicinal Chemistry</i> , 2022 ,	2.2	2
25	Computer-aided diagnosis of COVID-19 from chest X-ray images using histogram-oriented gradient features and Random Forest classifier <i>Multimedia Tools and Applications</i> , 2022 , 1-18	2.5	O
24	Polarization insensitive dual band metamaterial with absorptance for 5G sub-6 GHz applications <i>Scientific Reports</i> , 2022 , 12, 8495	4.9	2
23	Drug eluting titanium implants for localised drug delivery. Journal of Materials Research,	2.5	2
22	Optimization of biodiesel production via transesterification of soybean oil using EMoO3 catalyst obtained by the combustion method. <i>Arabian Journal of Chemistry</i> , 2022 , 15, 104012	5.9	O
21	MicroRNAs in Non-Malignant Diseases. 2022 , 41-68		
20	Ultra-intense vortex laser generation from a seed laser illuminated axial line-focused spiral zone plate. <i>Optics Express</i> ,	3.3	
19	Improved YOLOv3 detection method for PCB plug-in solder joint defects based on ordered probability density weighting and attention mechanism. <i>AI Communications</i> , 2022 , 1-16	0.8	
18	Towards prediction of oil recovery by spontaneous imbibition of modified salinity brine into limestone rocks: A scaling study. <i>Journal of Petroleum Exploration and Production</i> ,	2.2	

CITATION REPORT

17	Synergistic data fusion of satellite observations and in-situ measurements for hourly PM2.5 estimation based on hierarchical geospatial long short-term memory. <i>Atmospheric Environment</i> , 5.3 2022 , 286, 119257	O
16	Carbon Quantum Dots: A Promising Nanocarrier for Bioimaging and Drug Delivery in Cancer. Materials Today Communications, 2022 , 104068	3
15	Structural, functional, and molecular docking analyses of microbial cutinase enzymes against polyurethane monomers. <i>Journal of Hazardous Materials Letters</i> , 2022 , 3, 100063	1
14	Longitudinal Magneto-optical Kerr Effect in Insulator/Metal/Insulator Grating Structure.	
13	Protocol and reference values for minimal detectable change of MyotonPRO and ultrasound imaging measurements of muscle and subcutaneous tissue. 2022 , 12,	2
12	Gamma irradiation as a tool to produce cowpea (Vigna unguiculate (L.) Walp.) genotypes resistant to aphid pests.	Ο
11	Notch-insensitive, underwater adhesive, and self-healing ionic skins. 2022 , 259, 125246	0
10	Low maintenance anammox enrichment and nitrogen removal with an anaerobic baffled reactor. 2022 , 128047	O
9	Detection of indigenous gut bacteria related to red chilli pepper (Capsicum annuum) in murine caecum and human faecal cultures.	0
8	Novel Analysis of Two Kinds Hybrid Models in Ferro Martial Inserting Variable Lorentz Force Past a Heated Disk: An Implementation of Finite Element Method. 2023 , 135, 1393-1411	O
7	Detecting Pneumonia Based On Chest X-Ray Images Using Reinforcement Learning. 2022,	1
6	Correlative surface and bulk analysis of deep cryogenic treatment influence on high-alloyed ferrous alloy. 2022 ,	1
5	Partitioning evapotranspiration and carbon flux in ungrazed and grazed tallgrass prairie. 2023, 343, 108285	0
4	LWSNet - a novel deep-learning architecture to segregate Covid-19 and pneumonia from x-ray imagery.	1
3	MMLN: Leveraging Domain Knowledge for Multimodal Diagnosis. 2022 , 192-203	O
2	EVALUATION OF IMPACT ACCELERATION IN RUNNING FOOT STRIKE DEPENDING ON PAVEMENT TYPES. 2023 , 78, I_144-I_151	O
1	Lighthatter interaction empowered by orbital angular momentum: Control of matter at the micro- and nanoscale. 2023 , 88, 100459	Ο